Calhoun
Institutional Archive of the Naval Postgraduate School

Calhoun: The NPS Institutional Archive

DSpace Repository

Theses and Dissertations | 1. Thesis and Dissertation Collection, all items

1991

Measurement of surface layer turbulence above AMOS

Mattingly, Timothy Scott

Monterey, California. Naval Postgraduate School

http://hdl.handle.net/10945/43780

This publication is a work of the U.S. Government as defined in Title 17, United States Code, Section 101. Copyright protection is not available for this work in the United States.

Downloaded from NPS Archive: Calhoun

http://www.nps.edu/library

Calhoun is the Naval Postgraduate School's public access digital repository for research materials and institutional publications created by the NPS community. Calhoun is named for Professor of Mathematics Guy K. Calhoun, NPS's first appointed -- and published -- scholarly author.

Dudley Knox Library / Naval Postgraduate School
411 Dyer Road / 1 University Circle
Monterey, California USA 93943

DUDLEY KNOX LIBRARY
NAVAL POSTGRADUATE SCHOOL
MONTEREY CA 93943-5101

NAVAL POSTGRADUATE SCHOOL
Monterey, California, 93943

Rear Admiral R.W. West, Jr.
Superintendent

H. Shull
Provost

This thesis was prepared in conjunction with research sponsored in part by Phillips Lab(Code PL/LIM), Kirtland AFB, Albuquerque, NM 87117.

Reproduction of all or part of this report is authorized.

Released By:

NAVAL POSTGRADUATE SCHOOL
Monterey, California, 93943

Rear Admiral R.W. West, Jr.
Superintendent

H. Shull
Provost

This thesis was prepared in conjunction with research sponsored in part by Phillips Lab(Code PL/LIM), Kirtland AFB, Albuquerque, NM 87117.

Reproduction of all or part of this report is authorized.

Released By:

NPS-PH-92-005

NAVAL POSTGRADUATE SCHOOL

Monterey, California

THESIS

MEASUREMENT OF SURFACE LAYER OPTICAL TURBULENCE ABOVE AMOS

by

Timothy Scott Mattingly

December, 1991

Thesis Advisor: Donald L. Walters

Approved for public release; distribution is unlimited

Prepared for:
Phillips Lab
Attn: Richard Frosch
Kirtland Air Force Base
Albuquerque, NM 87117

REPORT DOCUMENTATION PAGE

PORT SECURITY CLASSIFICATION ASSIFIED	1b RESTRICTIVE MARKINGS
CURITY CLASSIFICATION AUTHORITY	3 DISTRIBUTION/AVAILABILITY OF REPORT Approved for public release; distribution is unlimited.
ECLASSIFICATION/DOWNGRADING SCHEDULE	
FORMING ORGANIZATION REPORT NUMBER(S)	5 MONITORING ORGANIZATION REPORT NUMBER(S)

AME OF PERFORMING ORGANIZATION l Postgraduate School	6b. OFFICE SYMBOL *(If applicable)* CODE 33	7a. NAME OF MONITORING ORGANIZATION Naval Postgraduate School
DDRESS (*City, State, and ZIP Code*) terey, CA 93943-5000		7b. ADDRESS (*City, State, and ZIP Code*) Monterey, CA 93943-5000
IAME OF FUNDING/SPONSORING ANIZATION ips Lab	8b OFFICE SYMBOL *(If applicable)* PL/LIM	9. PROCUREMENT INSTRUMENT IDENTIFICATION NUMBER
DDRESS (*City, State, and ZIP Code*) and AFB querque, NM 87117		10 SOURCE OF FUNDING NUMBERS

Program Element No	Project No	Task No	Work Unit Accession Number

ITLE (*Include Security Classification*)
SUREMENT OF SURFACE LAYER OPTICAL TURBULENCE ABOVE AMOS

ERSONAL AUTHOR(S) Mattingly, Timothy S. in conjunction with Walters, Donald L.

TYPE OF REPORT	13b. TIME COVERED	14 DATE OF REPORT (*year, month, day*)	15 PAGE COUNT
er's Thesis	From To	December 1991	124

UPPLEMENTARY NOTATION
iews expressed in this thesis are those of the author and do not reflect the official policy or position of the Department of Defense or the U.S. rnment.

OSATI CODES			18 SUBJECT TERMS (*continue on reverse if necessary and identify by block number*)
LD	GROUP	SUBGROUP	Acoustic Echo-sounder, Atmospheric Optical Turbulence, Spatial Coherence Length, Wind Profile, Short and Long Term Exposures

BSTRACT (*continue on reverse if necessary and identify by block number*)

mperature fluctuations in the atmosphere severely limit the angular resolution of earth bound observation facilities to around 1 arcsecond. corresponds to an effective, coherent aperture size of 10 cm even thougb the telescope may have a 2-4 m primary mirror. Understanding the ial and temporal distribution of atmospheric optical turbulence is essential to maximize the performance of large astronomical telescopes. thesis made use of a 5 kHz high frequency, short range Doppler acoustic sounder to investigate the first 100 meters of the mountain boundary r turbulence above the Air Force Maui Observation Site, AMOS, Haleakala, Hi. These measurements were part of a coordinated site uation for a proposed 4 m telescope to be built at AMOS in the near future.

entative results revealed significant layering, 15-20 m and occasionally thicker, in the turbulent surface layer above AMOS. Additionally, a parison of two proposed construction sites near the top of Haleakala showed that the turbulent surface layer tends to follow the contours of the ntain.

DISTRIBUTION/AVAILABILITY OF ABSTRACT ☒ UNCLASSIFIED/UNLIMITED ☐ SAME AS REPORT ☐ DTIC USERS	21. ABSTRACT SECURITY CLASSIFICATION UNCLASSIFIED	
NAME OF RESPONSIBLE INDIVIDUAL Walters	22b TELEPHONE (*Include Area code*) (408)646-2267	22c OFFICE SYMBOL PH/WE

FORM 1473, 84 MAR — 83 APR edition may be used until exhausted; All other editions are obsolete — SECURITY CLASSIFICATION OF THIS PAGE: UNCLASSIFIED

Approved for public release; distribution is unlimited.

Measurement of Surface Layer Turbulence Above AMOS

by

Timothy Scott Mattingly
Lieutenant, United States Navy
B.S., Eastern Kentucy University

Submitted in partial fulfillment
of the requirements for the degree of

MASTER OF SCIENCE IN PHYSICS

from the

NAVAL POSTGRADUATE SCHOOL
December 1991

ABSTRACT

Temperature fluctuations in the atmosphere severely limit the angular resolution of earth bound observation facilities to around 1 arcsecond. This corresponds to an effective, coherent, aperture size of 10 cm even though the telescope may have a 2-4 m primary mirror. Understanding the spatial and temporal distribution of atmospheric optical turbulence is essential to maximize the performance of large astronomical telescopes. This thesis made use of a 5 kHz high frequency, short range Doppler acoustic sounder to investigate the first 100 meters of the mountain boundary layer turbulence above the Air Force Maui Observation Site, AMOS, Haleakala, Hi. These measurements were part of a coordinated site evaluation for a proposed 4 m telescope to be built at AMOS in the near future.

Tentative results revealed significant layering, 15-20 m and occasionally thicker, in the turbulent surface layers above AMOS. Additionally, a comparison of two proposed construction sites near the top of Haleakala showed that the turbulent surface layer tends to follow the contours of the mountain.

M 38315
c.1

TABLE OF CONTENTS

I. INTRODUCTION 1

A. OPTICAL TURBULENCE 1

B. MISSION OBJECTIVES 1

II BACKGROUND 4

A. ATMOSPHERIC TURBULENCE 4

B. ECHO-SOUNDER OPERATION 6

1. Acoustic Sounder Calibration 9

III. EQUIPMENT 14

A. OVERVIEW 14

B. RECENT UPGRADES 16

IV. RESULTS 20

A. CALIBRATION 20

1. Equipment 20

2. Findings 22

B. AMOS FIELD MEASUREMENTS 28

MONTEREY CA 93943-5101

1. Turbulence Profile 28

2. r_o vs. Altitude 29

3. Comparison to Optical Data 37

a. AMOS Support 37

b. Zenith Angle Correction 42

c. Short Exposure Correction 42

4. Wind and Atmospheric Conditions 48

V. CONCLUSIONS AND RECOMMENDATIONS 52

A. MISSION OBJECTIVES 52

1. r_o vs. Altitude 52

2. Site Comparison 53

B. FUTURE CONSIDERATIONS 54

1. Atmospheric Turbulence 54

2. Artificial Turbulence 54

APPENDIX A. ACOUSTIC ECHO-SOUNDER OPERATING CODE 56

APPENDIX B. ACOUSTIC SOUNDER DATA FROM AMOS 72

APPENDIX C. WIND PROFILE DATA FOR AMOS 105

LIST OF REFERENCES 112

INITIAL DISTRIBUTION LIST 114

ACKNOWLEDGEMENTS

I would like to express my sincere thanks to those who made this project possible. The enthusiasm and diversification of my thesis advisor Dr. Don Walters, made the entire experience rewarding and enjoyable. To Captains Ann Slavin, Hiedi Beason, Kurt Guinn, and Andrew Terzakis of the Air Force Phillips Lab for coordinating our field trip to Maui, Hawaii. And last but not least to our ever-willing and capable technical support personnel, Dale Galarowicz and George Jaksha, without whose help on various hardware components, this project would have never been possible.

I. INTRODUCTION

A. OPTICAL TURBULENCE

The resolution of an astronomical telescope is known to be highly dependent upon localized optical turbulence characteristics. The ability to measure and to understand such phenomenon can enhance the optical viewing quality of earth-bound instruments. One method of monitoring these naturally occurring effects at low altitudes (<200m), is through the use of an acoustic echo-sounder. A variety of such devices have been proven to be both feasible and accurate [Refs. 1 through 4]. The echo-sounder used to obtain the data in this thesis has been developed over the past 4 years by Walters, Moxcey, Weingartner, Wroblewski, and McCrary [Refs. 5 through 9].

Temperature fluctuations in the atmosphere degrade optical seeing conditions by affecting the local index of refraction. The scattering of acoustic energy produced by an echo-sounder can reveal the spatial and temporal distribution of these fluctuations. The acoustic echo-sounder exploits this scattering phenomenon to model optical turbulence.

B. MISSION OBJECTIVES

The mission of this project was to assist in the site assessment for a proposed Air Force, 4 meter telescope at the Air Force Maui Observation Station,

AMOS, Haleakala, Hi. This was accomplished in two phases. The first of these investigated the existence, location, and significance of low altitude turbulence layers. The second performed a quick-look comparison between two proposed construction sites.

Sounder measurements extended between 26 June and 2 July, 1991, at both proposed sites. Additionally, the 1.6 meter Itek Compensated Imaging System, CIS, and the 1.2m Hughes seeing monitor gathered simultaneous stellar full width at half maximum (FWHM) data. The primary site, Site A, was at the summit of Haleakala in the center of a 30 m circular ring, 15 m higher and 100 m to the south-east of the current facility. The secondary site, Site G, was located 35 m to the south-east of, and at approximately the same elevation as, the current facility. A layout of the AMOS facility is given in Figure 1.

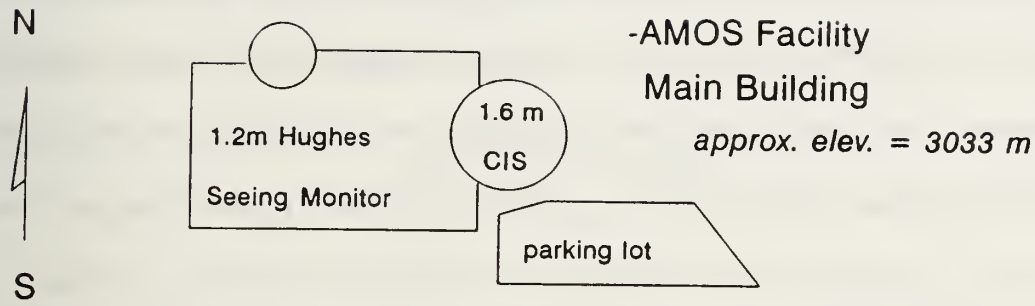

Site G

approx. elev. = 3036 m

Site A

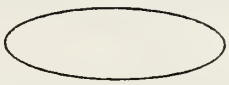

approx. elev. = 3048 m

Scale in meters :

0 *25*

Figure 1 AMOS Facility Layout Showing Locations of Proposed 4m Telescope Sites.

II BACKGROUND

A. ATMOSPHERIC TURBULENCE

An optical plane wave experiences random phase perturbations while passing through the atmosphere. The cause of these perturbations stems from the presence of small temperature fluctuations carried by turbulent velocity fields in the atmosphere. These phenomena affect the local index of refraction directly, and hence, degrade the resolution of earth-bound observation facilities. The following two parameters arise when describing this degradation: 1) the refractive turbulence structure parameter, C_N^2, and 2) the spatial coherence length of the atmosphere, r_o .

The more fundamental of these, C_N^2, is the mean-square statistical average of the difference between the indices of refraction of two points. Tatarski [Ref. 10] includes a detailed discussion of this parameter which is summarized more recently by Walters and Kunkel [Ref. 11] as follows,

$$C_N^2 = \langle (n_1 - n_2)^2 \rangle / r_{12}^{2/3} \qquad (1)$$

where n_1 and n_2 are the indices of refraction at points 1 and 2 respectively, and r_{12} is the separation between points 1 and 2 in the atmosphere. It is a measure of the local optical turbulence present in the atmosphere and is the starting point in analyzing that turbulence. It is important to note that the presence of significant

optical turbulence does not imply an appreciable degree of velocity turbulence and vice versa [Ref.9]. Regretfully, C_N^2 is a difficult parameter to measure directly. It is easier to make direct measurements of another atmospheric structure parameter, C_T^2.

The thermal structure parameter, C_T^2, is the mean squared temperature difference between two points in space,

$$C_T^2 = \langle (T_2 - T_1)^2 \rangle / r_{12}^{2/3} \qquad (2)$$

where T_1 and T_2 are the temperatures at points 1 and 2 respectively. As will be discussed in the following section, an acoustic echo-sounder measures this parameter indirectly. Tatarski [Ref. 10] develops a relationship between C_T^2 and C_N^2,

$$C_N^2 = (79 \times 10^{-6} P/T^2)^2 C_T^2 \qquad (3)$$

where P is the atmospheric pressure in millibars, and T is the temperature in kelvins. Equation (3) ignores a contributing factor that depends upon water vapor concentration. This is a good approximation for optical wavelengths under dry, non-maritime conditions [Ref. 11] such as those present at AMOS.

As mentioned previously, the spatial coherence length, r_o, is the second optical turbulence parameter. It represents the magnitude of the integrated,

optical-turbulence present. It depends on the integral of C_N^2 over the distance in question [Ref. 11]. For a plane wave,

$$r_o = 2.1 [\ 1.46 k^2 \int_o^L C_N^2(z)\, dz\ ]^{-3/5} \qquad (4)$$

where k is the wave number ($2\pi/\lambda$), and L is the optical path length along the vertical directon. Vertical path coherence lengths vary widely between observation sites. Historically r_o values can range from a few centimeters for a poor site to approximately 30 cm for a world class site. The following sections present data in the form of coherence lengths integrated over several different optical path lengths. In comparing r_o's between sites it is important to realize that the atmospheric turbulence above the site is not the only variable that degrades seeing ability. Of equal importance are the artificially induced conditions surrounding and within a facility [Ref. 12]. Some of the more prevalent of these sources are ventilation systems, electrical equipment, and convective heat from surrounding buildings, tarmacs, and optical components.

B. ECHO-SOUNDER OPERATION

Acoustic echo-sounders use a transmitted pulse of acoustic energy to investigate the properties of the atmosphere in much the same way as a ship-borne sonar detects the presence of a submarine. The temperature structure of the atmosphere backscatters a portion of the transmitted energy that the echo-

sounder receives. The echosonde equation, also known as the radar equation, relates the scattered acoustic signal to a number of atmospheric and instrumental parameters. This relationship, based on work by Tatarski [Ref. 10], and discussed by Neff [Ref. 2] for adaptation to an echo-sounder is,

$$P_R = P_T E_R E_T \, (c\tau/2) \, \{e^{(-2\alpha R)}\} \, \{\sigma_o(R, f)\} \, \{AG/R^2\} \qquad (5)$$

where,

- P_R is the acoustic power returned form a range R.
- P_T is the acoustic power transmitted at frequency f.
- E_R is the efficiency in converting from acoustic to electrical power.
- E_T is the efficiency in converting from electrical to acoustic power.
- τ is the length of the acoustic pulse (sec).
- R is the range to the scattering volume (meters).
- c is the local speed of sound (m/s).
- A is the area of the antenna (m^2).
- G is the effective aperture factor for the antenna.
- exp(-2αR) is the round trip power loss, where α is the average attenuation factor over the path.
- σ(f) is the scattering cross section per unit volume.

As mentioned in the previous section, the acoustic sounder measures atmospheric turbulence, C_T^2, values from the scattering cross section, σ. Tatarski

[Ref. 10] shows the backscattering cross section is proportional to C_T^2 through the following relationship,

$$\sigma(R,f) = 0.0039\ k^{1/3}\ (C_T^2/T^2) \tag{6}$$

where,

- T is the absolute temperature in kelvins,
- k is the acoustic wave number $= 2\pi/\lambda$,
- λ is the acoustic wavelength.

This is the case only for backscattered acoustic energy, that is, energy scattered through an angle of π. For other angles, the amount of energy scattered depends upon the velocity structure parameter of the atmosphere [Ref. 10]. Combining Eqs. (5) and (6), and solving for C_T^2 gives,

$$C_T^2 = \left\{\frac{2P_R}{0.0039P_TE_TE_RAG}\right\}\frac{T^2}{k^{1/3}}\left\{\frac{P_R}{(ct)\,(P_T)}\right\}R^2\ e^{(2\alpha R)} \tag{7}$$

Several of the factors appearing Equation (7), such as E_T, E_R, G and α, are difficult to determine accurately. Therefore, a certain degree of error exists with an acoustic sounder that must be dealt with when calibrating such a device. The following section discusses these effects.

1. Acoustic Sounder Calibration

The advantages of an echo-sounder lie in its simplicity of operation, portability, and its ability to map the spatial distribution of turbulence. Regretfully,

calibration of the data from an acoustic sounder is complex. A more common means of measuring temperature variations as a function of altitude is through the use of high speed temperature probes. Mounting these probes at specific heights along a rigid tower can provide direct temperature measurements. However, such devices lack the portability of the echo-sounder and are costly to build and to maintain.

Historically, acoustic echo-sounders are considered to be semi-quantitative devices. Inherent uncertainties include such factors as difficulties in measuring transducer efficiencies, determination of the effective aperture factor, G, and in obtaining a precise attenuation factor, α, over the optical path length in question. As with any experimental system, judicious selection of equipment, close monitoring of operating parameters, and strict experimental procedures will minimize these effects.

Figure 2 is a plot illustrating the dependence of the attenuation factor on both water vapor pressure and frequency. Determining a precise value for the atmospheric attenuation factor as a function of altitude is extremely complicated. Tower mounted humidity probes could measure the height dependence but then the portability benefit of the sounder is lost. In order to solve this problem an approximation must be made. One such method is to take a ground level reading and to assume it to be the average value over the path length. Since this project was concerned with low-altitude measurements, this approach was taken.

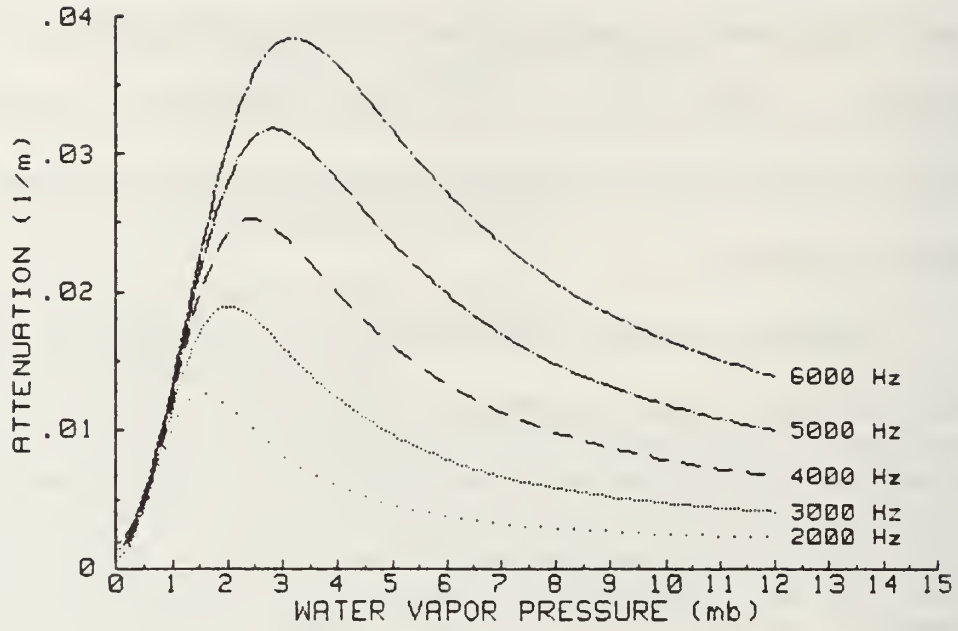

Figure 2. Attenuation vs Water-Vapor Pressure for Temperature = 20°C and Atmospheric Pressure = 1013 mb.

The inner and outer scales determine the dimensions of the thermal turbulence. These refer to the smallest and largest scale sizes of the turbulence structure, respectively. Typical values for these parameters range from millimeters to hundreds of meters. These happen to be of the same order of magnitude as acoustic wavelengths. Acoustic sounders measure optical turbulence effectively because of this match between acoustic wavelength and characteristic scale size, combined with the fact that the acoustic scattering cross section is orders of magnitude larger than the optical scattering cross section.

As mentioned, one of the more common means of measuring thermal turbulence profiles is through the use of tower mounted temperature probes. An acoustic sounder may be calibrated by positioning it in the vicinity of such a tower and comparing simultaneous measurements. In doing so, the difference in scale sizes measured by each device will introduce some degree of discrepancy between the two sets of readings.

An acoustic echo-sounder, unlike a temperature probe system, is susceptible to inner scale errors due to the finite dimensions and wavelength spectrum of its acoustic pulse. Tatarski [Ref. 10] shows that the Bragg scattering expression $n\lambda = 2d \sin\theta$ determines the turbulent scale size probed by an acoustic sounder. For the 5 kHz acoustic sounder used here, this scale corresponds to 3.4 cm, which is between the inner and outer scales of turbulence. As an illustrative example consider the set of conditions such that the mean wind speed is 6 m/sec. The corresponding inner scale length, l_o, of the turbulence present for these winds was calculated by Ochs and Hill to be $\approx$ 3 mm. [Ref. 13] using,

$$l_o = [\frac{\nu}{\epsilon}]^{1/4} \qquad (8)$$

where ν is the kinematic viscosity and ϵ is the turbulent dissipation rate. Figure 3 is a plot of the spatial power spectrum of temperature fluctuations, Φ_T, versus scaled wave number, $\kappa\eta$ taken from Reference 14 (both are dimensionless). The

dotted line represents the Kolmogorov spectrum including dissipation for velocity fluctuations. The solid line is the theoretical model of Hill [Ref. 14] and corresponds to the spectrum of temperature fluctuations. The most significant feature of this plot is the bump present in the Hill model. This occurs at the edge of the inner scale of turbulence and arises from residual temperature gradients as the turbulence enters the viscous convective region. Viscosity dissipates the kinetic energy of the turbulence while temperature gradients diffuse at a slower rate. The scaled wave number consists of κ, which is equal to 2π/scale length, and η, which is equal to $l_o/7.14$ (for air). Using the sounder wave length of 3.4 cm, the calculated scaled wave number is approximately 7.8×10^{-2}. From Figure 3 it is evident that this point lies along the viscous-convective bump and corresponds to a Φ_T of $\approx$ .88. This translates to an enhancement of $\approx$ 20% compared to the other model. The position of this bump depends on the inner scale which is sensitive to the local dissipation rate ϵ. From this error source alone, C_T^2 values measured by the acoustic sounder at 5kHz should be approximately 20% greater than those recorded by a temperature probe. Of course, this calculation was conducted only for a specific inner scale. This value of $\approx$ 3 mm was chosen since it was representative of the conditions encountered at AMOS.

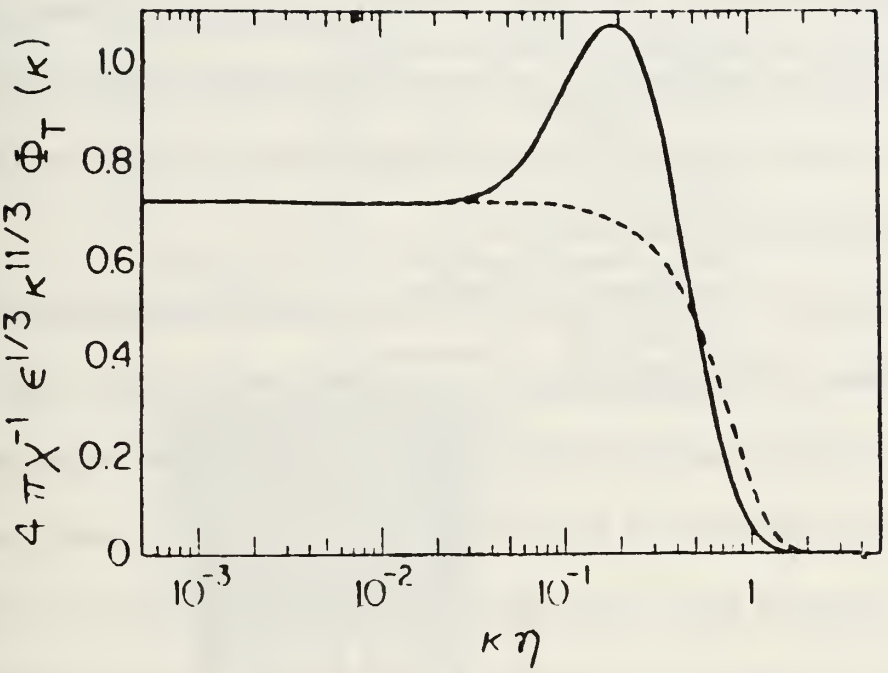

Figure 3. Spatial Power Spectrum, Φ_T, of Temperature Fluctuations in Air (both axes are dimensionless). The Solid Curve is the Accurate Model; the Dashed Curve is the Tatarski Model. (from Ochs and Hill [Ref. 13])

III. EQUIPMENT

A. OVERVIEW

The majority of the components of the echo-sounder used in this project were identical to those described by Moxcey [Ref. 6] and McCrary [Ref. 9]. The system as a whole has been used by Walters over the past 4 years for a variety of projects. The hardware has undergone minor refinements during this time, while the software has undergone three major revisions. Figure 4 is a schematic of the entire echo-sounder system.

The acoustic heart of the system is a 19 element hexagonally shaped array of piezo-electric speakers. Figure 5 is a sketch of this array. The individual elements are Motorola KSN 1005A speakers and were chosen for their resonance properties as well as their high efficiencies in both the transmit and receive modes. The array beam lobe pattern was studied extensively in an anechoic chamber and found to be highly directional [Ref. 6]. The experimentally determined parameters associated with this transducer antenna array are:

- efficiencies: $E_T = E_R = 0.5$,
- resonant frequency = 5kHz,
- area of antenna = A = 0.0866 m^2,
- effective aperture factor = G = .4.

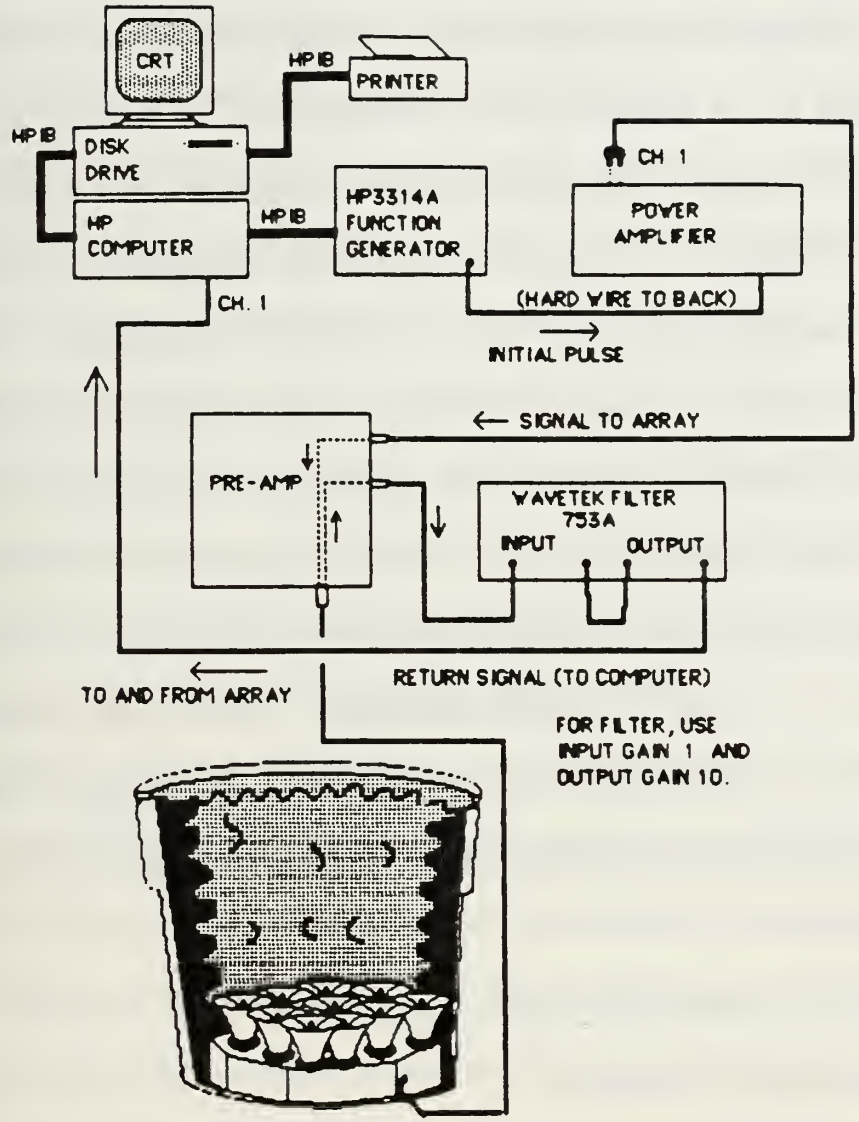

Figure 4. Echosounder System Set-up.

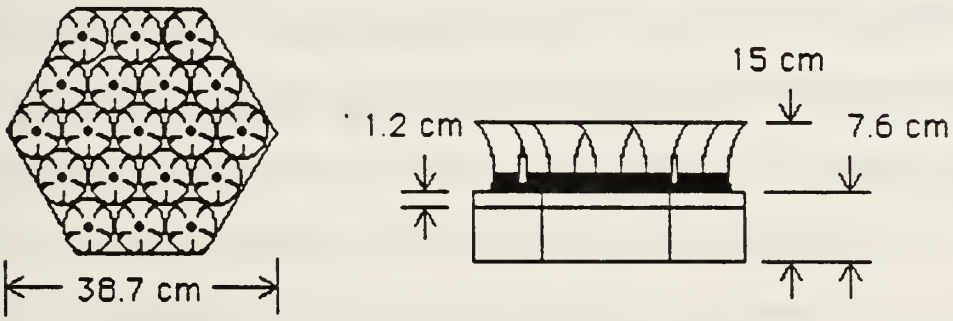

Figure 5. Dimensions of Acoustic Array

To accomplish the project's mission, the sounder had to operate in a mode that would provide high-resolution data over the 0 to 100 meter altitude range. From Figure 2, it is apparent that the attenuation of an acoustic signal by the atmosphere increases with frequency. This suggests using a low operating frequency. However, the resolution of the sounder depends on wavelength size and is inversely proportional to the frequency. Additionally, driving the transducers at their resonant frequency of 5 kHz provides a high efficiency of nearly 50%. However, exploiting this resonance condition also has a slight drawback. After transmitting the 5 kHz pulse, the transducers continue to ring momentarily as does any oscillator when driven at resonance. The effect of this ringing was to create a brief post-transaction period when reception was impossible. The consequence was a minimum range of $\approx$ 5-7 meters. The following acoustic pulse parameters were used in analyzing the 7.5 to 100 meter layer at AMOS.

- frequency of sinusoidal pulse = 5kHz,
- Pulse length = 75 cycles,
- Magnitude of Pulse = 40 volts,
- Resolution = $(c*\tau)/2$ = (.5)(75*340m/s)/(5kHz) = 2.55 meters.

Past experience has shown that this is an optimum choice of operating parameters.

B. RECENT UPGRADES

Upgrades have been made in the areas of computing power, mass data storage, Doppler processing and acoustic attenuation. The control of all components is now handled by a Hewlett-Packard 9836C P. C., vice the previous H-P 217. This is an upgrade over the previous system in that speed of operation has been significantly increased through the addition of a Newport Digital 33MHz 68020 control processing board. The standard H.P. 3.5" disk drive has been replaced with a Bering 600 megabyte optical disk drive. This enables storage of individual pulses of raw turbulence data which were previously recorded only as line printer plots. The massive storage capability of the optical disks provides the ability to record several weeks of data on the same disk.

The last equipment modification is in the preamplifier. This change was made in order to avoid R.F. interference problems that were experienced earlier [Ref. 6]. The new preamp can be operated at several gains (measured to be 987, 1906, or 3895) and was designed by D. L. Walters and built by D. Glarowicz. For the data presented in this paper, a gain of 1906 was used throughout.

The computer software provides instrument control and real time data processing. Acoustic pulse length, number of cycles, pulse strength, filtering of obvious noise signals, data storage and data display are all functions controlled by the sounder data collection program. This software, [Appendix A], has undergone numerous revisions since the first version was drafted in 1987 by Wroblewski and Walters [Ref. 8]. Of these changes, three stand out as being

especially significant. The first of these involves the addition of a Doppler algorithm. This was written by D. L. Walters and investigated by McCrary [Ref. 9]. It provides for the collection of horizontal wind speeds by tilting the sounder slightly off the vertical and measuring the Doppler shift in the backscattered signal. This enables additional turbulence information regarding the velocity field of the atmosphere to be recorded. The second significant software change involves the gain of the reflected signal. Previously, a constant gain of approximately 100,000 was used to amplify the reflected signal over the entire range of altitude concerned. This often caused some overloading on the filter during periods of excessive, low-altitude turbulence, but was necessary in order to obtain measureable return from heights of 100 m. Now there is a gain change accomplished during acquisition. From 0 to 30 meters, the Infotek AD-200 analog to digital converter provides unity gain to the signal received from the filter. From 30 to 100m, the AD-200 imparts an additional gain multiple of 10. This extends the operating range without causing an overload at short ranges. Numerically, this translates to the following gains. Over the altitude range of 0 to 30 meters, the total gain = (pre-amp gain)(filter gain) (soft ware gain) = (1906)(10)(1) = 19,060. Over the altitude range from 30 to 100 meters, the total signal gain is = (1906)(10)(10) = 190,600. A 16 bit A-D converter would alleviate the need for such a gain change, but at the time of this project none was readily available. The third of these software refinements involves a modification to the water vapor acoustic attenuation algorithm, based on a recent publication by H. Bass [Ref.

15]. The effect of this modification is to significantly change (by as much as a factor of 2) the absorption coefficient at very low and very high humidity values as compared to the previous algorithm. In the middle humidity range, there is little change from the previously determined value [Ref. 2].

IV. RESULTS

A. CALIBRATION

1. Equipment

Remote sensors must be calibrated to provide accurate data. In the case of acoustic echo-sounders, this is usually accomplished through the use of temperature probes positioned along a tower at specified heights. This provides a means for obtaining an independent C_T^2 vs. altitude profile for comparison. Ideally, probes are positioned along the tower over the entire altitude range of the sounder being calibrated. However, due to cost, equipment, and time constraints, the calibration conducted for this project consisted of a single point comparison at heights of 10 and 14 meters. These heights were chosen for two reasons. First, they were consistent with reasonable pedestal heights for the AMOS 4m facility. Secondly, the lower altitude region was of special interest since it allowed comparisons with optical data from the 1.6m CIS and 1.2m Hughes telescopes. This calibration experiment was conducted on the roof of Spanagel Hall, Naval Postgraduate School, Monterey, California. Figure 6 shows the equipment positioning for the calibration. To conduct an accurate calibration, the sounder and the temperature probe should be measuring the identical atmospheric volume. However, since the probe itself will scatter acoustic energy, it must be offset from the sounder. As depicted in Figure (6), the predominant wind direction

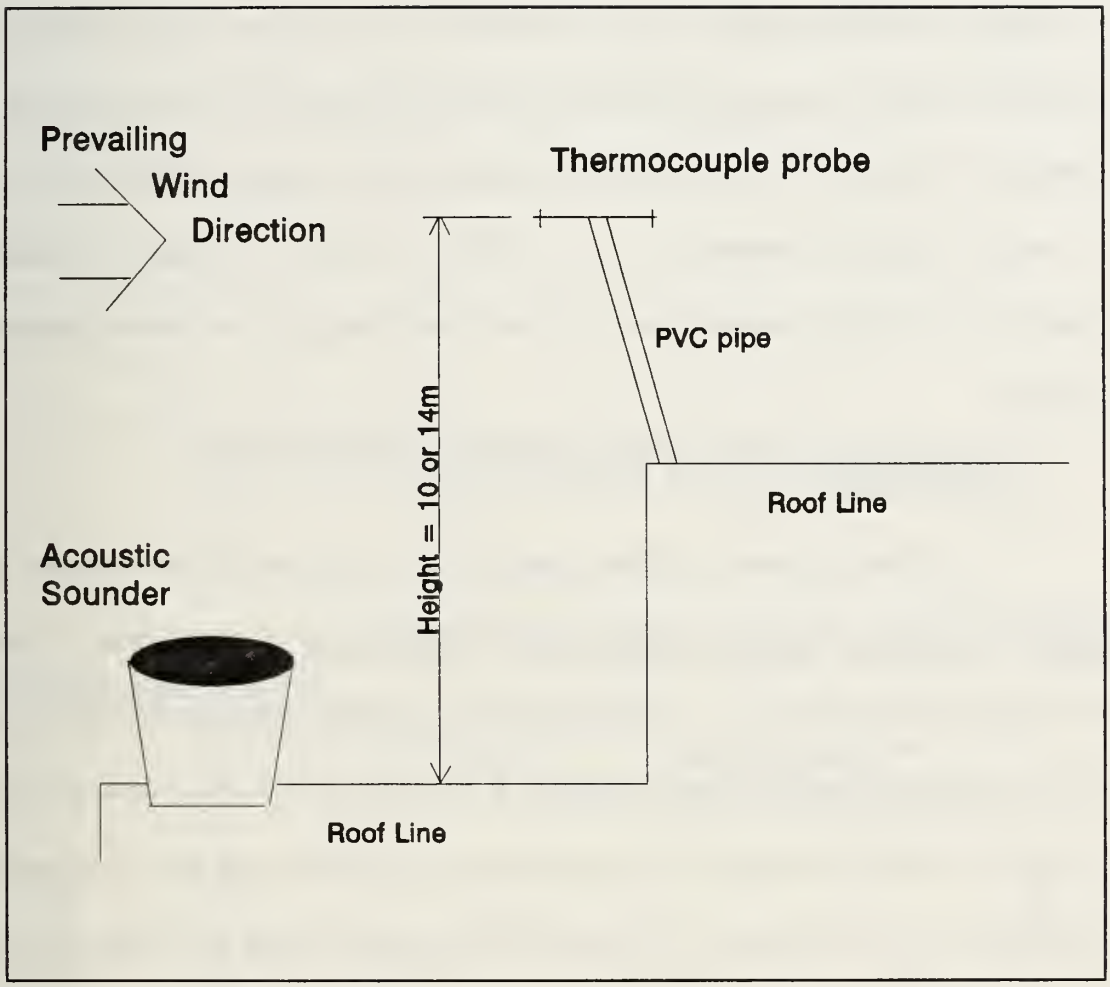

Figure 6. Equipment Positioning for Acoustic Sounder Calibration.

during the calibration would appear to allow both devices to measure the same C_T^2, while minimizing building or probe induced turbulence contributions.

The differential thermocouple probe used is one which was designed by Walters and investigated by Olmstead [Ref. 15]. It consists of two 0.00254 cm. diameter Copper-Constantan thermocouples rigidly attached to the ends of a 1 meter aluminum rod. This comprises a device that is capable of determining a C_T^2 value within a sensitivity of $\approx 10^{-6}$ ($K^2/m^{2/3}$). Figure 7 contains a baseline measurement of this sensitivity taken in the Naval Postgraduate School anechoic chamber.

2. Findings

Data were taken on three days, Oct. 10, 23, and 24, when wind and weather conditions were appropriate. Initial data taken at 10 m indicated a major discrepancy between the C_T^2 values measured by the the sounder and the probe. As discussed in the Background section, it was anticipated that there would be a 15-20% difference between the two values due to scale size effects. However, comparing the two data sets revealed that the sounder data was a factor of 2-4 times smaller than the thermal probe results. Additionally, there were several other trends in the data which were not understood. Figures 8, 9, and 10 contain these results. Figure 8 contains the only set of data taken at a height of 10 meters. Notice that the data points in this plot appear to be in closer agreement than those of the other two. The purpose for taking measurements at two altitudes was to ascertain some measure of the dynamic range of the sounder.

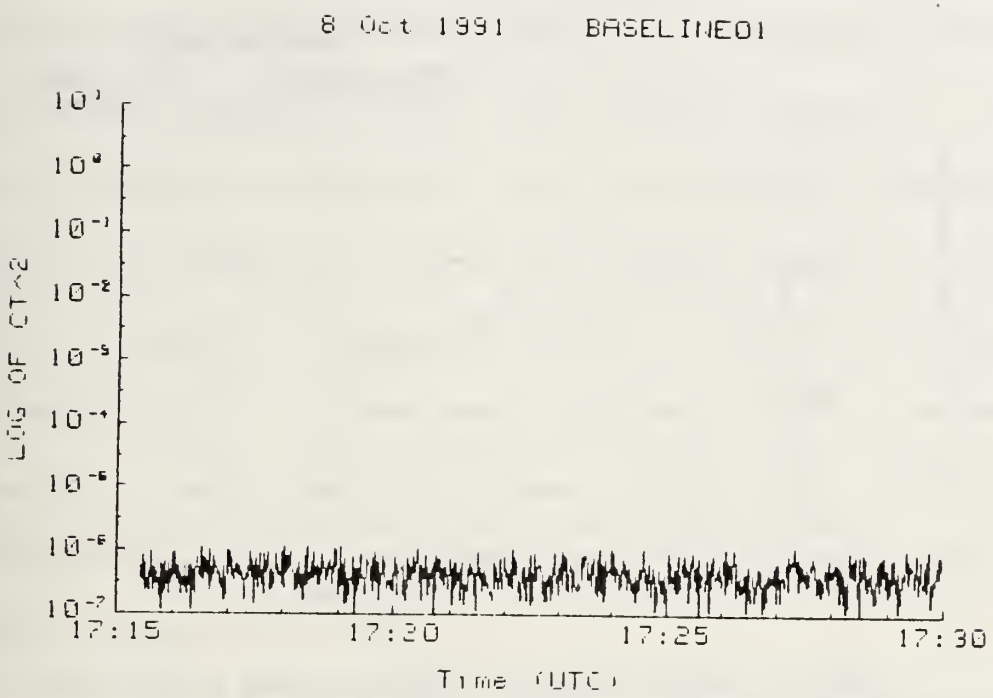

Figure 7. Differential Thermocouple Probe Sensitivity Baseline Sensitivity Measurement.

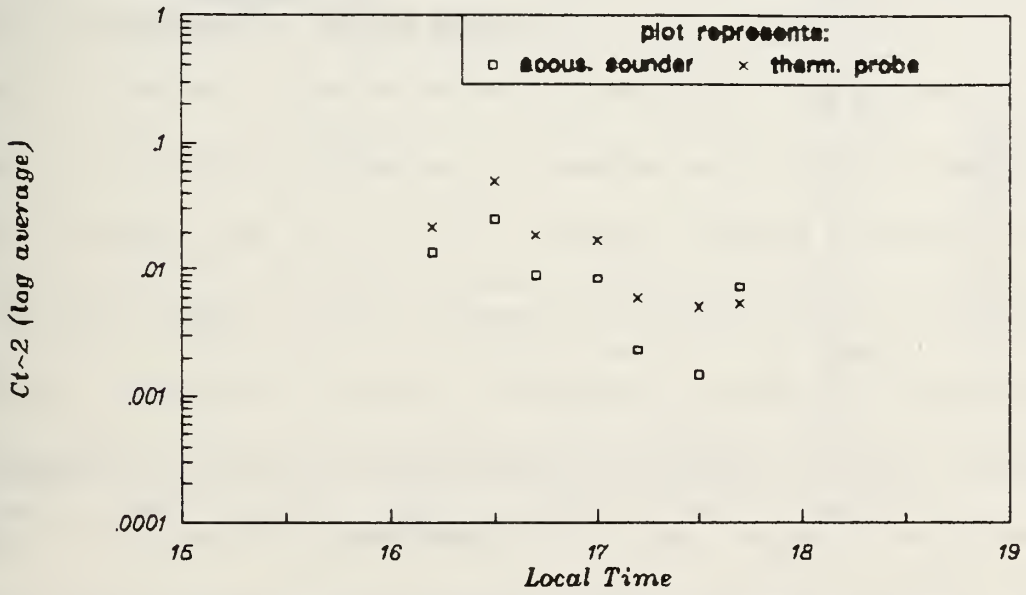

Figure 8. Acoustic Sounder Calibration Data for 10 October, 1991 at a Height of 10m.

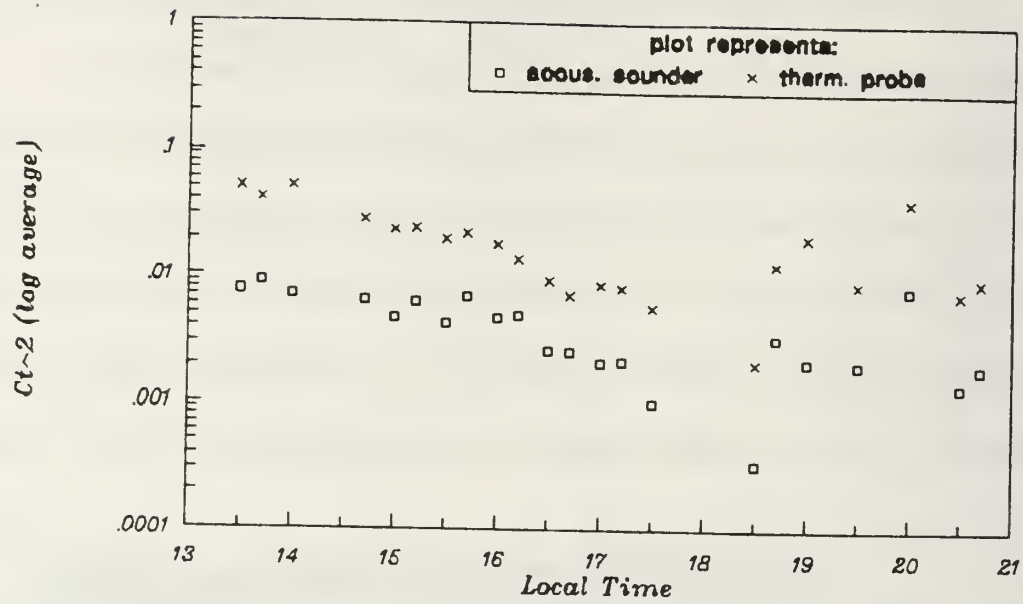

Figure 9. Acoustic Sounder Calibration Data for 23 October, 1991 at a Height of 15m.

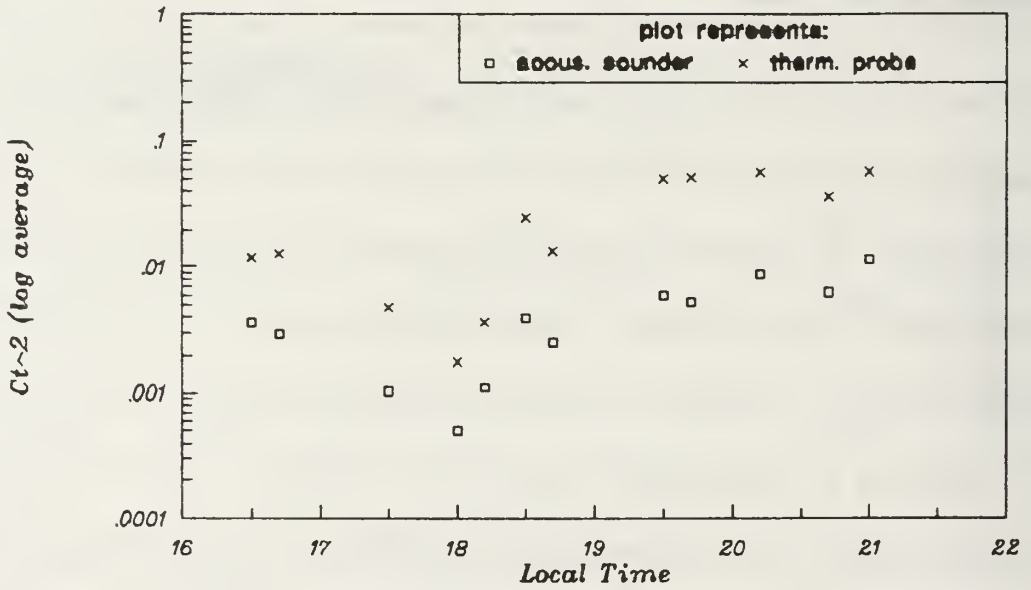

Figure 10. Acoustic Sounder Calibration Data for 24 October, 1991 at a Height of 15m.

The fact that a noticeable difference existed over such a small range of altitudes was intriguing. Initial investigation into the cause of these discrepancies centered around possible hardware causes. This included replacement of both thermocouples, detailed measurements of both the sounder and probe amplifier parameters, and replacement of several lower efficiency transducer elements. Discovering no significant changes, the investigation shifted towards possible contamination sources. Was there some contamination of the measurements from building induced effects at the lower altitude? Upon reviewing the equipment positioning, and observing the trends in the prevailing winds, the following conclusions were made.

To record data at a height of 10m the thermocouple probe was positioned over the sounder at nearly the same height as the upper roof line in Figure 6. As discussed, the set up was chosen so that the prevailing winds would allow both devices to measure the same uncontaminated atmospheric volume. However, upon closer analysis the 10 m location was found to be sensitive to eddy formation near the roof. This artificially induced turbulence would undoubtedly cause the sounder to measure different C_T^2 values at 10m than at 15m when compared to the probe. This reasoning explained the discrepancy between the 10m and 15m sounder data but still didn't explain the persistent factor ≈ 4 between the two devices in the 15m data. Additionly, the 23 and 24 Oct. data still contained other inconsistencies that required explanation.

Both days contained differences between successive sets of data that varied by a factor of two or more. To explain these, some interaction between the building and the wind-borne turbulence structure was suspected. The observed weather conditions for each day were similar; clear and sunny in the morning, gusty afternoon winds becoming more directional as the afternoon passed, and becoming near calm near sunset (approx. 17:30 local time). Accurate calibration required that the winds come consistently from the ocean. Searching for trends in the data revealed that the measurements differed by a consistent factor of four during several hours of the day. Upon reviewing the weather observations, the winds blew steadily from the ocean during these hours. Prior to these periods the winds were gusty. Following these periods the winds became light and variable. Both of these conditions would influence the turbulence detected by both devices. The atmospheric volume each was measuring was not only different but was also artificially contaminated. Eddying effects as well as convective interaction with the rooftop and exterior building walls during these periods invalidated the measurements. Based on these arguements, the only data from the two days considered trustworthy were those taken during the mid-afternoon hours when sea breeze wind conditions prevailed. Subsequently, a detailed review of the sounder operating software was conducted. The intent of this was to find an explanation for the consistent factor of 4 ratio between the two devices during these valid periods.

In programmimg Equation 7 into the data processing code, an error was discovered in the placement of the receive and transmit efficiency factors. This mistake lowered the measured C_T^2 sounder values by a factor of four. By comparing the sounder and probe calibration data, it was found that the sounder measured a C_T^2 value $\approx$ 3.8 times lower than the probe. This factor of 3.8 is consistent with the factor of four coding error after including the correction for the inner scale bump in Figure 3. The 3.8 value was used as a calibration for all the AMOS data, and is appropriate for all data previously recorded by this instrument. Figures 11 and 12 show the corrected plots of the calibration data from 23 and 24 Oct. 1991.

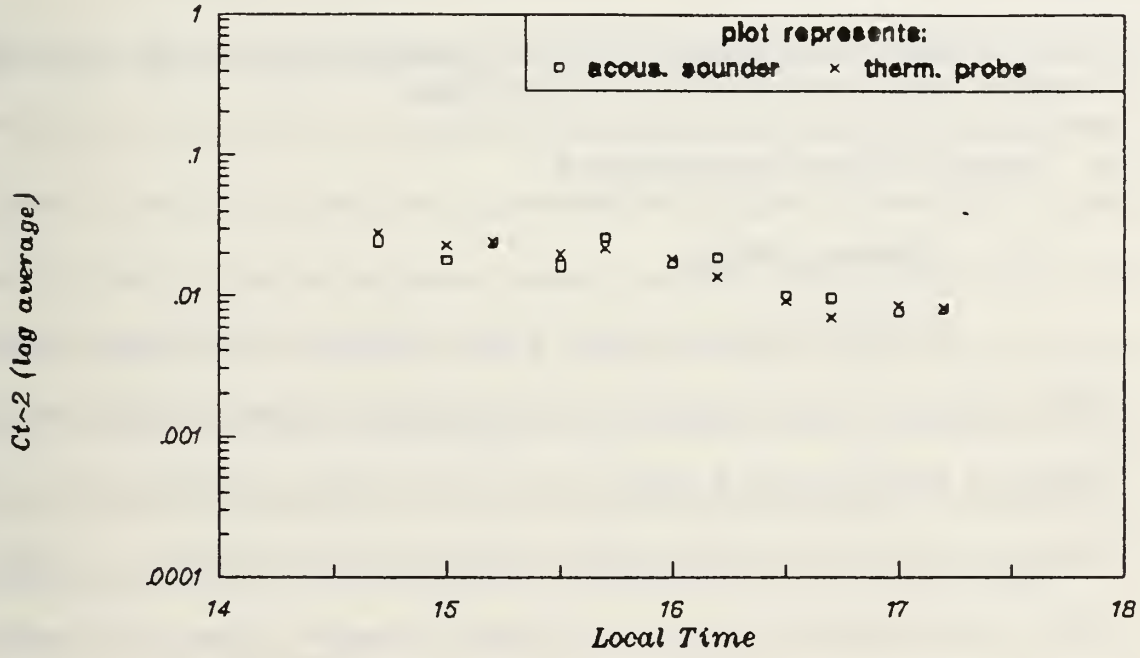

Figure 11. Acoustic Sounder Calibration Data for 23 Oct., 1991 Corrected Using Factor of 3.8 x Sounder Data.

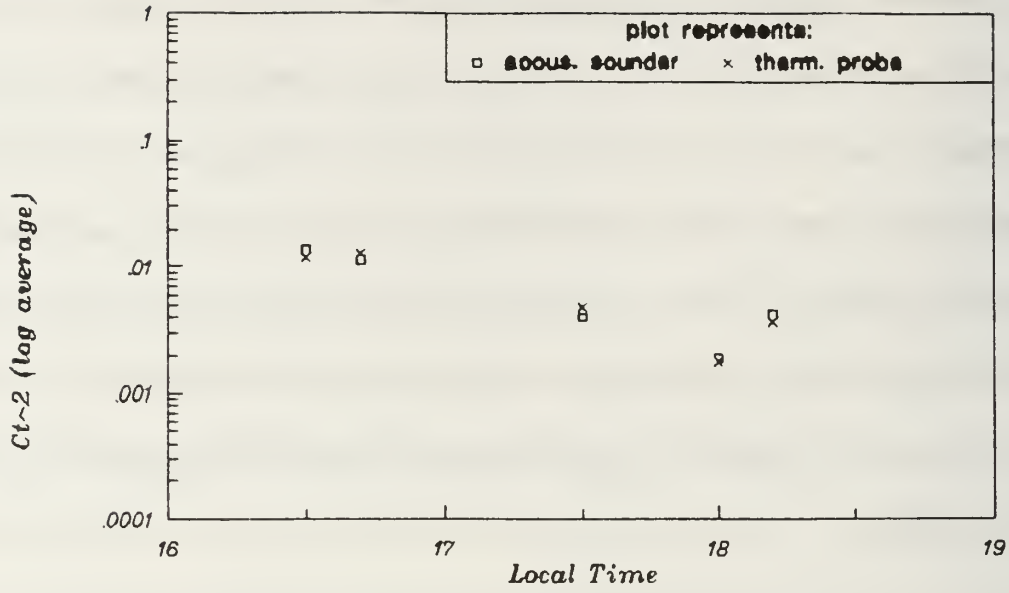

Figure 12. Acoustic Sounder Calibration Data for 24 Oct., 1991 Corrected Using a Factor of 3.8 x Sounder Data.

B. AMOS FIELD MEASUREMENTS

1. Turbulence Profile

The AMOS mission required a high-resolution, low-altitude turbulence profile. Hence, the sounder operating parameters were chosen to collect accurate turbulence readings over a range of 7.5 to 100 meters. As discussed in the Equipment chapter, the resolution of the sounder in this mode was $\approx$ 2.6 meters, which was considered ideal for the ranges in question. Some representative examples of the data taken at Site A are given in Figures 13 through 16. The uppermost of the plots displayed in each set is a time vs. altitude plot of the

backscattered signal received by the sounder. The intensity of the signal received is proportional to the degree of shading of the plot. The lower of the two plots in each example is a 15 min. time-averaged plot of the measured C_T^2 value vs. altitude. Most of the data was for Site A, the primary proposed site under consideration. In comparing these four examples, it is evident that the conditions present varied considerably from day to day. The profiles illustrated in Figures 13 and 14 are representative of the typical conditions observed at AMOS. Though Figures 15 and 16 are atypical, it is interesting to note that even during these high turbulence periods there is little if any signal return above 90 meters. Appendix B contains additional examples of sounder data plots.

Moving the acoustic sounder antenna between sites A and G on 6 different occasions provided a rough intercomparison between the two locations. This was done to reveal any possible gross differences between the two sites. Figures 17 and 18 contain a few representative examples of these Site G plots. No significant differences appeared between the two locations even though Site G was located 10 m lower than Site A and on the back side of the mountain peak. Although this was unexpected, it was consistent with observations of fog flowing over the mountain. The fog, and apparently the turbulent boundary layer, followed the contour of the mountain for moderate, 6-10 m/s wind speeds.

2. r_o vs. Altitude

As well as measuring the turbulent boundary layer profile, an equally important question was finding the relative contribution of the first 100 m to the

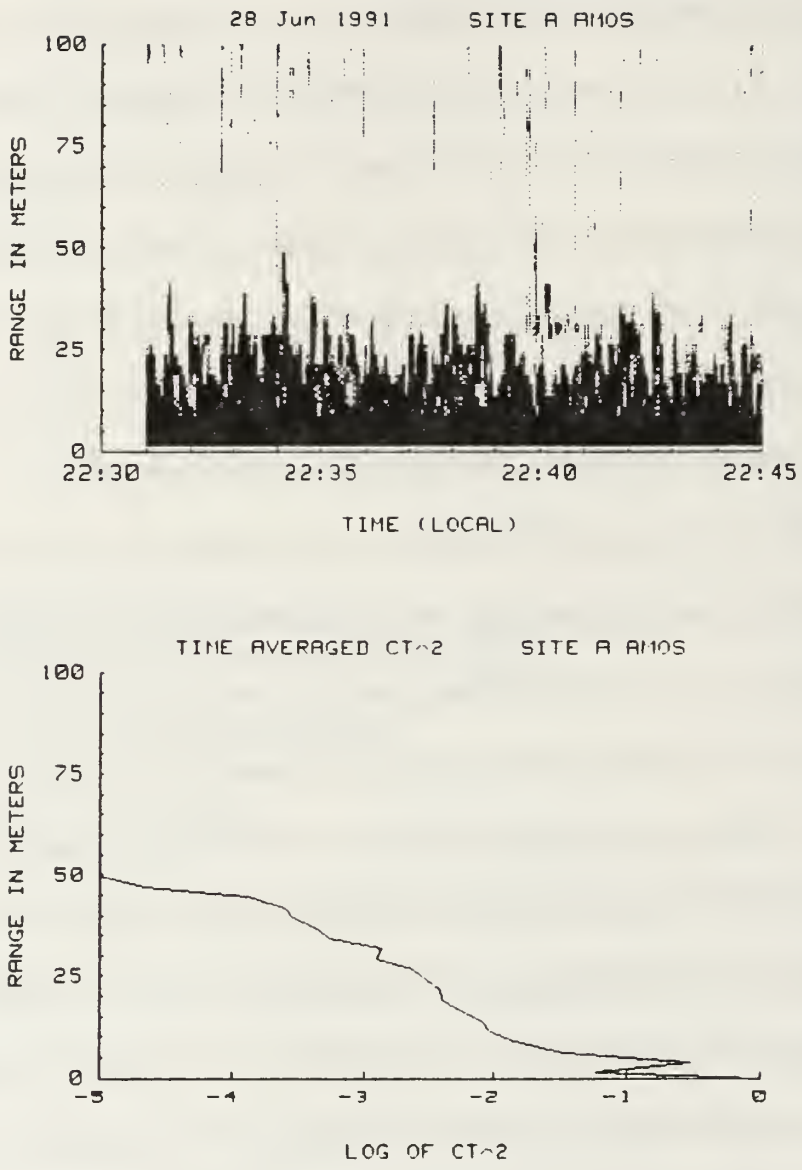

Figure 13. Sample #1 of Acoustic Sounder Data Plots.

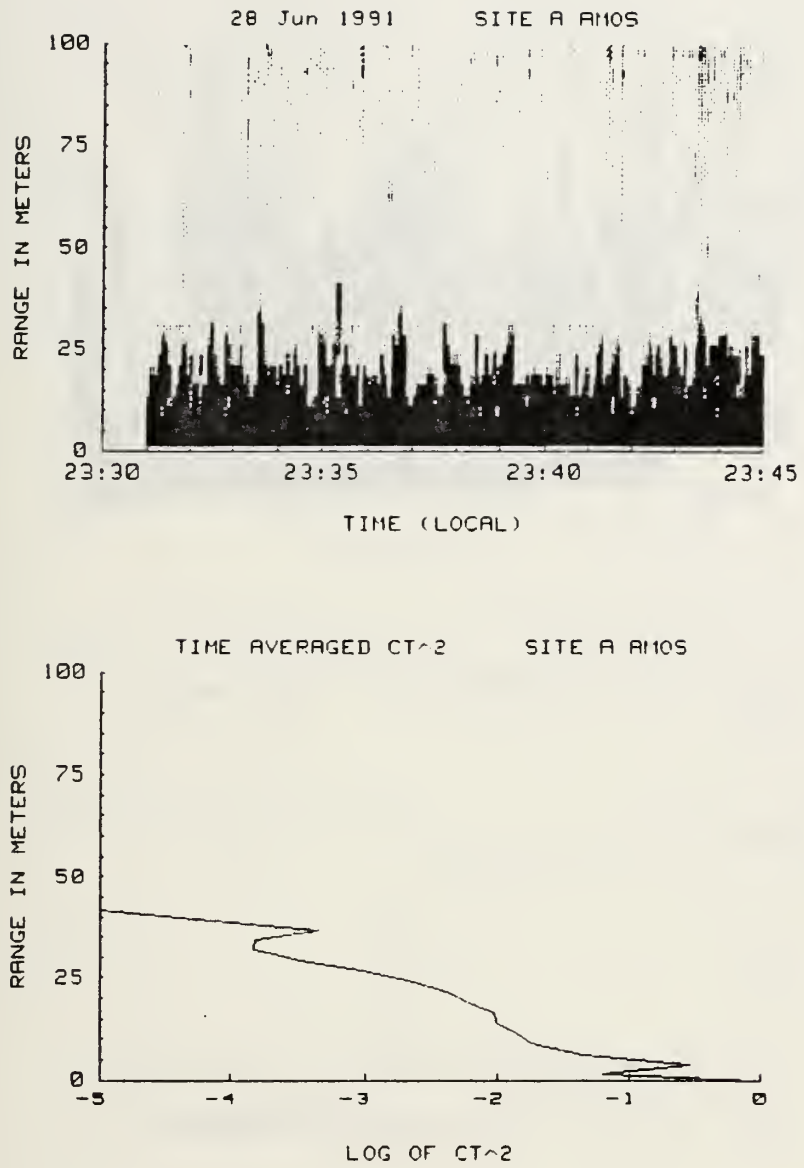

Figure 14. Sample #2 of Acoustic Sounder Data Plots.

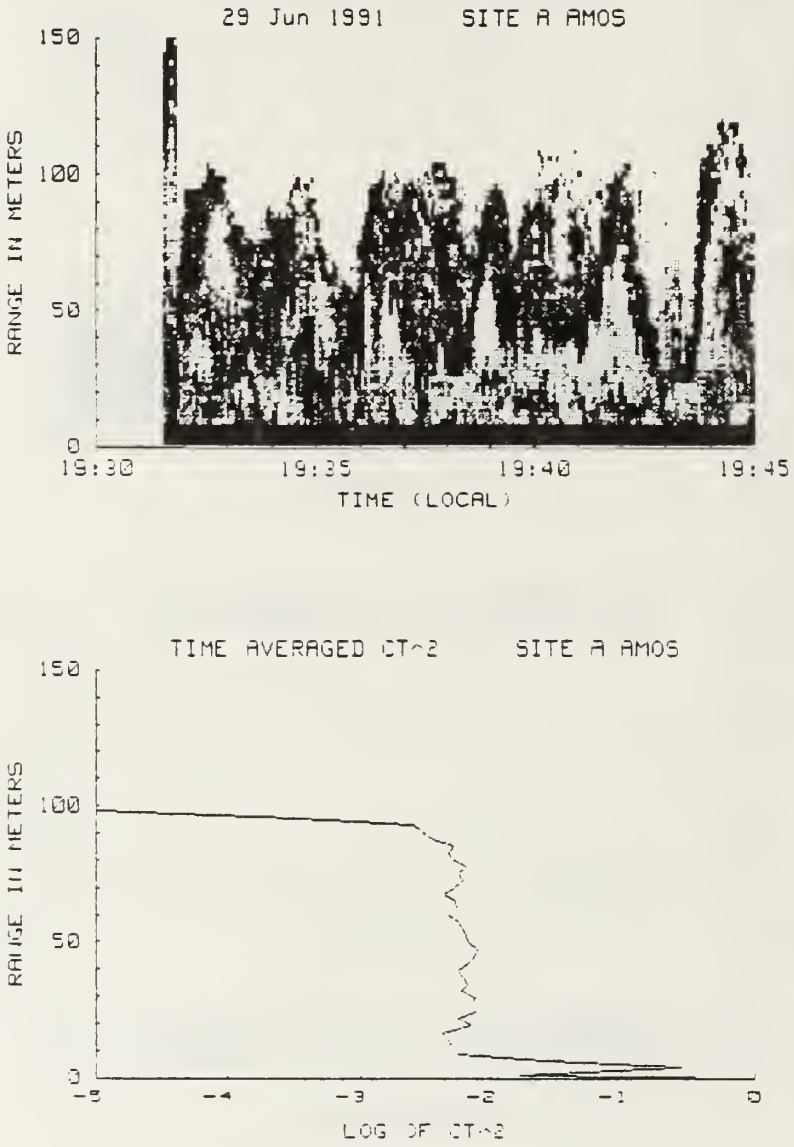

Figure 15. Sample #3 of Acoustic Sounder Data Plots.

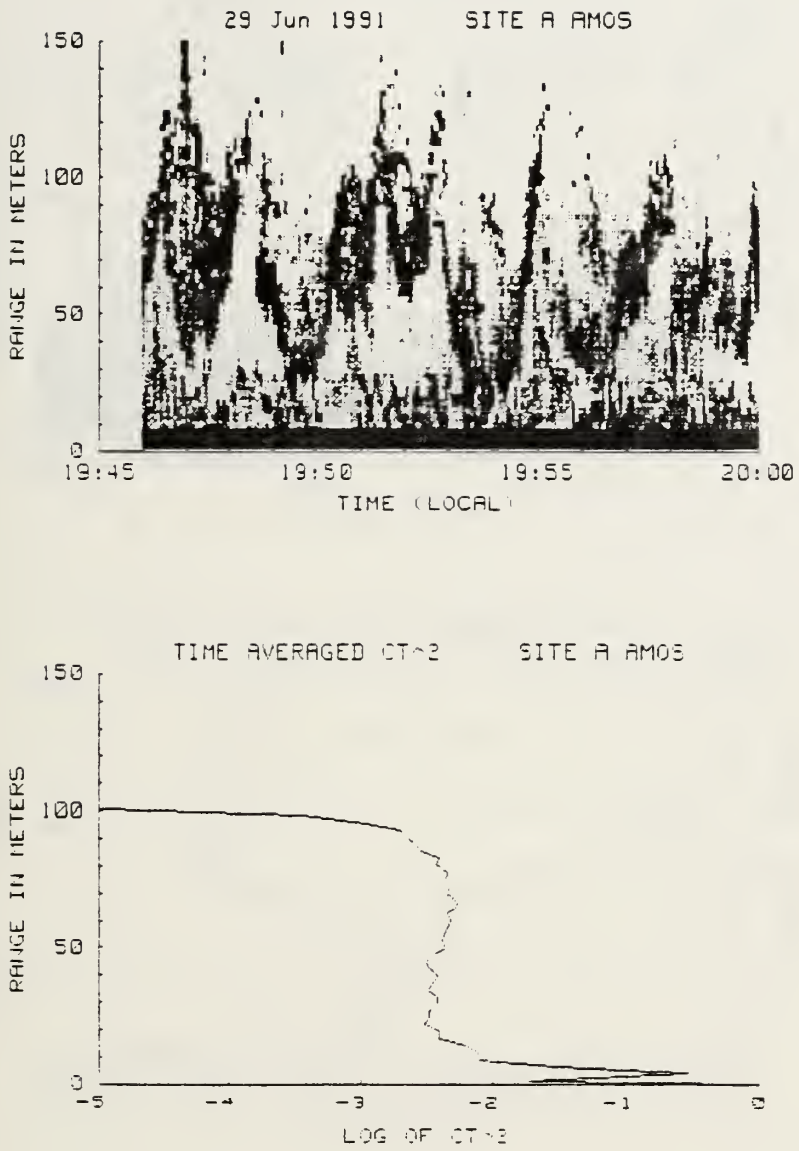

Figure 16. Sample #4 of Acoustic Sounder Data Plots.

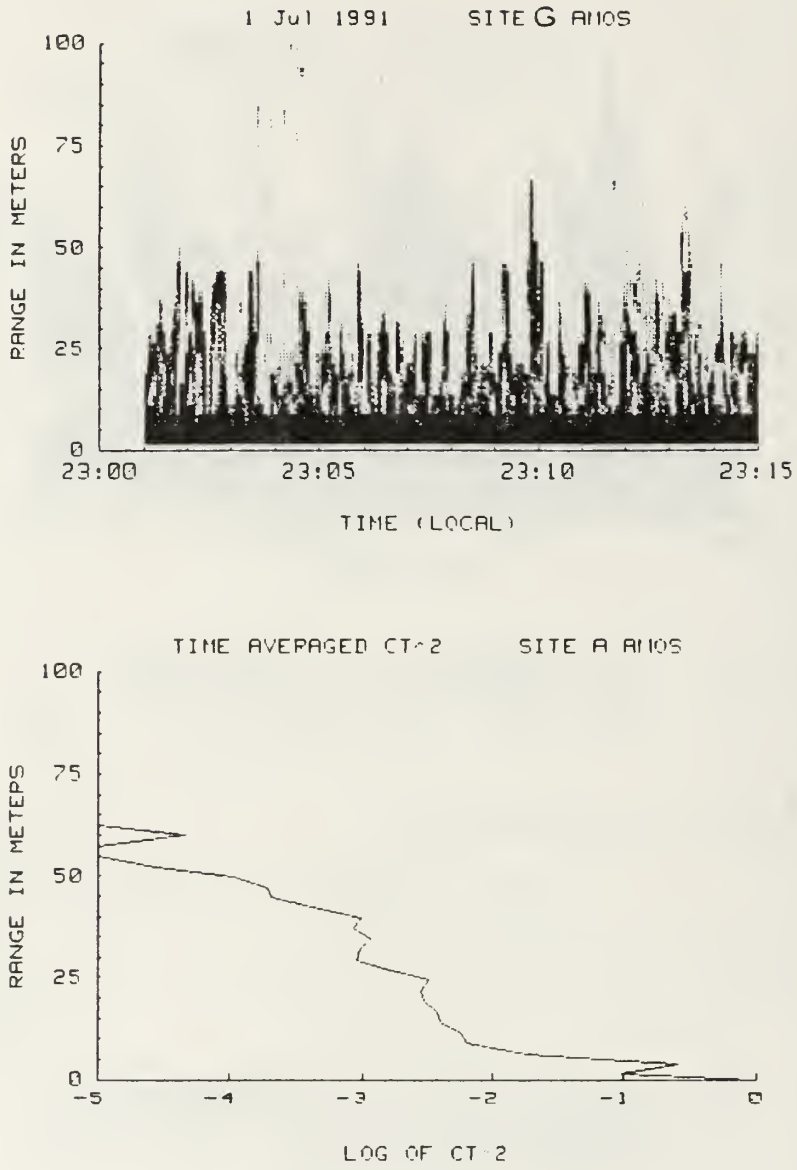

Figure 17. Example of Site G Acoustic Sounder Data Plot.

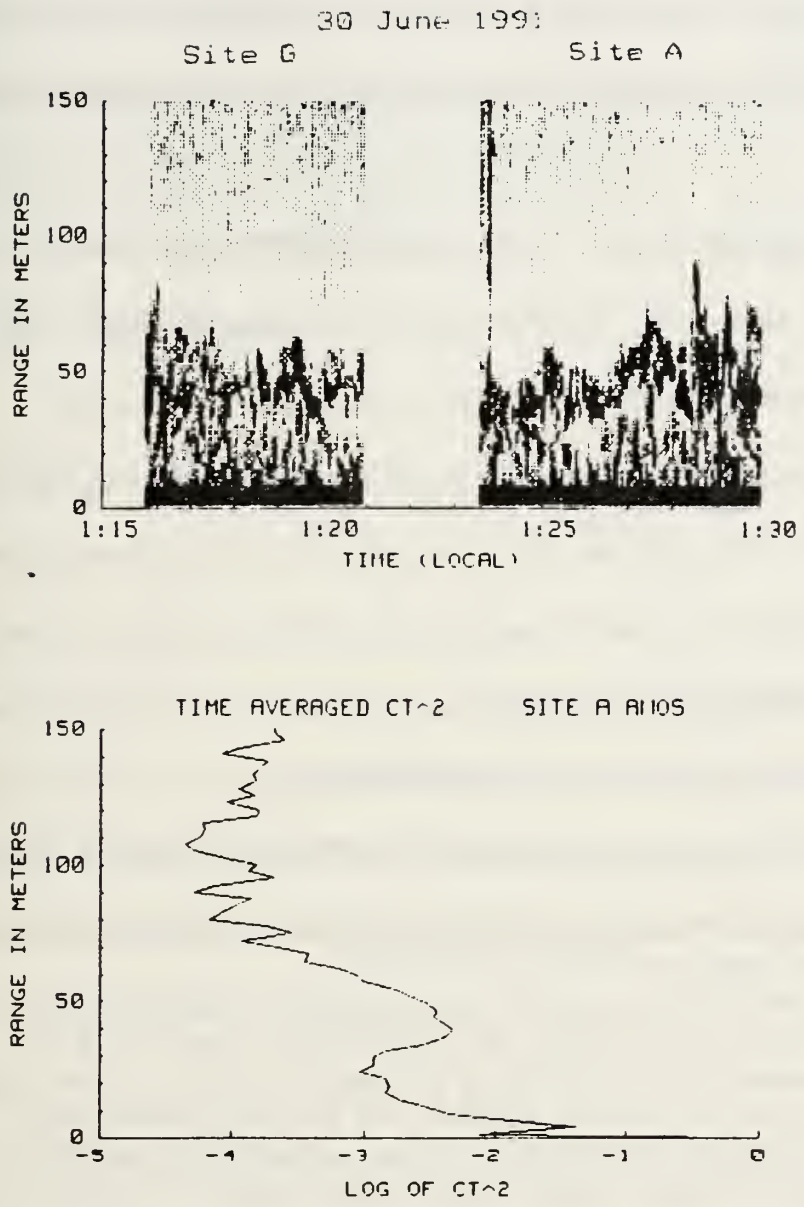

Figure 18. Comparison Plot of Sites G and A.

entire r_o integral. This information reveals the advantages of placing the 4 m instrument on a tower or pedestal and allows a tradeoff of optical quality vs. cost of a tower. Both the Kitt Peak and Mauna Kea telescopes are 4 m instruments with towers, 50 m and 20 m high respectively, that demonstrate the feasibility of this option.

Breaking Equation 4 into two separate integrals over the optical path length gives a relation for determining spatial coherence length, r_o, as a function of height, z, in the low altitude layer,

$$r_o = H* [\int_{7.5}^{100} C_N^2(z)\,dz + \int_{100}^{\infty} C_{n1}^2(z)\,dz]^{-3/5} \qquad (9)$$

where

- z is the height above ground,
- C_N^2 is the measured structure parameter,
- C_{N1}^2 is the structure parameter for the atmosphere above 100 meters,
- H is the product of all constants from Equation 4 for an optical wavelength of 500nm and is = 5.0647×10^{-9} ($m^{-6/5}$).

Equation 9 requires an approximation regarding the turbulence contribution from the second integral. The Canada-France-Hawaii Telescope, CFHT, located on Mauna Kea provides historical data to achieve this [Ref. 12]. Because CFHT is geographically close to AMOS, this data is representative of the seeing conditions above 4 km. Since CFHT averages 0.8 arcsec FWHM including its surface boundary layer, mirror and dome effects, a 20 cm coherence length

is reasonable for AMOS starting at 100 m above the surface. Figures 19 through 22 represent plots constructed using a 20 cm coherence length in Equation (9) for four different pedestal heights within the 7.5 to 100 m layer. Because of a combination of equipment malfunctions and rainy weather, reliable sounder data is missing for the evenings of 25, 27, and 30 June.

3. Comparison to Optical Data

a. AMOS Support

During the periods of sounder operation, both the 1.6m CIS and the 1.2 m Hughes seeing monitor at AMOS collected optical data for comparison. These data were in the form of stellar image full width at half maxima, FWHM, and provides a means for confirming the sounder results. Comparing the optical and acoustic data should reveal the presence of artificially induced turbulence within the 1.6 and 1.2 m facilities. Reference 12 is a recent paper discussing the effects of such turbulence at the CFHT. They discovered a significant amount of degradation from such factors as ventilation systems, wind turbulence across the dome, or inhomogeneous heating/cooling of the mirror itself. The following chapter addresses comments regarding the effects of such factors on the 1.6m device. To compare the optical and sounder results, the optical and acoustic data must be consistent.

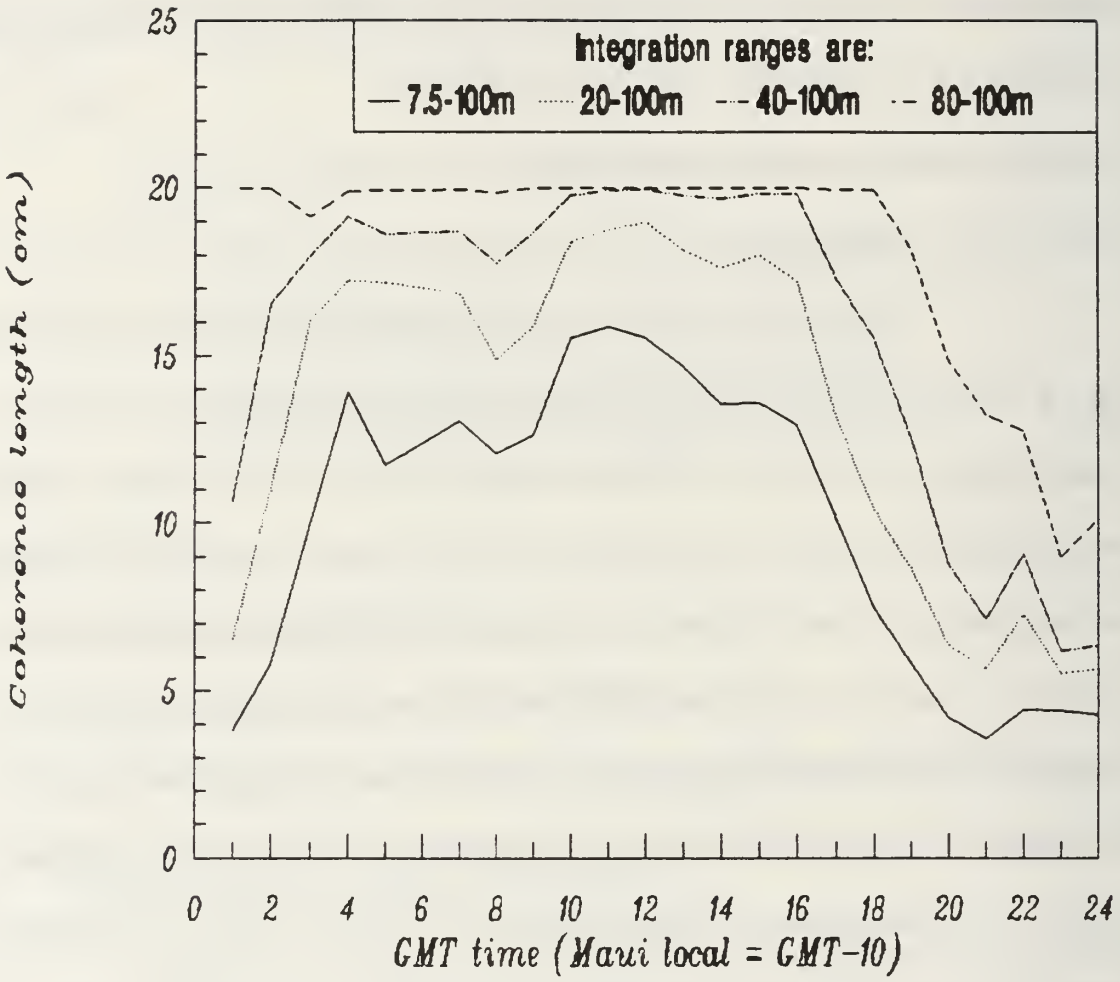

Figure 19. Acoustic Sounder Data for the Evening of 26-27 June 1991 Showing the Turbulence Layering Structure at AMOS.

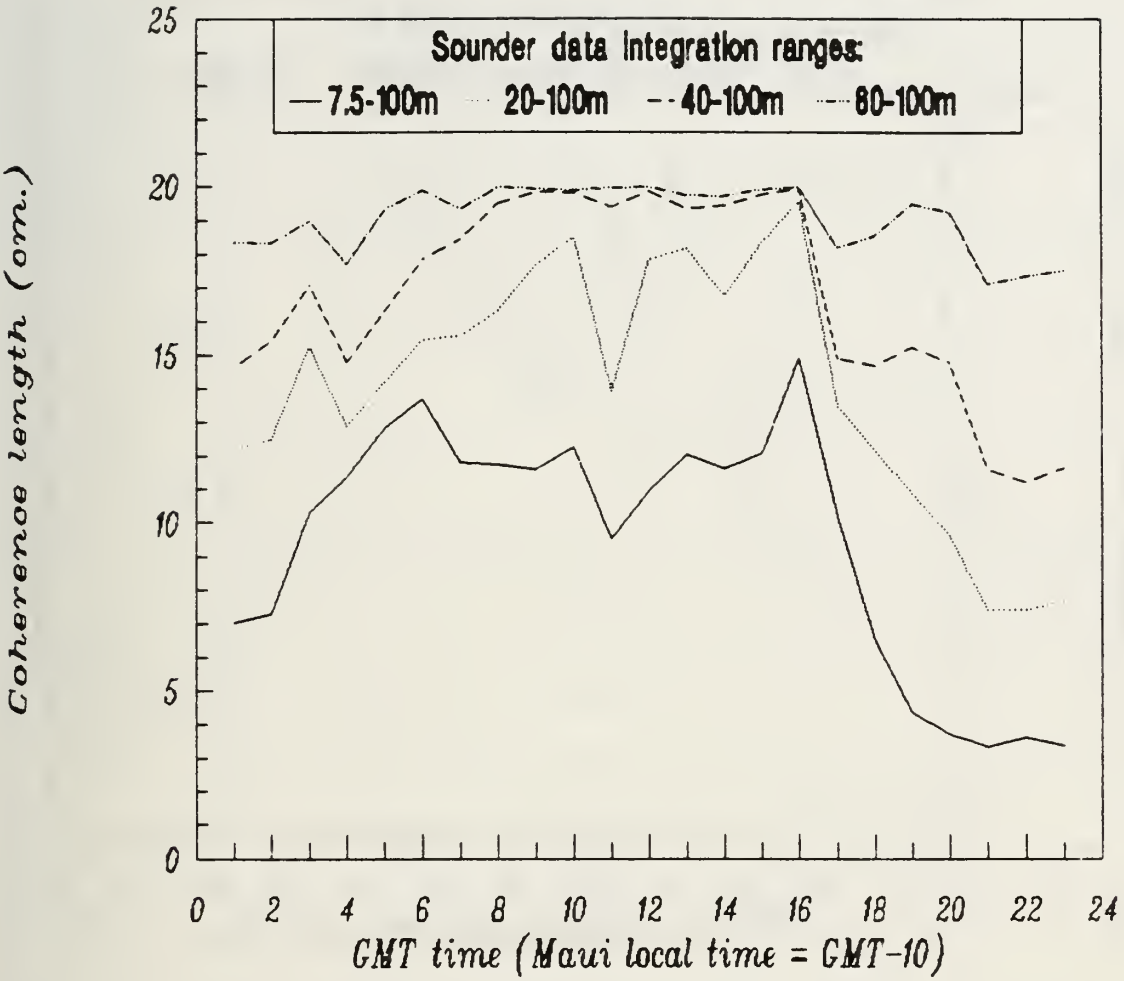

Figure 20. Acoustic Sounder Data for the Evening of 28-29 June, 1991 Showing the Turbulence Layering Structure at AMOS.

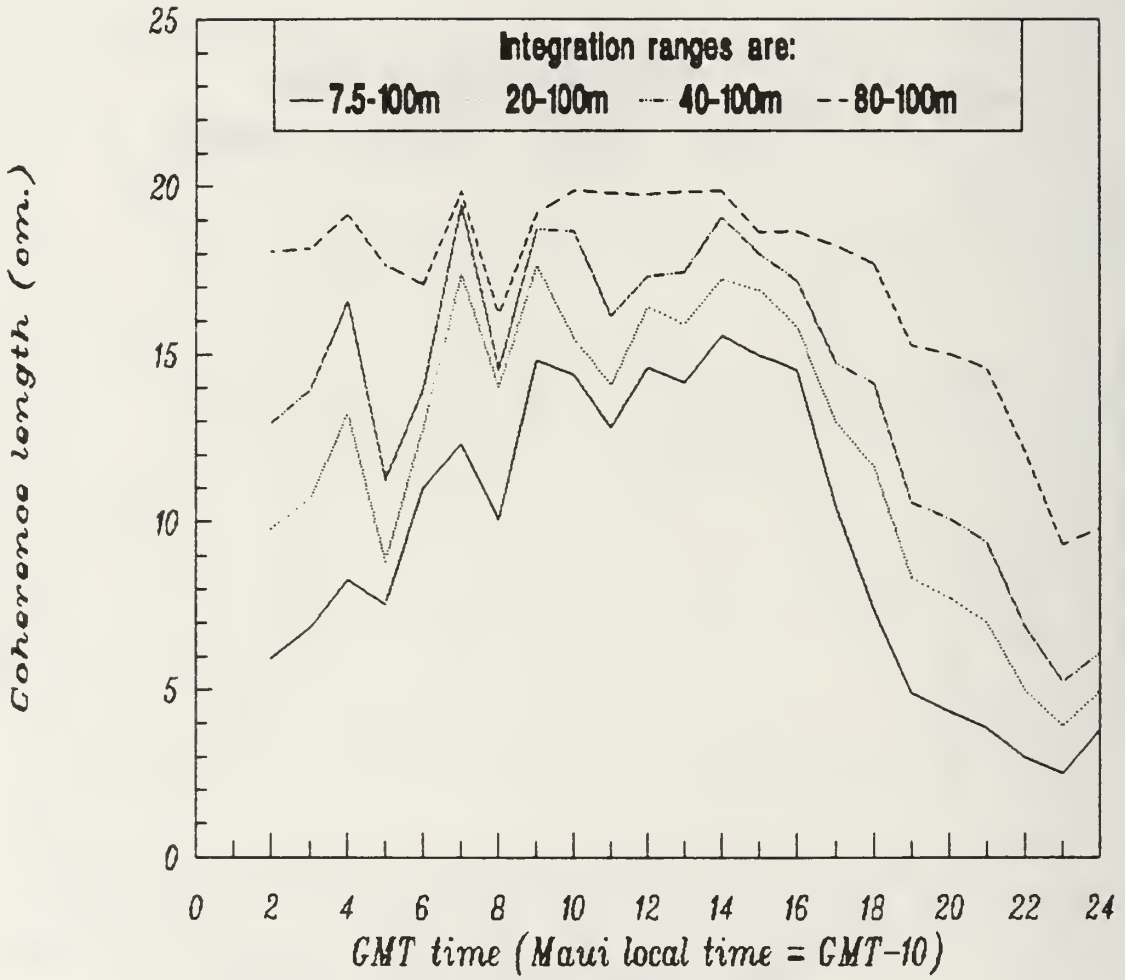

Figure 21. Acoustic Sounder Data for the Evening of 29-30 June, 1991 Showing the Turbulence Layering Structure at AMOS.

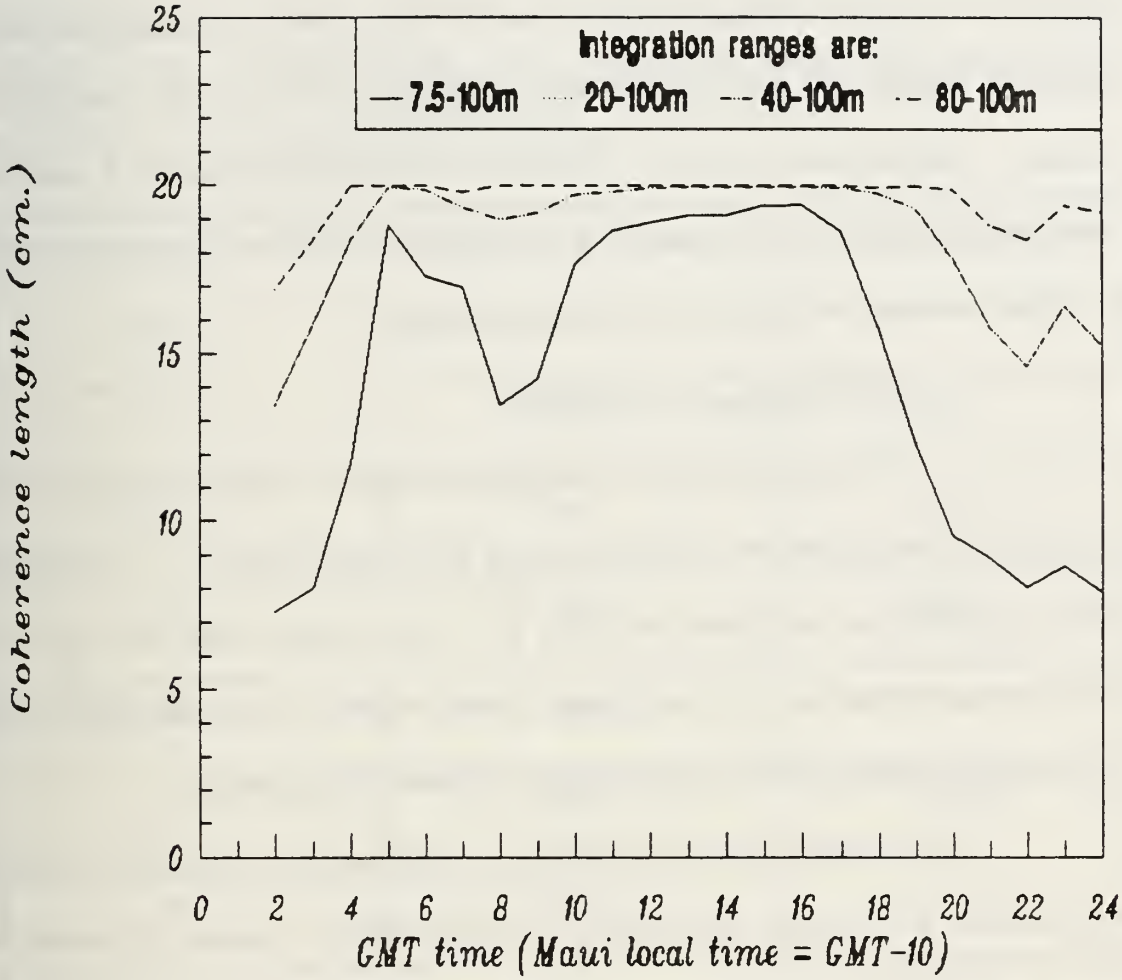

Figure 22. Acoustic Sounder Data for the Evening of 01-02 July 1991 Showing the Turbulence Layering Structure at AMOS.

b. Zenith Angle Correction

The first step in correcting the optical data for comparison is a zenith angle correction. This is a simple trigonometric technique that involves division of the optical measurement by $(\sec\theta)^{3/5}$ (where θ is the respective zenith angle) to rescale the data for the slant path length through the atmosphere. Caution must be exercised when applying this correction since it assumes horizontal turbulence stratification. It is not valid when large contributions of dome or mirror induced turbulence dominate the situation.

c. Short Exposure Correction

The second step in correcting the optical data is concerned with the effects of exposure time. Fried discusses this in detail [Ref. 17]. J. Oldenettal [Ref. 18] performed additional study for the 1.6 m device. Both the 1.2m and 1.6m devices measure a short exposure FWHM. However, inconsistencies in the 1.2m Hughes seeing monitor data, made comparison impossible.

The acoustic sounder obtains a C_T^2 profile of all turbulence it detects and provides a means for determining a corresponding r_o value. As mentioned above, the 1.6m CIS device measures this same turbulence in a short exposure manner. In essence, this means that the imaging system eliminates a portion of the turblence by compensating for long term phase tilts in the light received from a stellar object. Even though this tip/tilt correction is a necessary part of the 1.6m compensated imaging system, it causes the device to detect a lower level of

turbulence than the sounder. This lost, long exposure turbulence effect must be recovered before making a quantitative comparison. Table 1 contains the data taken from Reference 18 used to do this. The second, third, and fourth entries

TABLE 1. CALCULATED IMAGE FWHM FOR LONG AND SHORT EXPOSURES FOR THE 1.6m CIS TELESCOPE. [Ref. 18]

r_o (cm.)	long exp. @ 500nm (arcseconds)	short exp.@ 500nm (arcseconds)
6	1.69	.472
10	1.02	.702
14	.734	.186
18	.576	.328
22	.472	.234
26	.402	.186
30	.352	.142

in this table span the range of r_o values measured. A least-squares fit of the 1.6 m long exposure r_o values at 500 nm to the reciprocal of the short exposure FWHM values gave

$$r_o(cm) = 2.975 + \frac{4.925}{\theta_s} \quad (10)$$

with a correlation coefficient of r = 0.9999, where θ_s is the short exposure FWHM corrected for zenith angle and λ = 500nm. Figures 23 through 25 contain the final results of these conversion procedures.

Note that the optical r_o values tend to lie around 8 cm, which is considerably below the 12-15 cm acoustic results. In addition the optical r_o values around 14:00 on 2 July show an artificial enhancement produced by the zenith angle correction. Both of these results suggest that there was considerable dome or mirror turbulence in the immediate vicinity of the 1.6 m (and 1.2 m) devices.

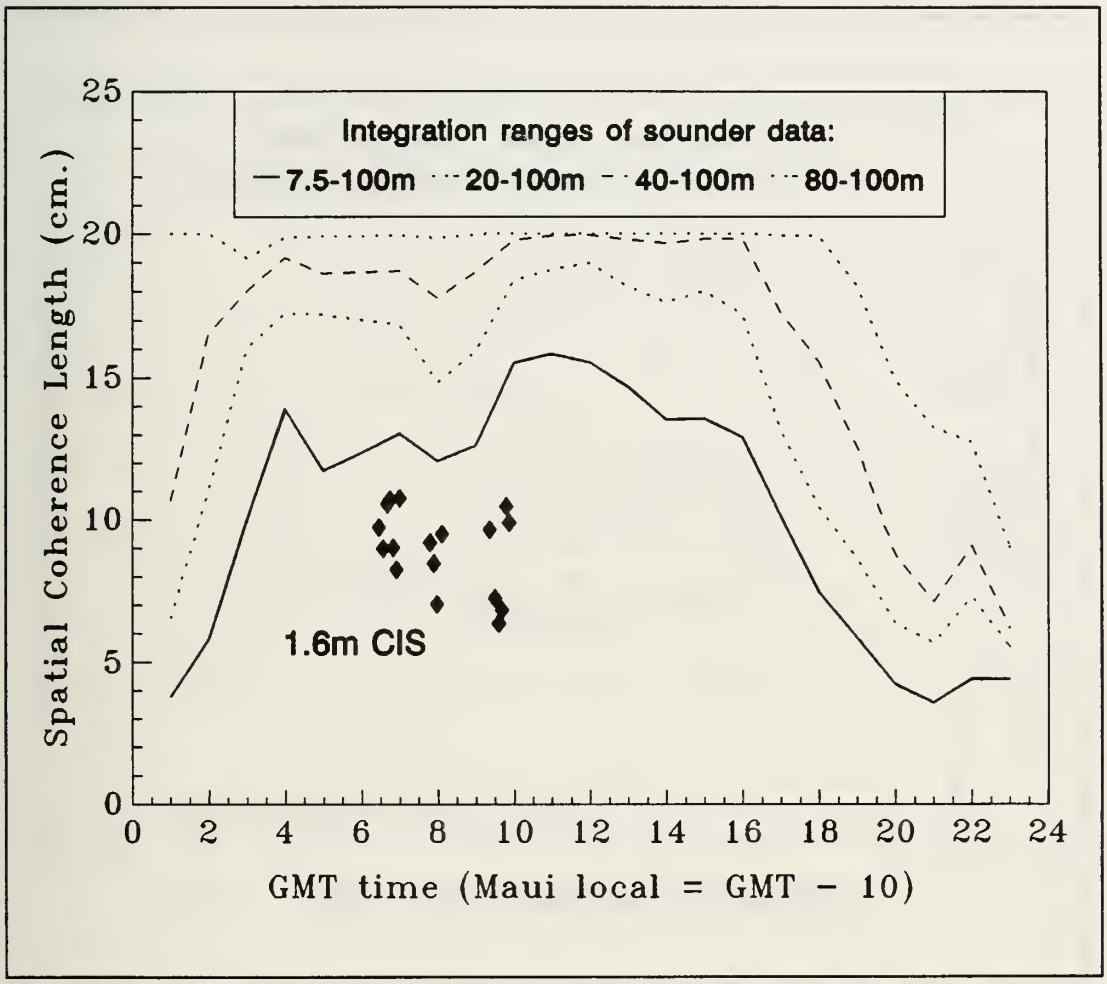

Figure 23. Acoustic Sounder Turbulence Layering Profile Data vs. Corrected 1.6m CIS Optical Data for the Evening of 26-27 June, 1991.

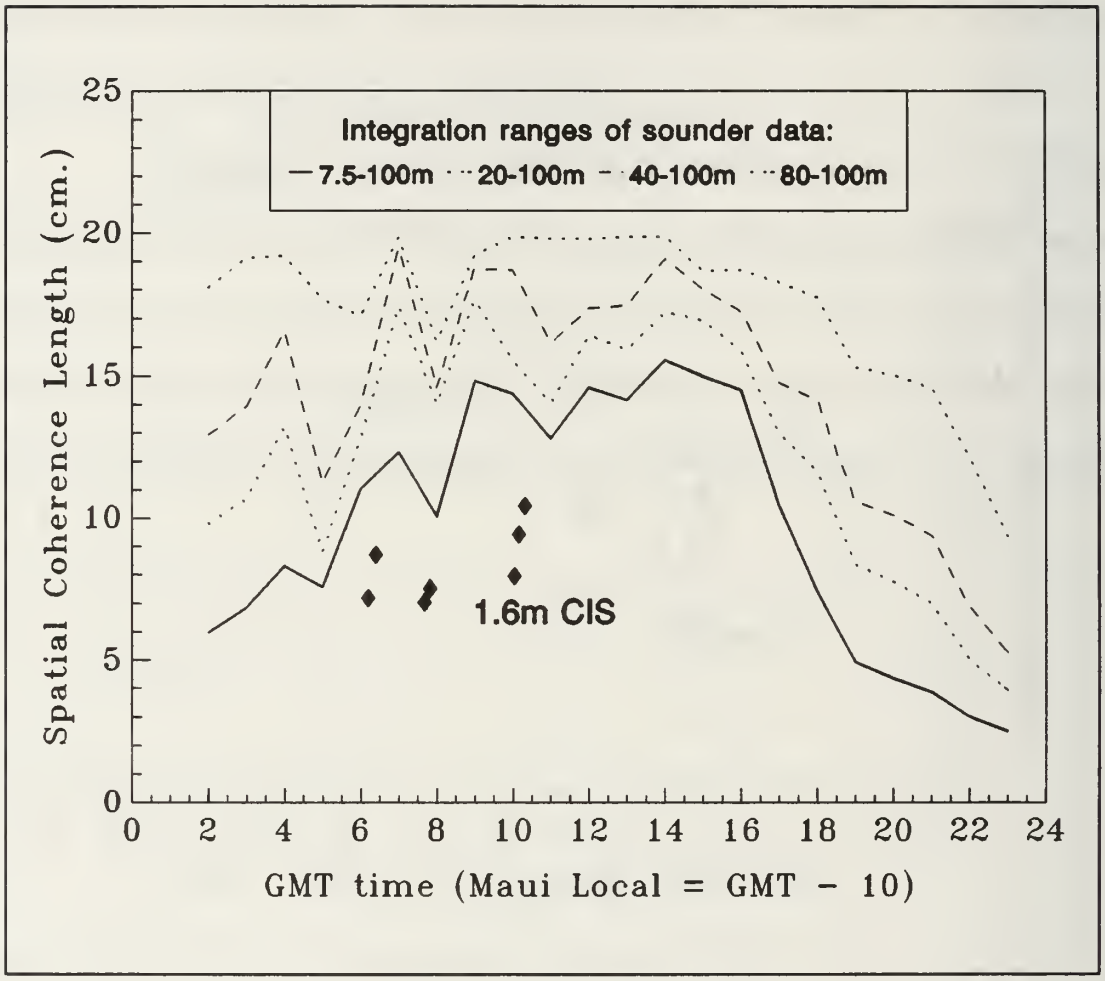

Figure 24. Acoustic Sounder Turbulence Layering Profile Data vs. Corrected 1.6m CIS Optical Data for the Evening of 29-30 June, 1991.

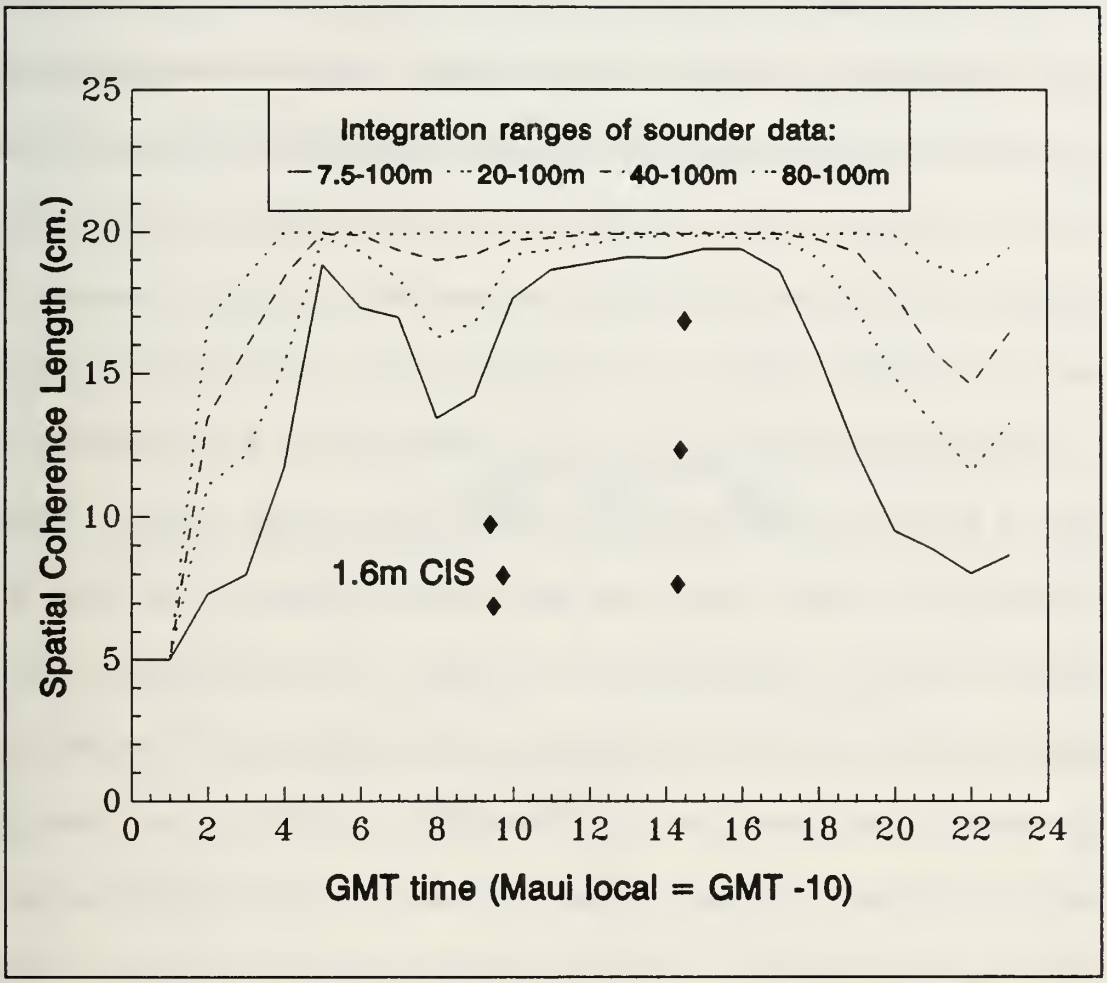

Figure 25. Acoustic Sounder Turbulence Layering Profile Data vs. Corrected 1.6m CIS Corrected Optical Data fro the Evening of 01-02 July, 1991.

4. Wind and Atmospheric Conditions

As discussed in the Equipment chapter, one of the recent updates made to the operating software was a Doppler algorithm. This allows for the collection of horizontal wind speed information corresponding to the turbulence under investigation. This data can be extremely useful in localizing regions of high turbulence within a given boundary layer. If these regions are low, then they can be completely negated through the use of an elevated platform. This is expected to be the case for smoothly contoured hilltop locations. However, in the case of the AMOS location, the mountaintop is not smoothly contoured. In fact, the entire facility is built on the rim of an ancient volcano. It was uncertain what type of boundary layer would be formed across such contours. Doppler information was taken during the Maui visit beginning on 28 June at an inclination angle of approximately 20 degrees off the vertical and into the direction of the predominant north-westerly winds. Figures 26, 27, and 28 contain representative examples of this data. The altitude cut-off for the wind data is the point at which the C_T^2 signal becomes insufficient to be considered trustworthy. This varies constantly and is a direct effect of the wind and humidity conditions. Appendix C contains a more extensive set of wind profile plots collected using the Doppler algorithm. The general pattern of the wind speed was essentially a constant 6 m/s with altitude, although a 10-20% increase appears around 40-50 m. The horizontal wind speeds on 28-29 June were slightly larger being around 10 m/s.

In addition to acoustic echo-sounder measurements, a VIZ 9000 microsonde system made measurements of humidity and temperature profiles above AMOS. This data is the subject of a Naval Postgraduate School Master's thesis being written by C. R. Hoover [Ref. 19]. Figures 29, and 30 are representatives of the low altitude portion of this data which are roughly coincident in time with the wind profiles of Figures 26 and 27.

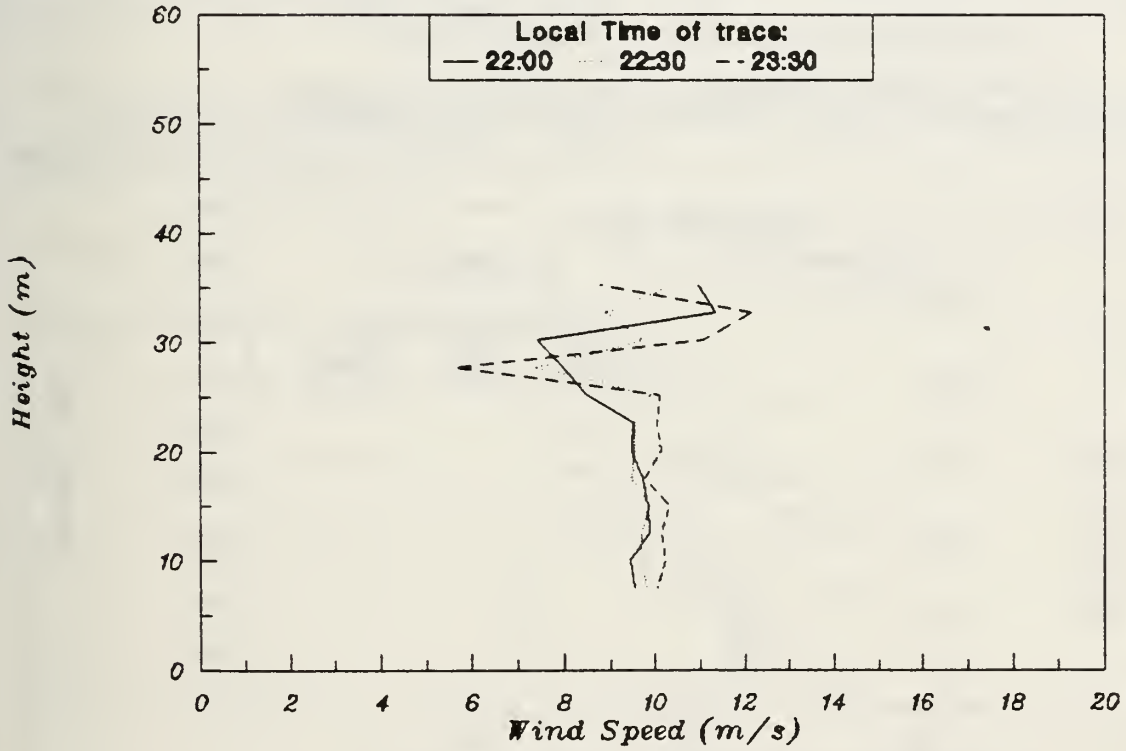

Figure 26. Wind Profile for Evening of 28-29 June 1991.

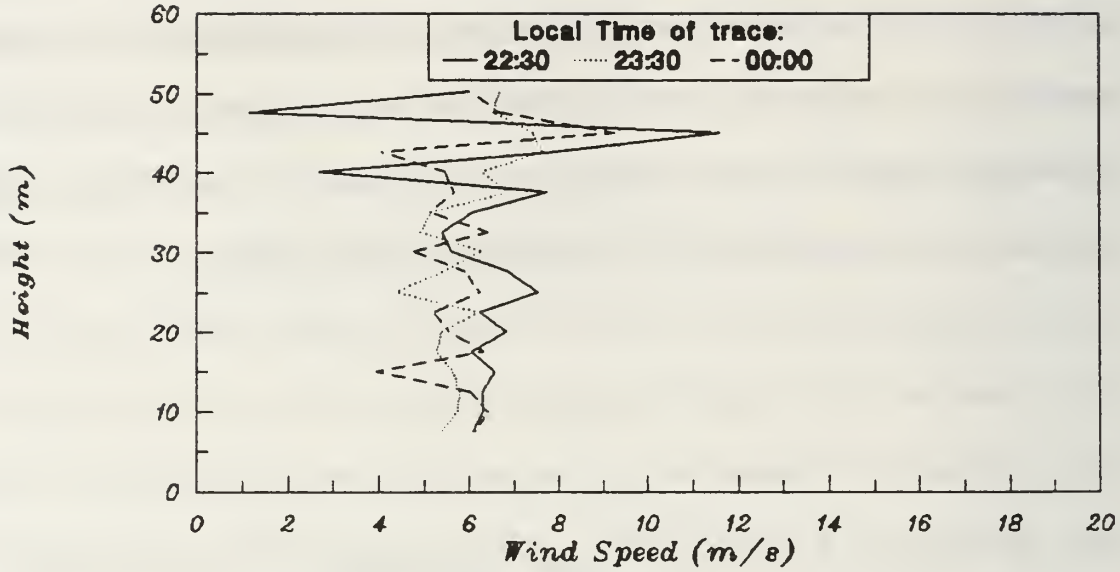

Figure 27. Wind Profile for Evening of 29-30 June 1991.

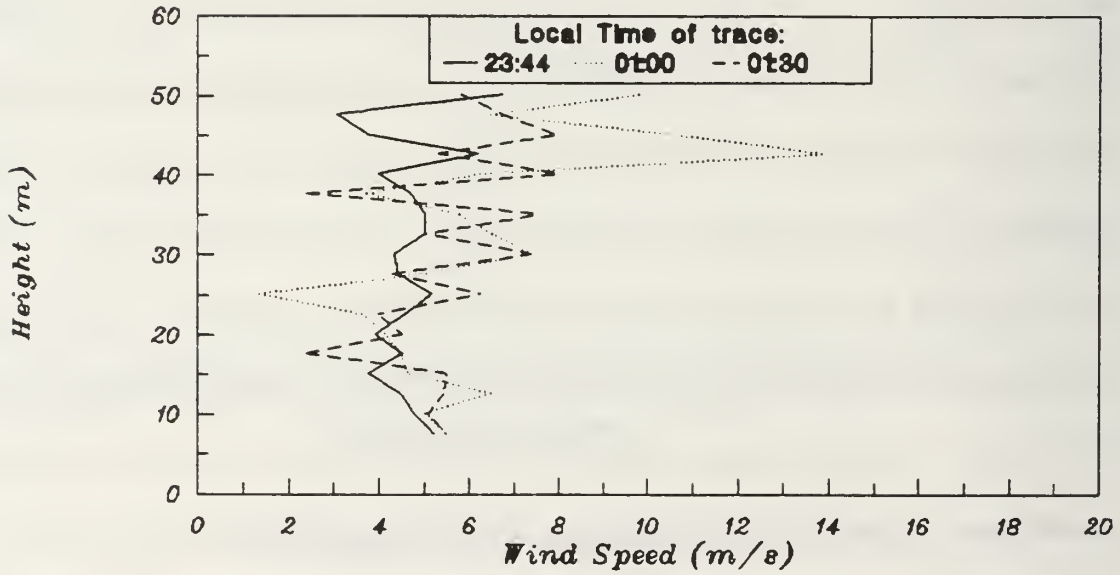

Figure 28. Wind Profile for Evening of 01-02 July 1991.

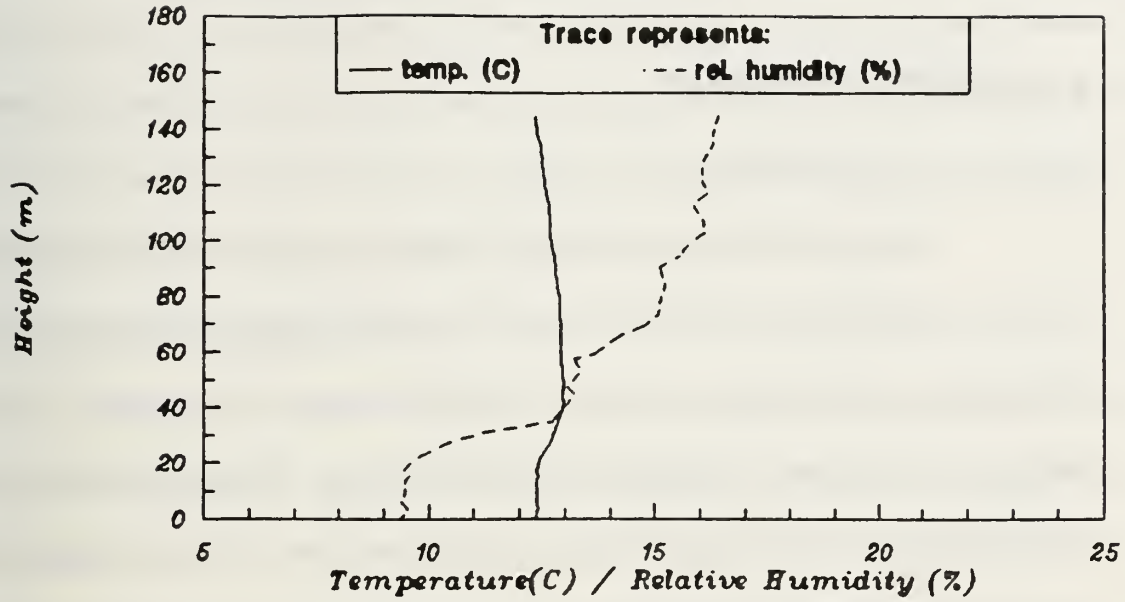

Figure 29. Low-Altitude Microsonde Temperature and Humidity Profiles at AMOS on the Evening of 28-29 June 1991.

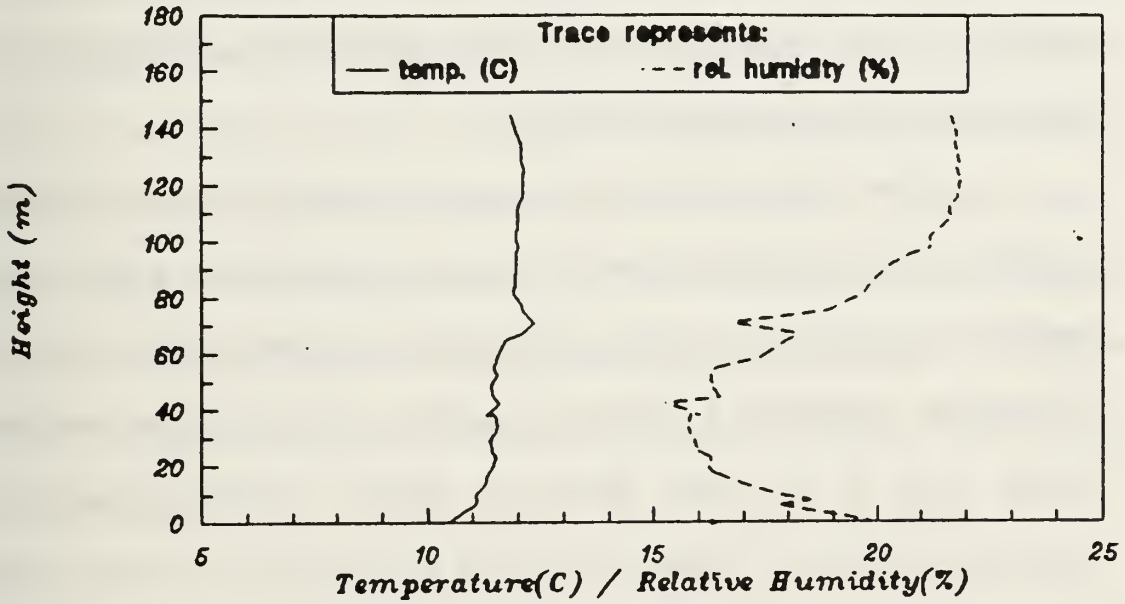

Figure 30. Low-Altitude Microsonde Temperature and Humidity Profiles at AMOS on the Evening of 29-30 June 1991.

V. CONCLUSIONS AND RECOMMENDATIONS

A. MISSION OBJECTIVES

1. r_o vs. Altitude

Figures 19 through 22 imply that the region from 7.5-100 meters contains a significant portion of the optical turbulence encountered above AMOS. Additionally, this turbulence occurs in stratified layers. This suggests that the resolution will improve by positioning the telescope on an elevated tower. Using Figures 23 and 24, this improvement would appear to be on the order of 30-40% for a 15-25 m tower. This value was found by comparing the existing seeing to that available at 15-25 m and neglecting other possible turbulence sources. The conditions on the evening of 01-02 July were anomalously good and were not considered in drawing these conclusions.

Other trends noticed in the sounder results are that the seeing conditions tend to improve slowly in the late evening hours and to reach a maximum at around 4 a.m. each morning. This suggests that, under similar wind/weather conditions, a window of optimum viewing may be predictable. Another trend is the rapid decline in viewing conditions beginning at approximately 5:30 a.m. each morning. This is caused by convection following sunrise. The interesting point is that it seems to take much longer for the conditions to improve after sunset than it does for them to decline after sunrise.

After reviewing the entire set of measured wind profiles, nothing conclusive can be said about the wind velocity boundary layer above AMOS. Characteristics vary considerably from plot to plot, making any conclusions sketchy at best. Since there is no apparent drop off in wind speeds, it seems that the wind shear layer extends to an altitude of at least 80 meters above AMOS, although this layer is only optically turbulent in its lower levels.

2. Site Comparison

As demonstrated in Figures 17 and 18, as well as in some of the plots in Appendix B, there appears to be no significant difference between the turbulence profiles at Sites A and G. This is not to say that there are no differences, but that this data set does not reveal any detectable differences. Surprisingly, since the two sites were at different heights on the mountaintop, this trend suggests that the turbulent layer follows the ground contour in a manner similar to observed fog advection. However, it is impossible to draw any definite quantitative set of conclusions based only on this data set. In order to do so would require not only additional data, but also data gathered during different weather and wind conditions. Additionally, data from tower mounted temperature probes located at each of the prospective sites would be useful in making any such conclusions.

B. FUTURE CONSIDERATIONS

1. Atmospheric Turbulence

Before making any definite conclusions regarding the atmospheric turbulence profile above AMOS, additional data must be taken. The data collected in this project spanned only a period of one week during the summer season. To conduct an accurate survey, it is recommended that additional measurements be taken during different seasons using a variety of equipment. This equipment should include not only an acoustic sounder, but balloon sonde, temperature probe, and optical devices as well.

2. Artificial Turbulence

The term 'artificial turbulence' refers to that turbulence caused by devices associated with the telescope being used for observation. These include all ventilation, electrical, and building-related heat or wind turbulence effects. Reference 12 presents a historical study of such effects at the CFHT. Figures 23 and 24 imply that 25-50% of the optical turbulence could be dome or telescope induced. The instrumental effects of the 1.6m telescope and the CIS were not removed from the optical data since they were unknown. If the optical quality factors were available and included, they would tend to improve the optical results and to reduce the difference with the sounder data. It is unlikely that this would compensate for all the differences. Measurements of dome-air temperature

differences and turbulence within the dome and over the mirrors are needed to resolve this issue.

APPENDIX A. ACOUSTIC ECHO-SOUNDER OPERATING CODE

The following computer code is used to operate the acoustic echo-sounder discussed in this paper. It is written in Rocky Mountain Basic and is for use on Hewlett-Packard computers.

```
10    !  ****************************************************************
20    !  *                      DOPPLER ACOUSTIC SOUNDER                *
30    !  *        Includes optical disc and dynamic gain change         *
40    !  *                   COMPLEX COVARIANCE ALGORITHM               *
50    !  *                     Prof. D. L. Walters                      *
60    !  *                    With contributions from                   *
70    !  *       LT. M. WROBLEWSKI AND LT. F. WEINGARTNER (1987)        *
80    !  *        Lt L. Moxcey (1988), Lt. J. McCrary (1990)            *
90    !  *              DOPPLER ADDITION: PROF. D. WALTERS              *
100   !  *                          JUNE 1991                           *
110   !  ****************************************************************
120   !  4 DEC 91, PREVIOUS:27 JUN 1991, DLW
130   !
140   !  The computer program receives information from an acoustic
150   !  array through an A-D converter.  This information is the
160   !  returned signal of an acoustic pulse as it passes through
170   !  the atmosphere.  The data is then used to display the return
180   !  intensity with distance as a function of time.  This is a
190   !  short range device (from 100m to 150m).
200   !
210   !
220   !  LIST OF VARIABLES
230   !
240   ! A  -  The area of the receiver (array)
250   ! Amp$ - Amplitude for HP3314A
260   ! Ap$,Frq$,Nm$,En$,Vo$,Hz$  -  strings needed to set the HP3314A
270   ! Count$ & Cnt  -  the string and real representation of
280   ! Ct(*)  -  the atmospheric temperature structure parameter
290   ! C0kelvin  -  the speed of sound at 0 degrees celcius in m/s
300   ! Ct_pts - the number of traces used in computing Ct(*)
310   ! Dat(*)  -  array of a-d converter output after sampling
320   ! Disc_address$  -  storage location of data file
```

```
330   ! End_pt  -  the last point of the plot vertically taking
340   ! Er  -  efficiency of coversion of acoustical power
350   !        to electrical power on the recieve side
360   !
370   ! Et  -  the efficiency of conversion of electrical
380   !        power to acoustical power on the transmit side
390   !         range correction from being applied to data very near
400   ! Freq$ & Freq  -  the frequency input of the HP3314A in kilohertz
410   ! G  -  The effective aperture factor
420   ! Gain  -  the electronic gain of the equipment
430   ! File$  -  file name used to store data
440   ! Hrs  -  the integer hours
450   !
460   ! I & J & K  -  counters for loops
470   ! Ilvl  -  the user input intensity level divisor; this value
480   !          sets the screen contrast in data return
490   ! Inc  -  The vertical increment along the plot
500   ! Kmax  -  total number of block averages computed
510   ! K3  -  the wave number to the 1/3rd power
520   ! M  -  the counter used in the plot label routines
530   ! Maxrng  -  the maximum range of the echosounder found
540   ! Min  -  the number of minutes
550   ! Noise  -  a running total of the noise accumulated at the
560   !           maximum range; used to find and remove the
570   !           average noise
580   ! Nrec -    record number for storage
590   ! Ns  -  the final average of the block of data points; also
600   !        used in the computation of the noise figure
610   ! N$ & Num  string and real representation of the number of
620   !              cycles in the transmitted burst
630   ! Num1  -  counter for computation of block averages
640   !
650   ! Num2  -  counter for the number of block averages made
660   ! Offset  -  the computed D-C offset for the system prior
670   ! Rec_num  - .real and integer representation of the
680   !                      record number for storage
690   ! Plotnum  -  counter used to insert form feeds between plots
700   ! Pls_lng  -  the pulse length of the burst
710   !
720   ! Pnt  -  the horizontal position on the Ct plot
730   ! Point(*)  -  real number representing the noise and range
740   !              corrected average over given number of points
750   ! Pt  -  The computed transmitted power to the array
760   !
770   ! Qtrhr & Qtrmin  -  keeps track of the passage of each
780   !                    15 minute interval
790   ! R  -  the range of a block of data samples
800   !
```

```
810   ! Rdist  -  the distance traveled in one time increment
820   !
830   !            by multiplying the distance per time increment
840   !            by the number of time increments
850   ! Rspd  -  the relative speed of sound that the echosounder
860   !          sees which is half the computed speed
870   ! Run_ave  -  the running sum of the block samples
880   !
890   ! Samfreq  -  the user input sampling frequency desired
900   ! Save_plt & Cntrl  -  on/off toggles used to determine whether
910   !                      a particular run will be saved to a disc
920   ! Site$  -  the name of the appropriate site of data collection
930   ! Spd  -  the speed of sound in air computed for the input
940   !         temperature
950   ! Temp  -  temperature of the surroundings in degrees celcius
960   ! Timcnt  -  time interval between data samples in
970   ! Time  -  the horizontal position of the trace on the plot
980   ! Timedist  -  the horizontal width of the trace on the plot
990   !            horizontal axis
1000  !             to data acquisition
1010  ! Time$  -  the string required by the A-D converter to
1020  !           sample at the desired rate
1030  ! Tminc  -  time interval between A-D samples
1040  ! Trig -    HP3314A trigger flag
1050  ! Ypl  -  the vertical position on the Ct plot
1060  ! Z  -  The final reduced data points which are output on the plot
1070  ! Zeff  -  Effective Impedence for input loading
1080  ! Zimp  -  the speaker array impedence
1090  ! Zone$  -  the appropriate time zone the operator desires
1100  !
1110  OPTION BASE 1
1120  !
1130  ! initialize the arrays  &  set dimensions
1140  ! declare all integer variables
1150  !
1160    DIM Disc_address$[20],File1$[30],File2$[30],D1(500),Ct(250),Point(
1170    DIM Doppler(300),Vdop(300),V_num(300),Davg(2000),Ct_dop(600)
1180    INTEGER Hr,I,Inum,J,K,Kmax,K1,K2,M,Ncnt,Nbin,Num,Num1,Num2
1190    INTEGER Plotnum,Print_key
1200    DIM Dat(18200)                  ! FOR 20 KHZ
1210  !
1220  !   initialization routines....set time, set HP3314A Function
1230  !   Generator
1240  !
1250 Rstrt:CALL Freq_init(Freq$,N$,V_out)
1260       CALL Init_ad200
1270       CALL Set_time(Zone$)
```

```
1280      INPUT "SITE NAME ",Site$
1290    !
1300    ! keyboard set_up  -  sets labels on the computer function
1310    !                     keys
1320    !
1330        OUTPUT KBD;"SCRATCH KEYE";    ! CLEAR THE KEYS
1340        CONTROL 2,2;1
1350        ON KEY 0 LABEL "NEW      TEMP" GOTO Speed
1360        ON KEY 1 LABEL "FILTER   GAIN" GOTO Set_gain
1370        ON KEY 2 LABEL "PRINT    TRACE" GOTO Plt_dmp
1380        ON KEY 3 LABEL "COLOR    SCALE" GOTO Doppler_fs
1390        ON KEY 4 LABEL "PLOT     RANGE" GOTO Plot_range
1400        ON KEY 5 LABEL "RESTART" GOTO Rstrt
1410        ON KEY 9 LABEL "QUIT" GOTO Quit
1420    GINIT
1430    !
1440    ! Set constants
1450    !
1460      Area=.0866                  ! Array area m^2  0.00456/driver
1470      Blue=2/3                    ! Color value for pure blue
1480      Count$="18200"              ! Total# A-D samples 11200 or 18200
1490      C0kelvin=331.6              ! Speed of sound at 0 C
1500      Disc_address$=":,704,0,0"
1510      Er=.5                       ! Receive efficiency
1520      Et=.5                       ! Transmit efficiency
1530      Filter_gain=10              ! Voltage gain for filter gain of 20 db
1540      Full_scale=5                ! Doppler full scale (red or blue)
1550      G=.4                        ! average antenna gain factor
1560      Green=1/3                   ! Value for green
1570      Ilvl=.01                  ! CT threshold for full scale
1580      Maxsec=900                  ! number of seconds in a 15 min plot
1590      Max_rec1=96                  ! 96 files in 24 hrs, 1 every 15 min
1600      Max_rec2=22000              ! #Ct2 traces stored in 24 hours @ 4sec
1610      Plotnum=1
1620      Pltrng=100                  ! Max range on plot
1630      Power_amp_gain=20.6         ! Power amp voltage gain
1640      Rin=100                     ! preamp input impedence, ohms
1650      Samfreq=20000               ! sample frequency
1660      Samave=0
1670      !Zimp=12.12                 ! 5 x 5 square array impedence
1680      Vloss=2.2                   ! Voltage loss in line and TR switch
1690      Zeff=12.94                  ! effective Z for 100 ohm input
1700      Zimp=19.5                   ! 19 ELEMENT HEXAGONAL ARRAY Z
1710      ! Derived constants
1720      INPUT "ENTER PRE-AMP GAIN: 987,1906 or 3895",Preamp_gain
1730      INPUT "SET FILTER GAIN ON PREAMP AND ENTER SETTING (0,10,20,30)",Db
1740      PRINT "FILTER GAIN = ",Db
1750      Filter_gain=10^(Db/20)
```

```
1760       !
1770       Vtpk=V_out*Power_amp_gain
1780       Pt=Et*(Vtpk-Vloss)^2/(2.*Zimp)      ! RMS acoustical power output
1790       Gain=Preamp_gain*Filter_gain
1800       !
1810       !
1820 Sfrq:!
1830       GCLEAR
1840       Tminc=1./Samfreq
1850       Timcnt=Tminc/1.E-9          ! Delta t in nsec
1860       Time$="TIME "&VAL$(Timcnt)
1870       Cnt=VAL(Count$)             ! Total # of A-D samples
1880       Navg_pts=2000               ! # points used to compute offset
1890       Ncnt=Cnt
1900       Num=VAL(N$)                 ! # cycles transmitted in burst
1910       Freq=VAL(Freq$)*1000        ! Transmitted frequency
1920       Full_scale=5                ! Doppler full red or blue shift
1930       Tau=Num/Freq                ! Pulse length (sec)
1940       Nbin=Samfreq*Tau            ! # of counts per range bin
1950       Ksave=INT(Ncnt/Nbin)        ! # of range bins
1960        Navg=Ncnt-Navg_pts+1
1970        Nbin2=Nbin/2
1980        Num1=Nbin-1
1990        Num2=Ncnt-Nbin+1
2000        Num_pts=Nbin+Nbin MOD 4
2010  !
2020       REDIM Ct(Ksave),Point(Ksave),Doppler(Ksave),D1(2*Ksave+10),Vdop(K
2030       REDIM V_num(Ksave),Ct_dop(2*Ksave)
2040  !
2050       CALL File_init(Disc_address$,Max_rec1,Max_rec2,Nlast1,Nlast2,Ksav
2060       ASSIGN @File1 TO File1$
2070       ASSIGN @File2 TO File2$
2080       Nrec_opt=Nlast2
2090  !
2100  !
2110  !    computation of the speed of sound at a given temp and the
2120  !    range of detection of the device
2130  !
2140  !
2150 Speed:INPUT "Enter the temperature (celsius) ",Temp
2160       INPUT "Enter the relative humidity in %",Rel
2170       INPUT "Enter the atmospheric pressure in mb",Atmos_pres
2180       Spd=C0kelvin*(SQR(1.+(Temp/273.)))
2190       Rspd=Spd/2.
2200       Rdist=Tminc*Rspd
2210       Maxrng=Cnt*Rdist
2220       Lambda=Spd/Freq
2230       K3=((2.*PI)/Lambda)^(1./3.)
2240       Pls_lng=(Rspd*Num)/Freq
```

```
2250  !
2260      CALL Attenuation(Freq,Temp,Rel,Atmos_pres,Atten)
2270      Atten2=2.*Atten
2280  !
2290 Start_plot:  !
2300  !
2310  !  Computation of the D-C offset
2320  !
2330   Noise=0
2340   Offset=0
2350   Offset_flag=0
2360   Vdoppler=Spd/(2*PI)
2370   Color_scale=1/(3*Full_scale)
2380   Volts_per_bit=5./(2048.*Gain*Rin/(Rin+Zeff))
2390  ! Compute CT calibration constant
2400        Ct_cal=Volts_per_bit^2/Zimp
2410        Ct_cal=Ct_cal*(Temp+273)^2/(.0039*K3)
2420        Ct_cal=Ct_cal/(Area*G*Pt*Er*Pls_lng)
2430  !
2440       Trig=0
2450       CALL Read_ad200(Dat(*),Time$,Trig)
2460       Trig=1
2470  !
2480      PRINT "COMPUTING D-C OFFSET AND NOISE BACKGROUND"
2490      Offset=SUM(Dat)/Cnt
2500      MAT Dat= Dat-(Offset)
2510  !
2520  ! Compute real and imaginary noise levels
2530  !
2540       K=0
2550       Zreal=0.
2560       Zimag=0.
2570  FOR I=1 TO Num2 STEP Nbin
2580       K=K+1
2590       Inum=I+Num1
2600       FOR J=I TO Inum STEP 4
2610          A=Dat(J)
2620          B=Dat(J+1)
2630          C=Dat(J+2)
2640          D=Dat(J+3)
2650          Zreal=A*C+B*D+Zreal
2660          Zimag=-A*D+B*C+Zimag
2670       NEXT J
2680  NEXT I
2690      Zrnoise=Zreal/K
2700      Zi=Zimag/K
2710      Zinoise=Zrnoise*TAN(1/Vdoppler)        ! +1m/s noise offset
2720      PRINT Zrnoise,Zi,Zinoise
2730  !
```

```
2740  !   Compute total noise
2750  !
2760       MAT Dat= Dat . Dat
2770       Noise=SUM(Dat)/Cnt
2780  !
2790  !  set up the plot
2800  !
2810 FOR Nrec=Nlast1 TO Max_rec1
2820   CALL Plot_setup(Maxsec,Site$,Maxrng,Pltrng,Zone$)
2830       MAT Ct= (0.)          ! Zero arrays
2840       MAT Doppler= (0.)
2850       MAT Vdop= (0.)
2860       MAT V_num= (0.)
2870       Ct_pts=0.
2880       Nsec_last=0
2890       OUTPUT KBD;"L";
2900  !
2910  !   Compute 15 minute noise level
2920  !
2930        Trig=0
2940        CALL Read_ad200(Dat(*),Time$,Trig)
2950        Trig=1
2960  !
2970        Offset=SUM(Dat)/Cnt
2980        MAT Dat= Dat . Dat
2990        New_noise=SUM(Dat)/Cnt-Offset*Offset ! Noise variance
3000        IF Noise=0 THEN
3010           Noise=New_noise
3020        ELSE
3030          IF New_noise<2.*Noise THEN Noise=.5*Noise+.5*New_noise
3040        END IF
3050        Signal_thresh=2.*Noise                ! Signal threshold for w
3060  !
3070 Read_sig:    !  read the A-D converter
3080  !
3090  ! find the # seconds in the fifteen minute block
3100  !
3110        T0=TIMEDATE
3120        T1=(T0 MOD 86400)                    ! # sec past midnight
3130        Nsec=(T1 MOD 3600 MOD Maxsec)        ! # sec within 15 min block
3140        Delta_time=Nsec-Nsec_last            ! Time interval between puls
3150        Nsec_last=Nsec                       ! Old # seconds
3160        IF Delta_time<0 THEN GOTO Plt_dmp    ! Print plot after 15 minute
3170        Delta_time=Delta_time/2+2
3180        !
3190        CALL Read_ad200(Dat(*),Time$,Trig)
3200        !
3210        MAT Davg= Dat(Navg:Ncnt)
```

```
3220        Offset=SUM(Davg)/Navg_pts
3230        MAT Dat= Dat-(Offset)
3240        MAT Vdop= (0.)
3250        !
3260        K=0
3270        ALPHA OFF
3280  FOR I=1 TO Num2 STEP Nbin
3290        R=(I+Nbin2)*Rdist                    ! Mean range of range bin
3300        K=K+1
3310        Raw_sig=0.
3320        Inum=I+Num1
3330        Zreal=0.
3340        Zimag=0.
3350        FOR J=I TO Inum STEP 4
3360           A=Dat(J)
3370           B=Dat(J+1)
3380           C=Dat(J+2)
3390           D=Dat(J+3)
3400           Zreal=A*C+B*D+Zreal
3410           Zimag=-A*D+B*C+Zimag
3420           Raw_sig=Raw_sig+A*A+B*B+C*C+D*D
3430        NEXT J
3440        Raw_sig=Raw_sig/Num_pts
3450        Point(K)=Ct_cal*R*R*(Raw_sig-Noise)*EXP(R*Atten2)
3460        IF Raw_sig>Signal_thresh THEN
3470          Vdop(K)=ATN((Zimag-Zinoise)/(Zreal-Zrnoise))*Vdoppler
3480          V_num(K)=V_num(K)+1
3490        END IF
3500  NEXT I
3510        Kmax=K
3520  !
3530  !
3540  !     Add data to Ct average if the noise is sufficiently low
3550  !
3560        IF Raw_sig<20.*Noise THEN            ! Add Points TO Ct
3570          MAT Ct= Ct+Point
3580          MAT Doppler= Doppler+Vdop
3590          Ct_pts=Ct_pts+1
3600        ELSE
3610          DISP "HIGH BACKGROUND NOISE- SIGNAL REJECTED"
3620        END IF
3630  !
3640  !  Plotting of the data
3650  !
3660  WINDOW 0,Maxsec,0,Pltrng
3670  GRAPHICS ON
3680  !
3690  Inc=Nbin*Rdist                             ! Vertical increment
```

```
3700  IF Delta_time>10 THEN Delta_time=10    ! account for delays
3710  Color_scale=1/(3*Full_scale)           ! Set full scale color
3720  !
3730  ! compute the intensity of the return, move to the proper
3740  ! coordinates and plot the appropriate dithered block
3750  !
3760  FOR K=1 TO Kmax
3770     Pointk=Point(K)
3780     IF Pointk>0. THEN
3790        Z=SQR(Pointk/Ilvl)
3800        IF Z>1. THEN Z=1.
3810     ELSE
3820        Z=0
3830     END IF
3840     Vcolor=Vdop(K)*Color_scale+Green
3850     IF Vcolor<0 THEN Vcolor=0              ! Red
3860     IF Vcolor>Blue THEN Vcolor=Blue        ! Blue
3870     AREA COLOR Vcolor,1,Z
3880     Range=(K-.5)*Inc
3890     MOVE Nsec,Range
3900     RECTANGLE Delta_time,Inc,FILL
3910  NEXT K
3920  !
3930  Point(1)=T0
3940  MAT Ct_dop(1:Ksave)= Point
3950  MAT Ct_dop(Ksave+1:2*Ksave)= Vdop
3960  OUTPUT @File2,Nrec_opt;Ct_dop(*)
3970  Nrec_opt=Nrec_opt+1
3980  !
3990  GOTO Read_sig
4000  !
4010  !  graphics dump of plot after 15 minute intervals
4020  !
4030 Plt_dmp:    PRINTER IS 701
4040     PRINT "     "
4050     PRINT "     "
4060     PRINT "     "
4070     Plotnum=Plotnum+1
4080     DUMP GRAPHICS #701
4090     !
4100     MAT Ct= Ct/(Ct_pts)
4110     FOR I=1 TO Kmax
4120      IF Ct(I)<1.E-6 THEN Ct(I)=1.E-6
4130      IF V_num(I)>0. THEN Doppler(I)=Doppler(I)/V_num(I)
4140     NEXT I
4150     !
4160     CALL Ct_plot(Ct(*),Pltrng,Maxrng,Kmax,Site$)
4170     ! Save the Ct data
```

```
4180      MAT D1= (0.)                          ! ZERO ARRAY
4190      D1(1)=T0                              ! T0 = TIMEDATE
4200      D1(2)=Atmos_pres
4210      D1(3)=Temp
4220      D1(4)=Rel
4230      D1(5)=Atten
4240      D1(6)=Inc
4250      D1(7)=Ct_cal
4260      D1(8)=Gain
4270      D1(9)=Kmax
4280      D1(10)=Offset
4290      !
4300      Ki=10+Ksave
4310      FOR I=1 TO Kmax
4320        D1(I+10)=Ct(I)
4330        D1(I+Ki)=Doppler(I)
4340      NEXT I
4350      !
4360      OUTPUT @File1,Nrec;D1(*)
4370      !
4380      !  start the next 15 minute plot
4390      !
4400 NEXT Nrec
4410      !
4420 Doppler_fs:  !
4430      INPUT "Enter Doppler full scale in m/s. (5 is normal)",Full_scale
4440      GOTO Read_sig
4450 Plot_range:  !
4460      INPUT "Enter CT plot full scale 100 or 150 m",Plot_rng
4470      Pltrng=INT(Plot_rng/50)*50
4480      GOTO Start_plot
4490 Set_gain:  !
4500        INPUT "Enter filter gain, 0, 10, 20, 30, 40 DB",Db
4510        IF Db=0 OR Db=10 OR Db=20 OR Db=30 OR Db=40 THEN
4520          Filter_gain=10^(Db/20)
4530        ELSE
4540          PRINT "WRONG GAIN SETTING"
4550          GOTO Set_gain
4560        END IF
4570        Gain=Filter_gain*Preamp_gain
4580        GOTO Start_plot
4590 Quit: !
4600        PRINT "Output has been written to ";File$
4610        ASSIGN @File1 TO *
4620        END
4630        !
4640        !
4650        !  SUBROUTINE SECTION
```

```
4660        !
4670  SUB Freq_init(Freq$,N$,V_out)
4680  !
4690  !
4700  !      SETUP OF THE HP3314A  FUNCTION GENERATOR
4710  !
4720  !
4730     Ap$="AP"
4740     Frq$="FR"
4750     Nm$="NM"
4760     En$="EN"
4770     Vo$="VO"
4780     Hz$="KZ"
4790     INPUT "FREQUENCY DESIRED (kHZ) (5 RECOMMENDED)",Freq$
4800     INPUT "AMPLITUDE DESIRED (V . .2.0V MAX) ",Amp$
4810     IF VAL(Amp$)>2.0 THEN
4820         Amp$="2.0"
4830         PRINT "AMPLITUDE OF FUNCTION GENERATOR IS 2.0 V"
4840     END IF
4850     V_out=VAL(Amp$)
4860     INPUT "NUMBER OF CYCLES PER BURST (INTEGER) (100 RECOMMENDED)",N$
4870     OUTPUT 707;"MO3"
4880     OUTPUT 707;"SR2"
4890     OUTPUT 707;Ap$&Amp$&Vo$&Frq$&Freq$&Hz$&Nm$&N$&En$
4900  SUBEND
4910  !
4920  !
4930  SUB Init_ad200
4940  !
4950  !
4960  ! INITIALIZATION OF THE A-D CONVERTER
4970  !
4980  !
4990     Ad_sel_code=17
5000     Dummy=READIO(Ad_sel_code,3)
5010     WRITEIO Ad_sel_code,0;0
5020     CONTROL Ad_sel_code,0;1
5030  SUBEND
5040  !
5050  !
5060  SUB Set_time(Zone$)
5070  !
5080  !
5090  !  SET THE TIME DATE RECORDER
5100  !
5110  !
5120        PRINT "WHAT TIME REFERENCE ARE YOU USING?  INPUT:"
5130        PRINT "      1 FOR UNIVERSAL TIME"
```

```
5140        PRINT "      2 FOR LOCAL TIME"
5150        PRINT "      3 FOR YOUR OWN CLASSIFICATION"
5160        INPUT K
5170        IF K=2 THEN
5180            Zone$="(LOCAL)"
5190        ELSE
5200            IF K=3 THEN
5210                INPUT "WHAT IS YOUR TIME REFERENCE",Zone$
5220            ELSE
5230                Zone$="(UTC)"
5240            END IF
5250        END IF
5260        INPUT "Do you want to reset the clock ?",Q$
5270        IF Q$="YES" OR Q$="Y" THEN
5280            INPUT "ENTER ""DD MMM YYYY""",Date$
5290            INPUT "ENTER ""HR:MIN:SC""",Time$
5300            SET TIMEDATE DATE(Date$)+TIME(Time$)
5310            PRINT DATE$(TIMEDATE),TIME$(TIMEDATE)
5320        END IF
5330  SUBEND
5340   !
5350   !
5360   SUB Read_ad200(Dat(*),Time$,Trig)
5370   INTEGER D1(1:3200) BUFFER
5380   INTEGER D2(1:15000) BUFFER
5390   Count1$="3200"
5400   Count2$="15000"
5410   !
5420   !
5430   ! INFOTEK A-D ROUTINE SET UP FOR EXTERNAL TRIGGER
5440   !
5450   !
5460      Ad_sel_code=17
5470   !
5480   !INITIALIZATION OF THE A-D CONVERTER
5490   !
5500        OUTPUT Ad_sel_code;"RESET"
5510        OUTPUT Ad_sel_code;"INTERNAL","COUNT "&Count1$,"HOLDON"
5520        OUTPUT Ad_sel_code;"DELAYON","SELECT 1s1 end",Time$
5530        OUTPUT Ad_sel_code;"STATUS"
5540        ENTER Ad_sel_code;Resp$
5550        IF Resp$="--------" THEN
5560           ASSIGN @Ad200 TO Ad_sel_code;WORD
5570    !
5580    !  triggering of the HP3341A
5590    !
5600           ASSIGN @Buf1 TO BUFFER D1(*)
5610           ASSIGN @Buf2 TO BUFFER D2(*)
```

```
5620            IF Trig=1 THEN TRIGGER 707
5630            TRANSFER @Ad200 TO @Buf1;WAIT
5640            OUTPUT Ad_sel_code;"COUNT "&Count2$,"SELECT 1s10 end"
5650            TRANSFER @Ad200 TO @Buf2;WAIT
5660            MAT Dat(3201:18200)= D2
5670            MAT Dat= Dat*(.1)
5680            MAT Dat(1:3200)= D1
5690       ELSE
5700          PRINT "ERROR DURING INITIALIZATION =";Resp$
5710       END IF
5720    SUBEND
5730    !
5740    !
5750    SUB Plot_setup(Maxsec,Site$,Maxrng,Pltrng,Zone$)
5760    !
5770    !
5780    ! SET-UP OF THE TIME PLOT ON THE CRT
5790    !
5800    !
5810    IF Pltrng=150 THEN
5820      Num_labels=3
5830      Num_ticks=15
5840    END IF
5850    IF Pltrng=100 THEN
5860      Num_labels=4
5870      Num_ticks=20
5880    END IF
5890         GCLEAR
5900         GRAPHICS ON
5910         LINE TYPE 1
5920         VIEWPORT 15,120,15,80
5930         WINDOW 0,Maxsec,0,Pltrng
5940         AXES Maxsec/15,Pltrng/Num_ticks,0,0,Maxsec/3,Pltrng/Num_label
5950         CLIP OFF
5960         CSIZE 4,.6
5970         LORG 6
5980         T1=TIMEDATE MOD 86400
5990         Hrs=T1 DIV 3600
6000         T2=T1 MOD 3600
6010         Min=T2 DIV 60
6020         Qtrhr=Min DIV 15
6030         FOR M=0 TO Maxsec STEP INT(Maxsec/3)
6040            MOVE M,-Pltrng/45
6050            Qtrmin=Qtrhr*15+(M*3/Maxsec)*5
6060            IF Qtrmin=60 THEN
6070               Qtrmin=0
6080               Hrs=Hrs+1
6090            END IF
```

```
6100          LABEL USING "DD,A,ZZ";Hrs;":";Qtrmin
6110       NEXT M
6120       MOVE Maxsec/2,-15
6130       LABEL "TIME "&Zone$
6140  !
6150  ! LABEL ORDINATE
6160  !
6170       LORG 8
6180       FOR M=0 TO Pltrng STEP INT(Pltrng/Num_labels)
6190          MOVE 0,M
6200          LABEL M
6210       NEXT M
6220       LDIR PI/2
6230       LORG 6
6240       MOVE -Maxsec/7,Pltrng/2
6250       LABEL "RANGE IN METERS"
6260  !
6270  !  TITLE
6280  !
6290       LDIR 0
6300       LORG 4
6310       MOVE Maxsec/2,Pltrng+3
6320       LABEL DATE$(TIMEDATE);"      ";Site$
6330       CLIP ON
6340   SUBEND
6350  !
6360  !
6370  SUB File_init(Disc_address$,Nrec1,Nrec2,Nlast1,Nlast2,Ksave,File1$,File2$)
6380  !
6390  !
6400  !  CREATE THE STORAGE FILE ON THE DISC FOR
6410  !  THE REDUCED DATA
6420  !
6430  !
6440     INPUT "ENTER THE REDUCED DATA OUTPUT FILENAME ",File1$
6450     INPUT "Is this the first entry in the file?",Q$
6460     File2$=File1$[1,7]&"EXT"&Disc_address$
6470     File1$=File1$&Disc_address$
6480     IF Q$="YES" OR Q$="Y" THEN
6490       CREATE BDAT File1$,Nrec1,8*(2*Ksave+10)
6500       CREATE BDAT File2$,Nrec2,8*2*Ksave
6510     END IF
6520       ASSIGN @File1 TO File1$
6530       STATUS @File1,7;Nlast1        ! next record in file 1
6540       ASSIGN @File2 TO File2$
6550       STATUS @File2,7;Nlast2        ! next record in file 2
6560  !
6570  SUBEND
6580  !
```

```
6590  !
6600  SUB Ct_plot(Ct(*),Pltrng,Maxrng,INTEGER Kmax,Site$)
6610  ! CT^2 PLOT ROUTINE
6620  ! Pltrng is the maximum range in 50 m increments (150m typically)
6630  ! Maxrng is the actual maximum range that depends on temperature
6640  ! Kmax   - the maximum number of Ct dat points Ct(Kmax).
6650     GCLEAR
6660     IF Pltrng=150 THEN
6670       Num_labels=3
6680       Num_ticks=15
6690     END IF
6700     IF Pltrng=100 THEN
6710       Num_labels=4
6720       Num_ticks=20
6730     END IF
6740     Decades=5
6750     VIEWPORT 15,120,15,80
6760     WINDOW 0,Decades,0,Pltrng
6770     AXES 1,Pltrng/Num_ticks,0,0,1,Pltrng/Num_labels
6780     CLIP OFF
6790     CSIZE 3,.9
6800     LORG 6
6810     FOR M=0 TO Decades
6820       MOVE M,-Pltrng/45
6830       LABEL (M-Decades)
6840     NEXT M
6850     MOVE Decades/2,-15
6860     CSIZE 4
6870     LABEL "LOG OF CT^2"
6880     LORG 8
6890     FOR M=0 TO Pltrng STEP INT(Pltrng/Num_labels)
6900        MOVE 0,M
6910        LABEL M
6920     NEXT M
6930     LDIR PI/2
6940     LORG 6
6950     MOVE -Decades/7,Pltrng/2
6960     CSIZE 4
6970     LABEL "RANGE IN METERS"
6980     LDIR 0
6990     LORG 4
7000     MOVE Decades/2,Pltrng+3
7010     LABEL "TIME AVERAGED CT^2     ";Site$
7020     CLIP ON
7030     MOVE Decades,0
7040     Inc=Maxrng/Kmax
7050     FOR I=1 TO Kmax
7060        Ypl=Inc*(I-.5)
```

```
7070        Pnt=LGT(Ct(I))+Decades
7080        IF Pnt>Decades THEN Pnt=Decades
7090        IF Pnt<0 THEN Pnt=0
7100        DRAW Pnt,Ypl
7110      NEXT I
7120      DUMP GRAPHICS #701
7130      PRINT "
7140      PRINTER IS CRT
7150      GCLEAR
7160      SUBEND
7170    SUB Attenuation(Freq,Temp,Rel,Atmos_pres,Alpha)
7180    ! 11 June 1991: DLW
7190    !
7200    ! This subprogram calculates the attenuation coefficient
7210    ! of sound in air based upon equations in H. BASS,
7220    ! Acoustical. Soc. Am.(xxx 1991)
7230    !
7240    ! Alpha  -  Intensiy attenuation coefficient of sound
7250    !           (alpha is normally calculated for pressure)
7260    ! Atmos_pres  -  atmospheric pressure in mb
7270    ! Es -  Saturation vapor pressure
7280    ! Freq - sound frequency in Hz
7290    ! H  -  absolute humidity (mb)
7300    ! Rel - relative humidity in %
7310    ! Temp - Celcius temperature
7320    !
7330    ! Saturation vapor pressure using Hooper formulation
7340      T=Temp
7350      A0=1.3521
7360      A1=1.6369E-2
7370      A2=3.1794E-5
7380      A3=-1.4892E-7
7390      Es=(A0+T*(A1+T*(A2+T*A3)))^6
7400      H=Rel*Es/Atmos_pres       ! Absolute humidity in %
7410    !
7420    ! H. Bass Attenuation calculation
7430    !
7440    F2=Freq*Freq
7450    Pso=Atmos_pres/1013.25  ! Relative pressure
7460    Tk=Temp+273.15          ! KELVIN TEMPERATURE
7470    Tr=293.15               ! REFERENCE TEMPERATURE K
7480    Tkr=Tk/Tr
7490    !
7500    ! Compute nitrogen and oxygen relaxation frequencies
7510    Frn=Pso/SQR(Tkr)*(9+280*H*EXP(-4.179*((1/Tkr)^.3333333-1)))
7520    Fro=Pso*(24+4.04E+4*H*(.02+H)/(.391+H))
7530    !
7540    Alpha=F2*(1.84E-11*SQR(Tkr)/Pso+Tkr^(-2.5)*(1.278E-2*EXP(-2239.1/Tk)/(Fro+
7550    Alpha=2*Alpha  !  convert to nepers/m (intensity)
7560    SUBEND
```

APPENDIX B. ACOUSTIC SOUNDER DATA FROM AMOS

The following is a representative set of acoustic echo-sounder C_T^2 profiles collected at AMOS during June-July, 1991. (Note: The C_T^2 profiles need to be multiplied by a factor of 3.8 to be calibrated.)

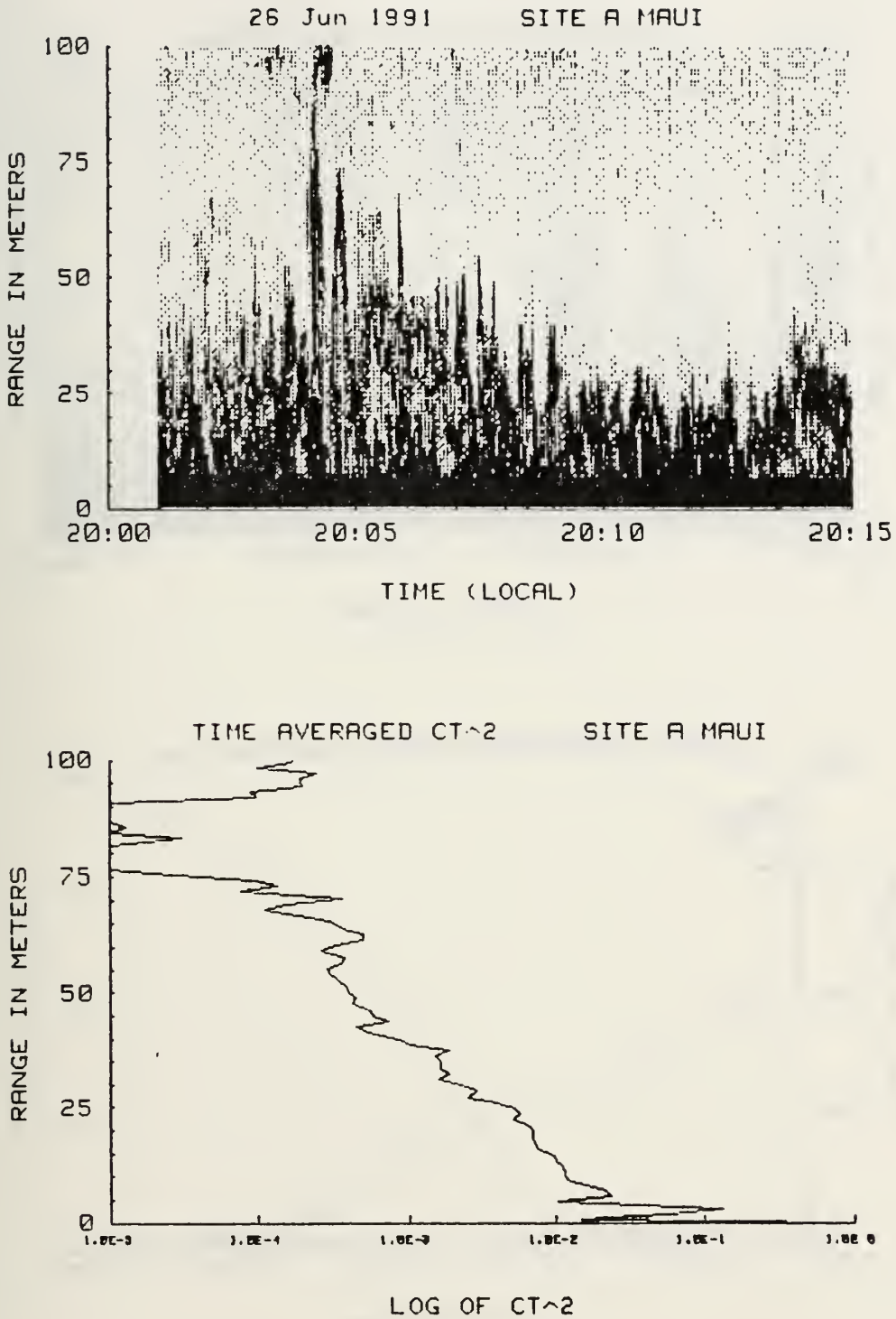

Figure 31. Echo-sounder Turbulence Profile, 26 June, 1991.

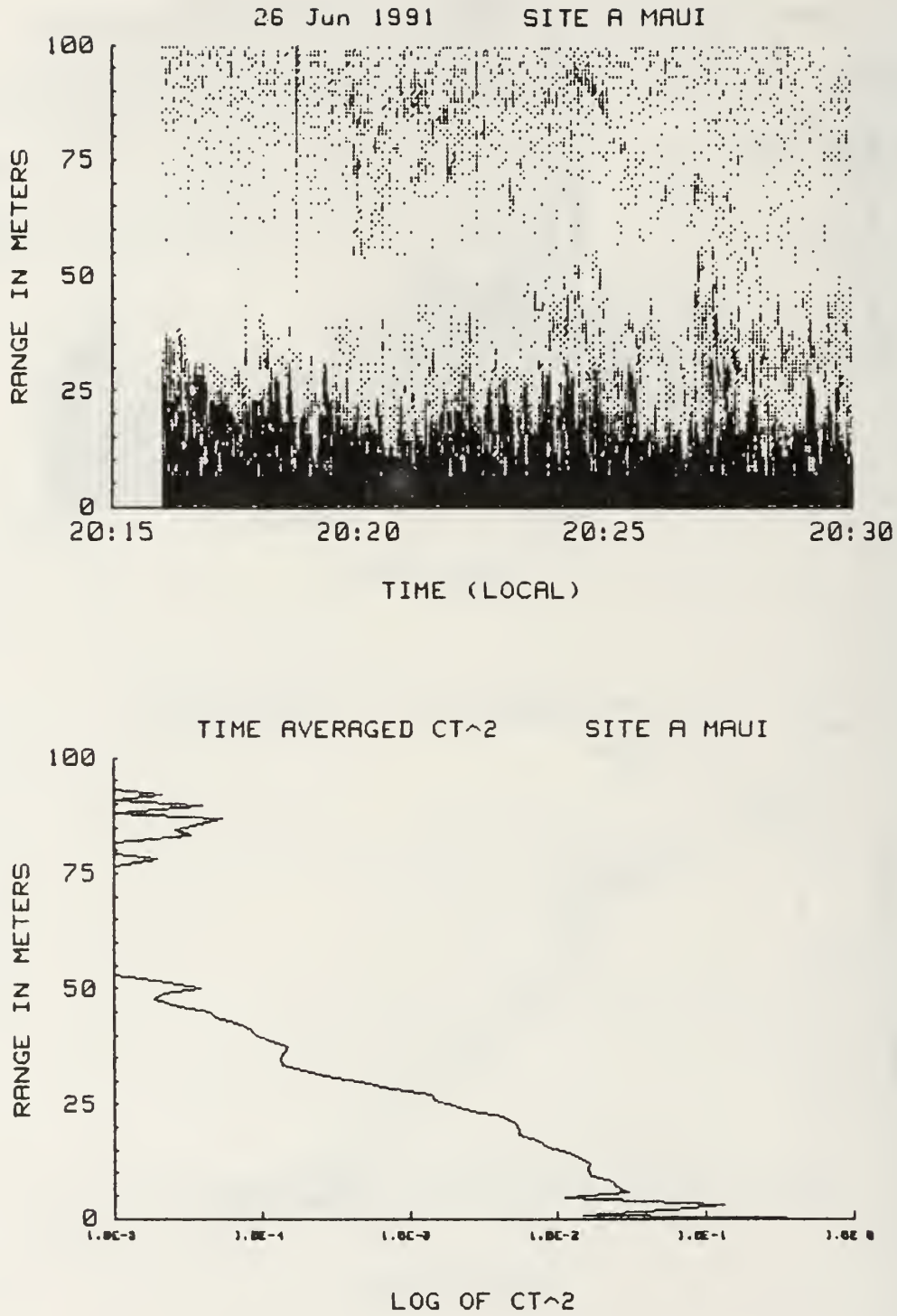

Figure 32. Echo-sounder Turbulence Profile, 26 June, 1991.

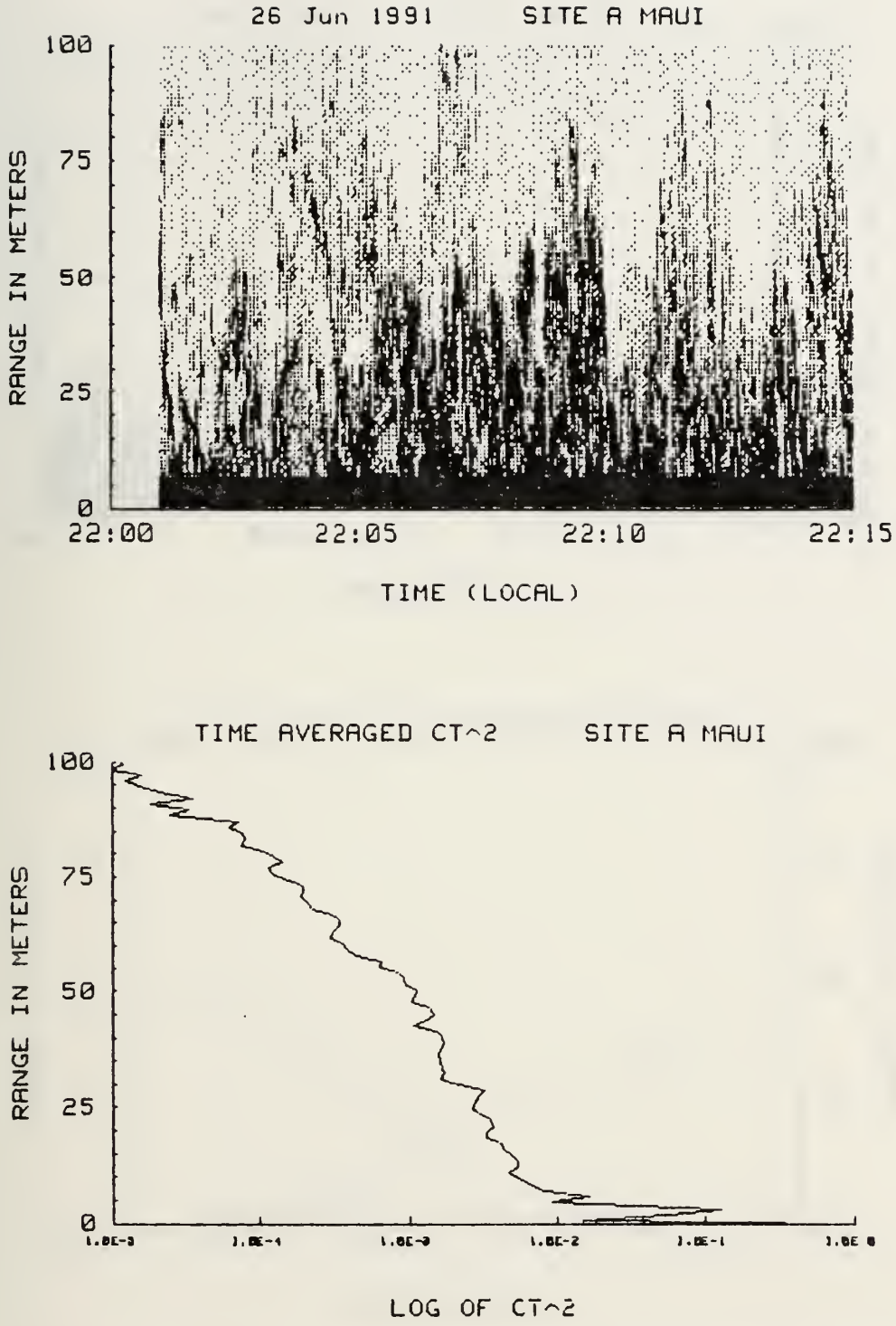

Figure 33. Echo-sounder Turbulence Profile, 26 June, 1991.

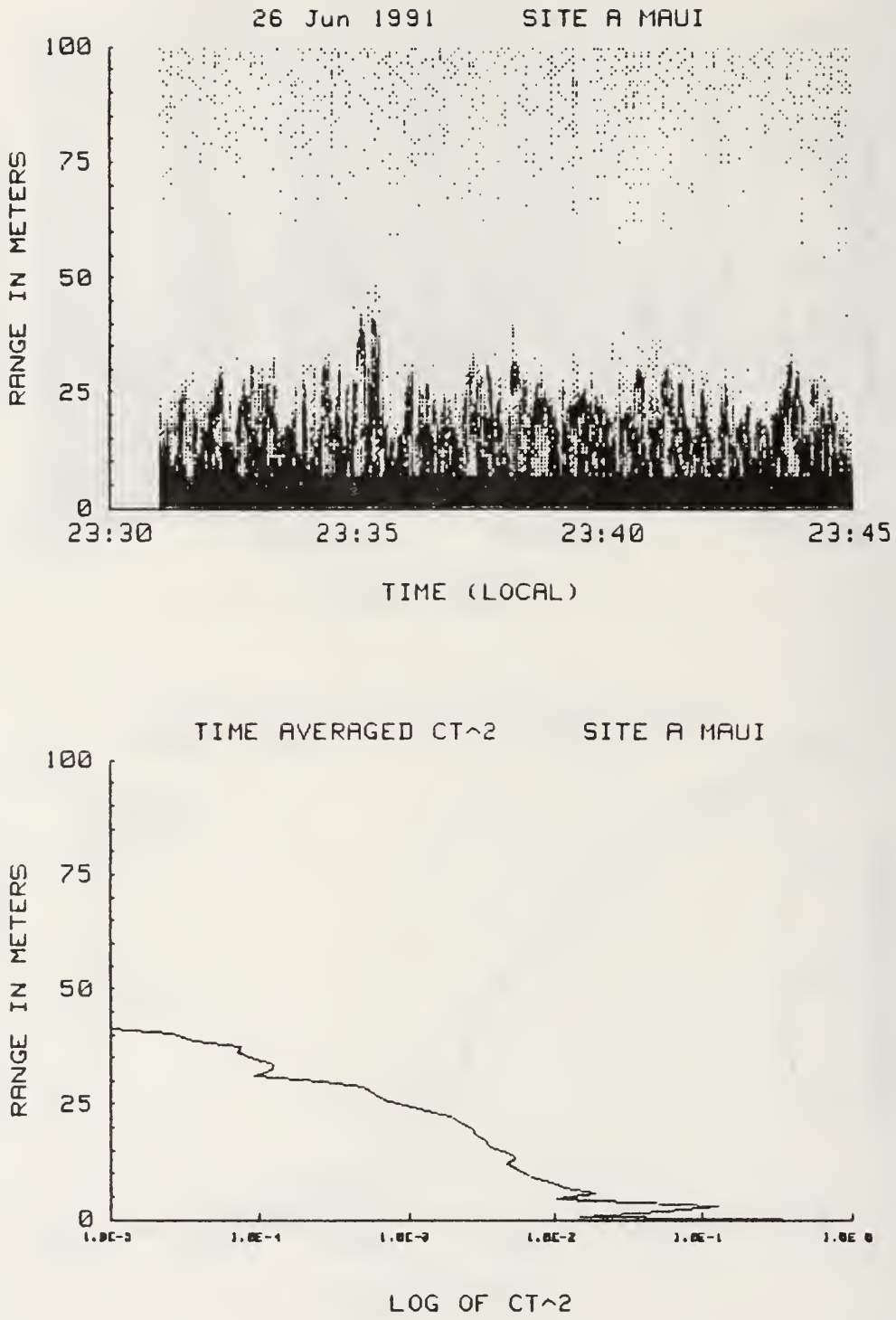

Figure 34. Echo-sounder Turbulence Profile,26 June, 1991.

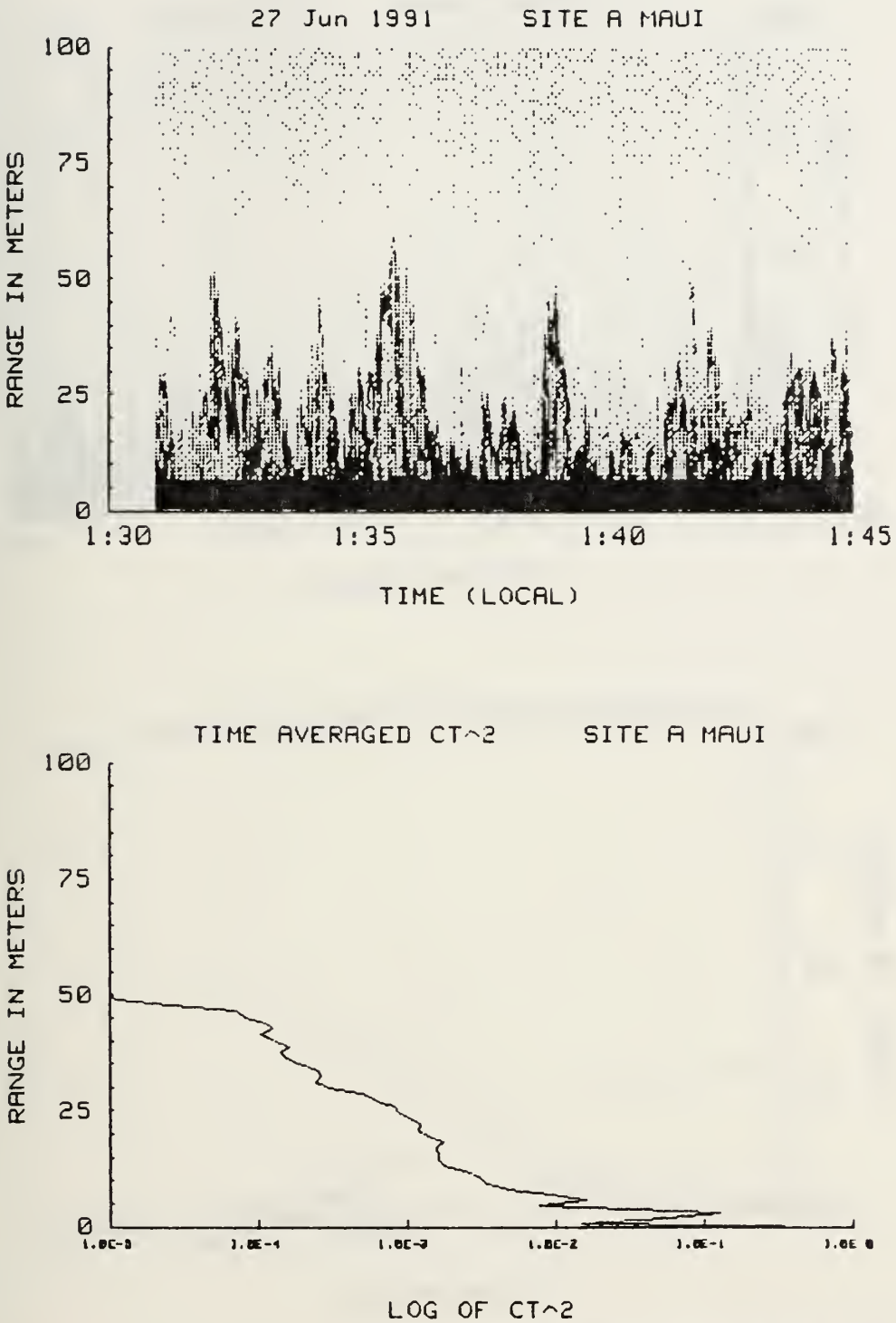

Figure 35. Echo-sounder Turbulence Profile, 27 June, 1991.

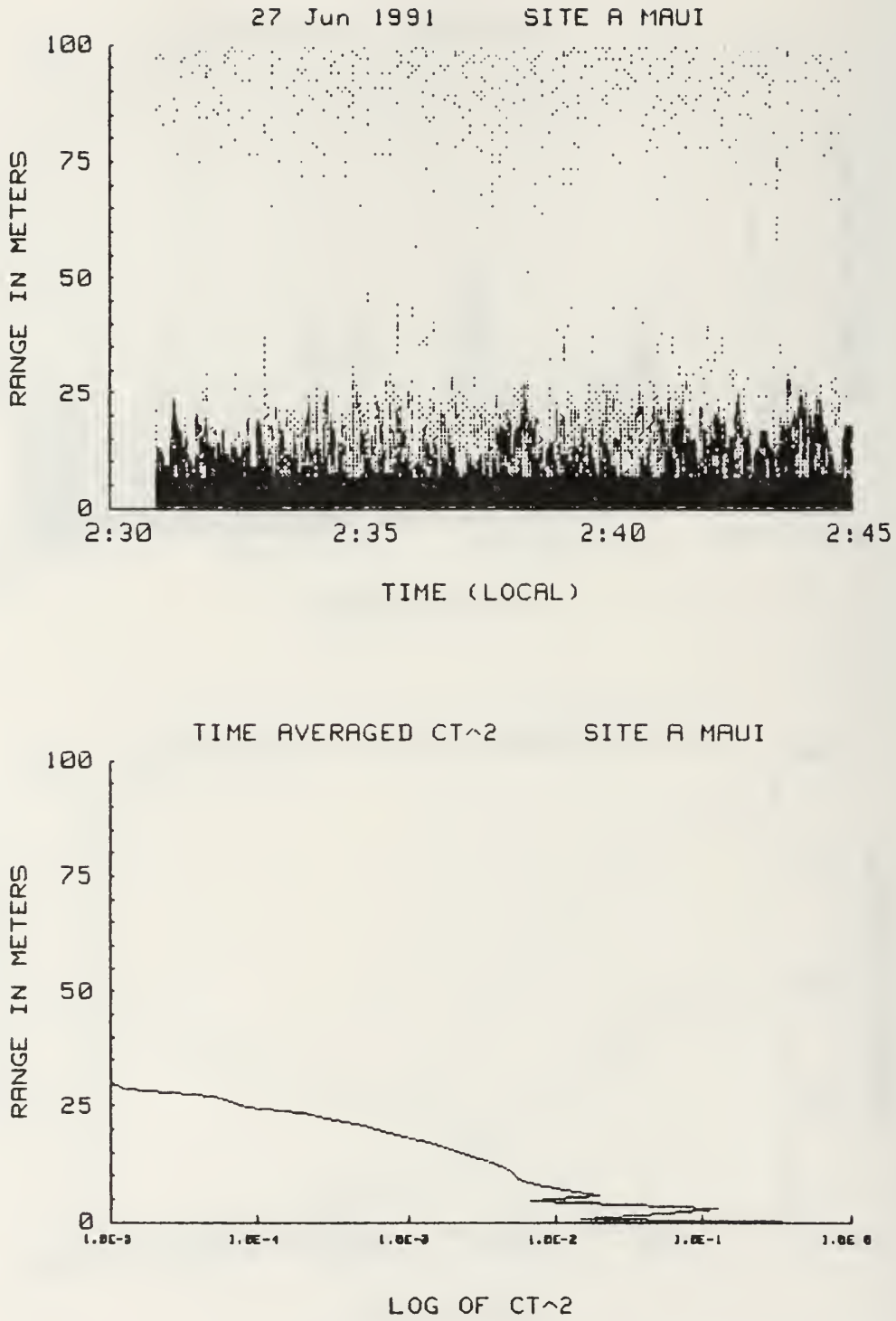

Figure 36. Echo-sounder Turbulence Profile, 27 June, 1991.

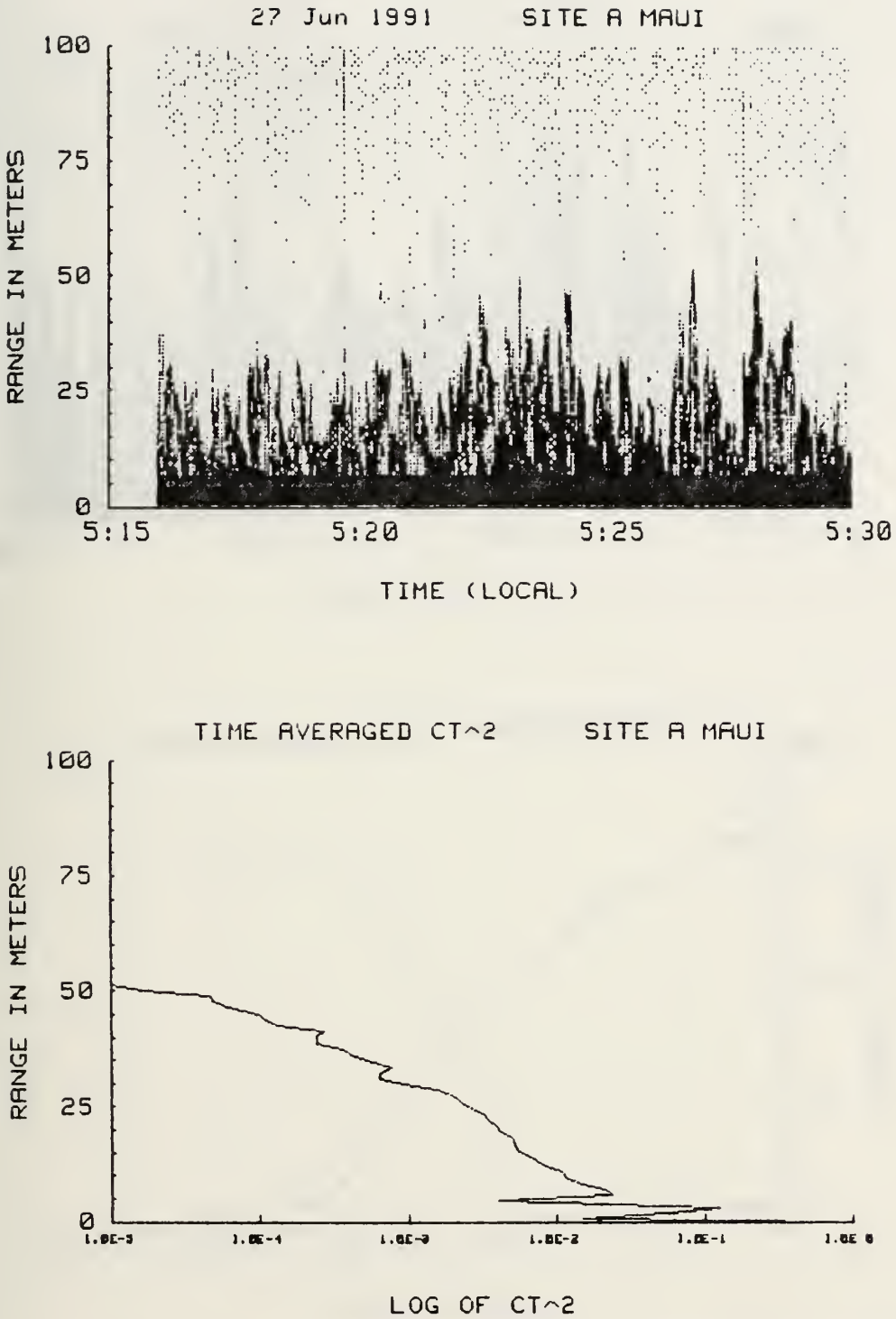

Figure 37. Echo-sounder Turbulence Profile, 27 June, 1991.

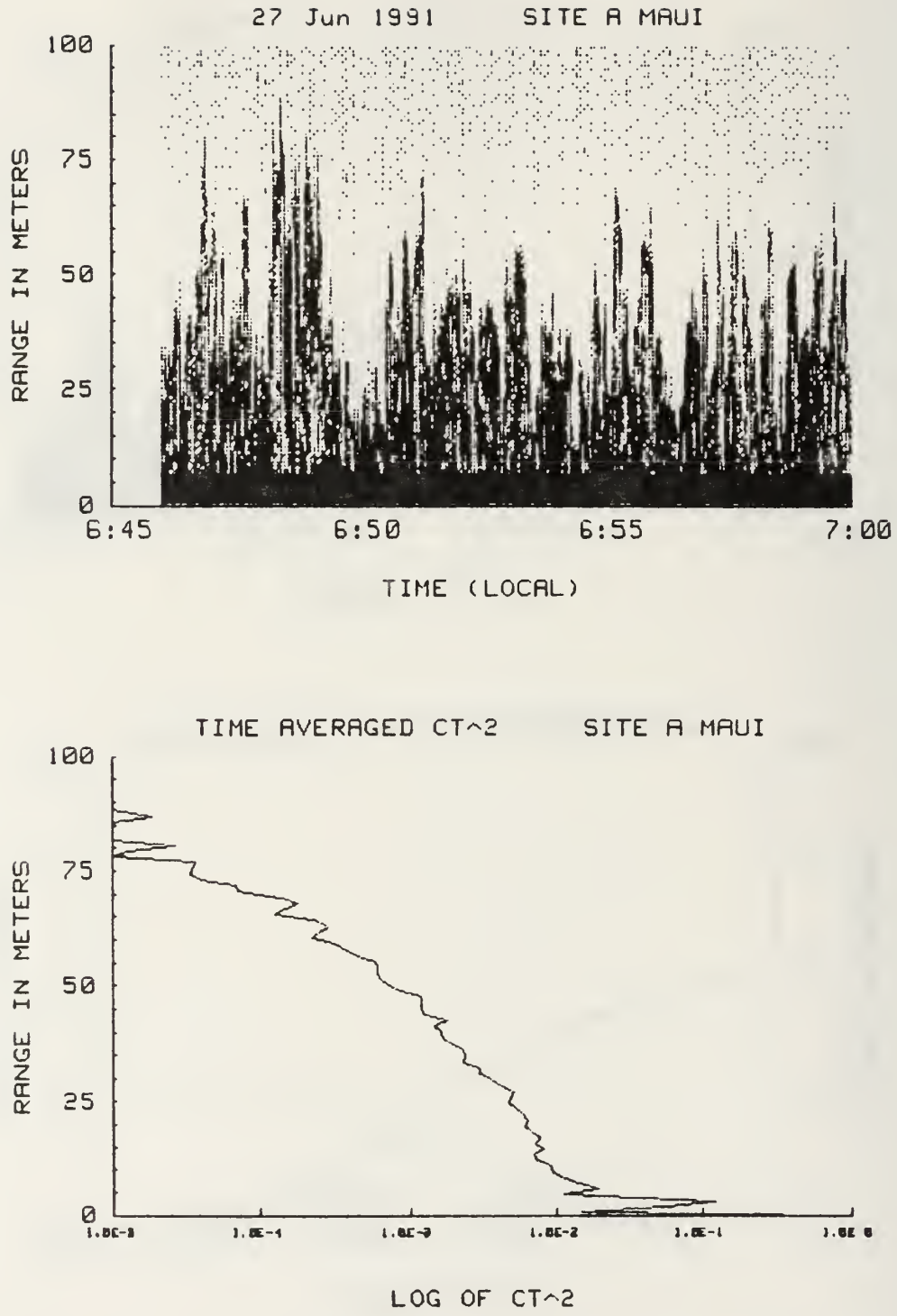

Figure 38. Echo-sounder Turbulence Profile, 27 June, 1991.

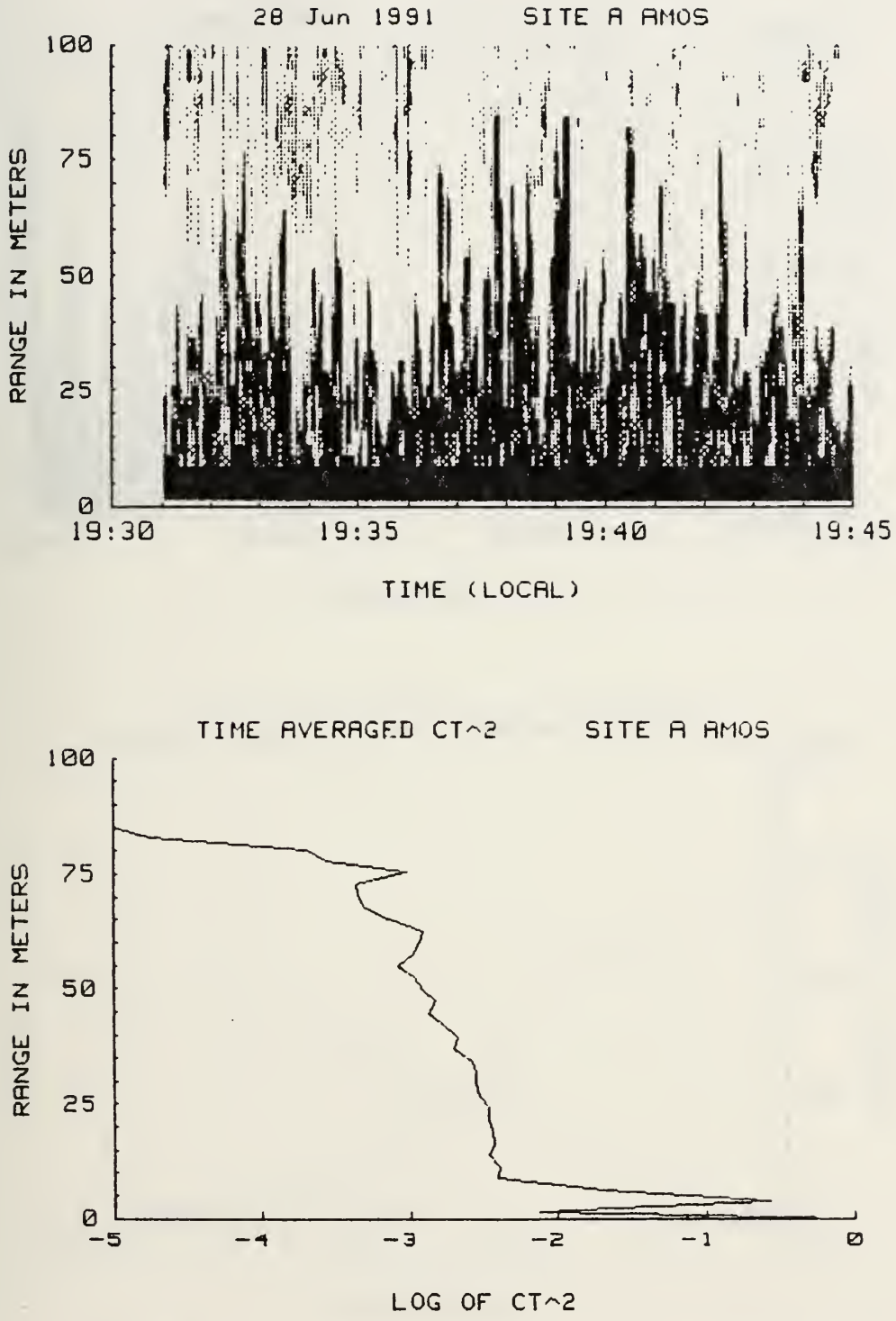

Figure 39. Echo-sounder Turbulence Profile, 27 June, 1991.

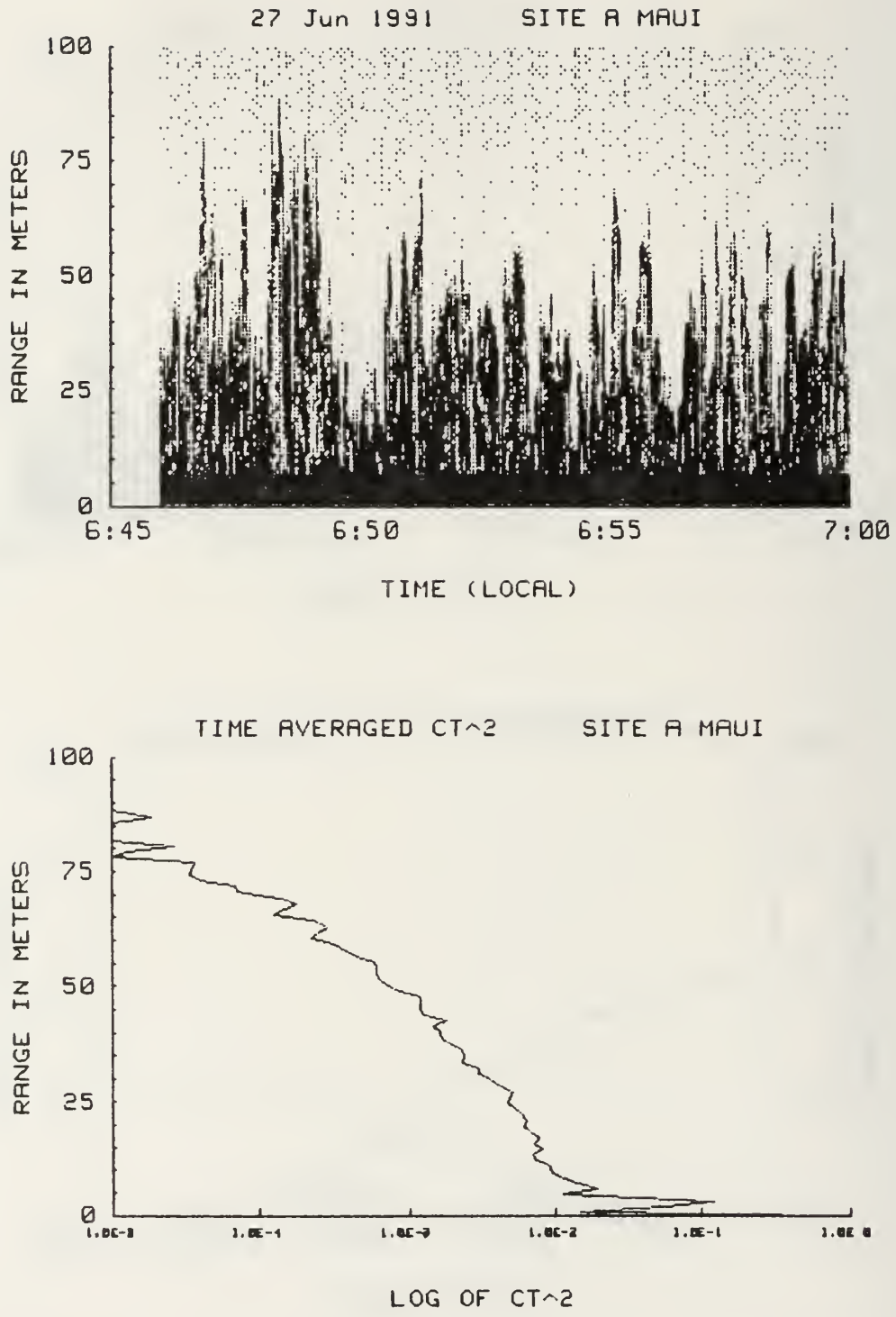

Figure 38. Echo-sounder Turbulence Profile, 27 June, 1991.

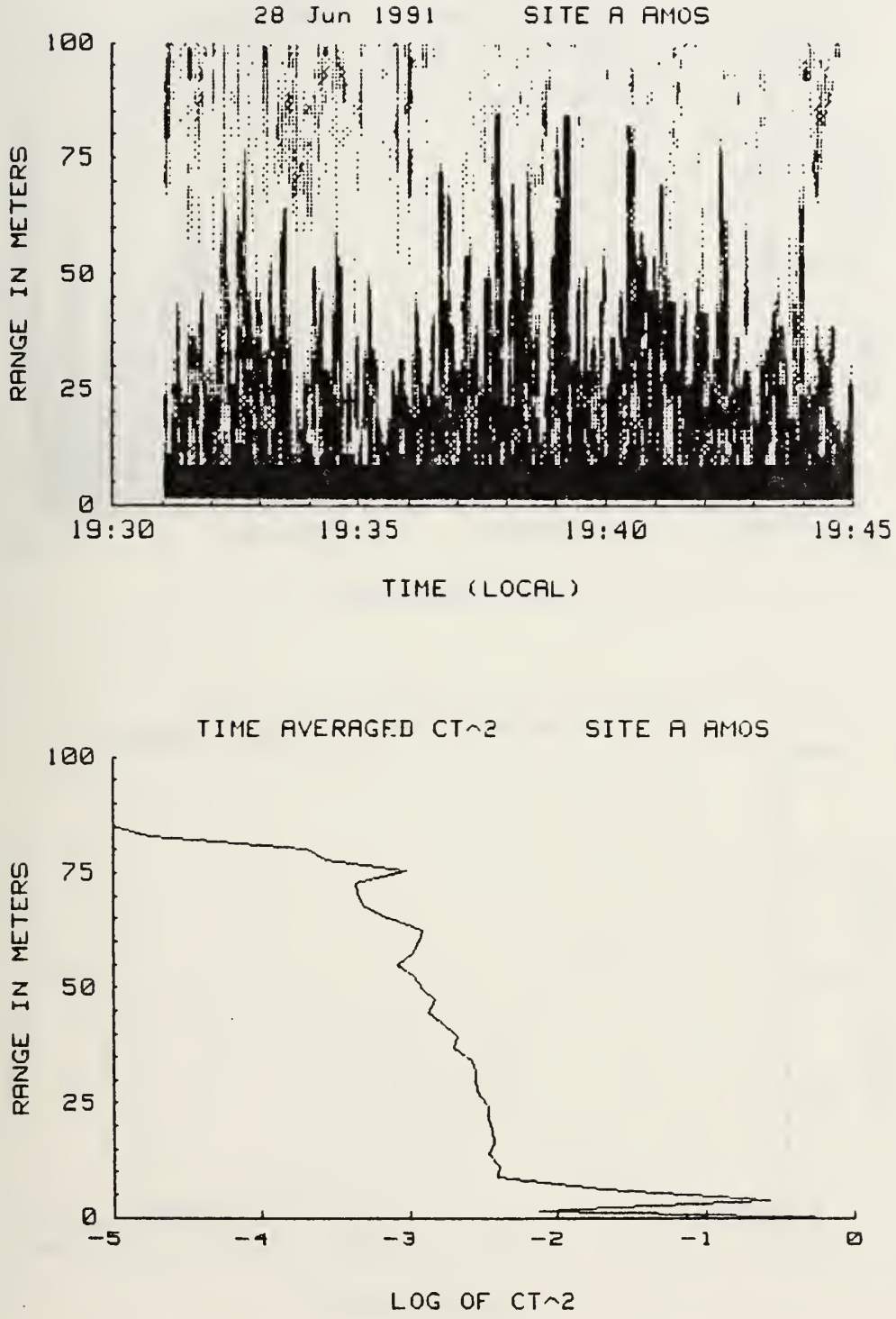

Figure 39. Echo-sounder Turbulence Profile, 27 June, 1991.

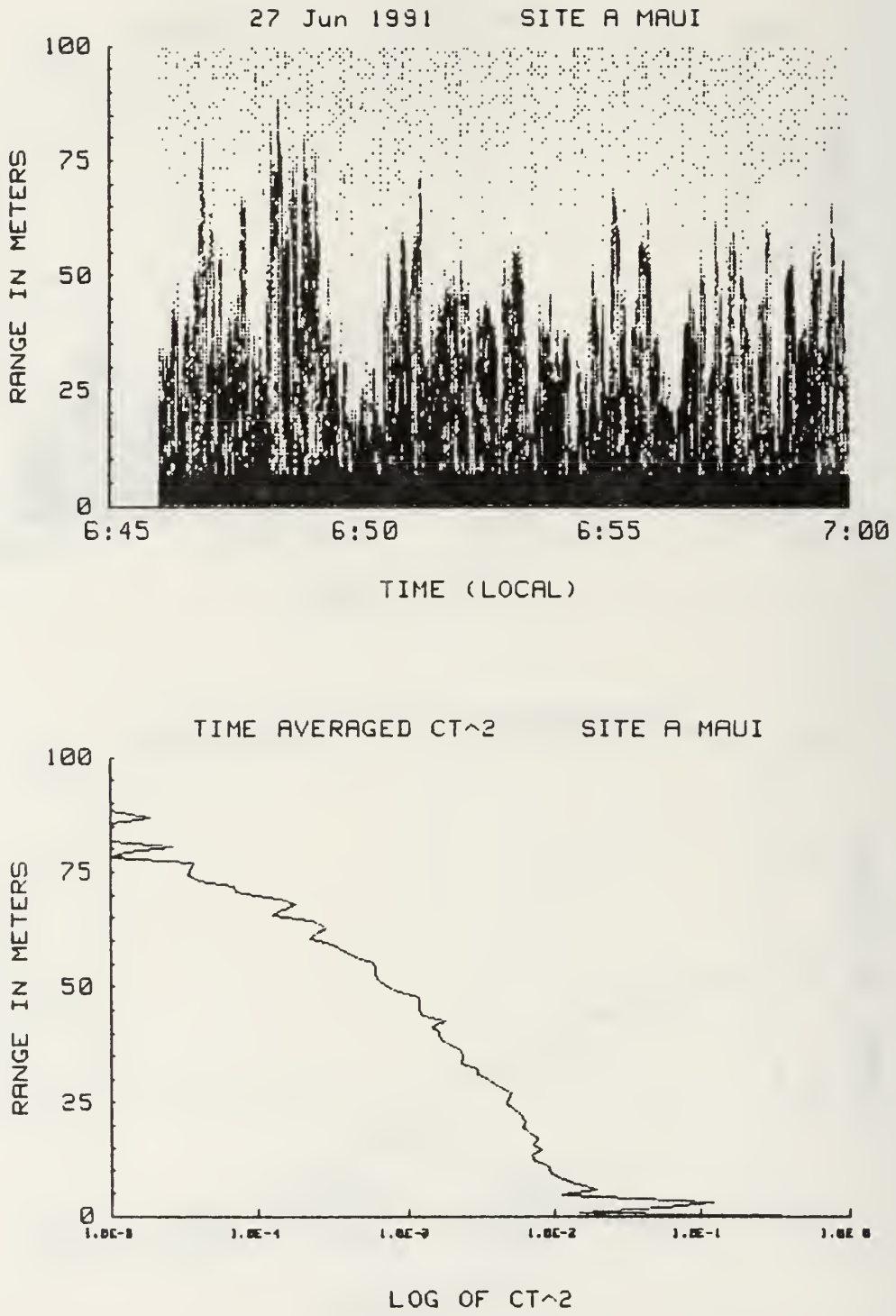

Figure 38. Echo-sounder Turbulence Profile, 27 June, 1991.

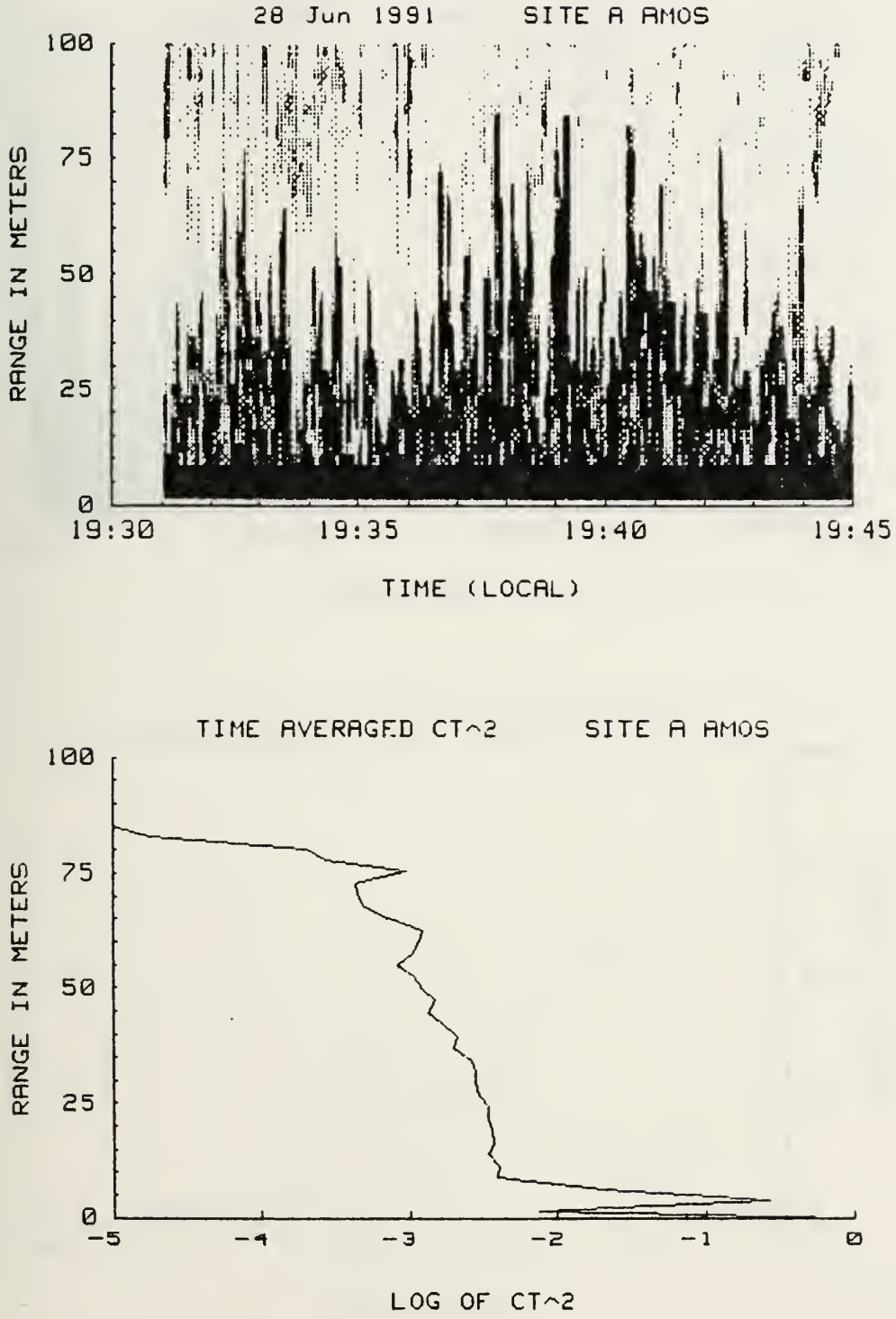

Figure 39. Echo-sounder Turbulence Profile, 27 June, 1991.

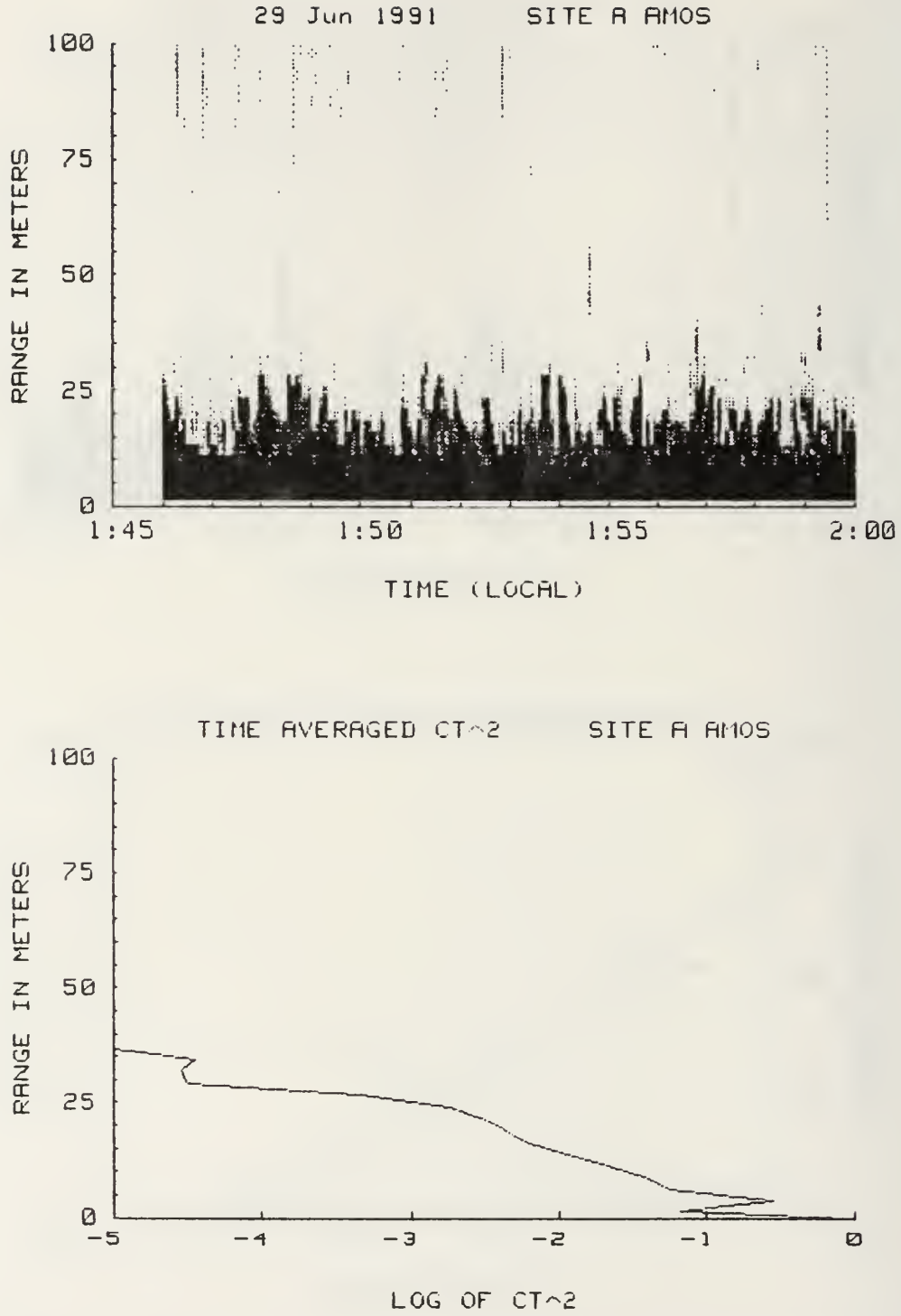

Figure 44. Echo-sounder Turbulence Profile, 29 June, 1991.

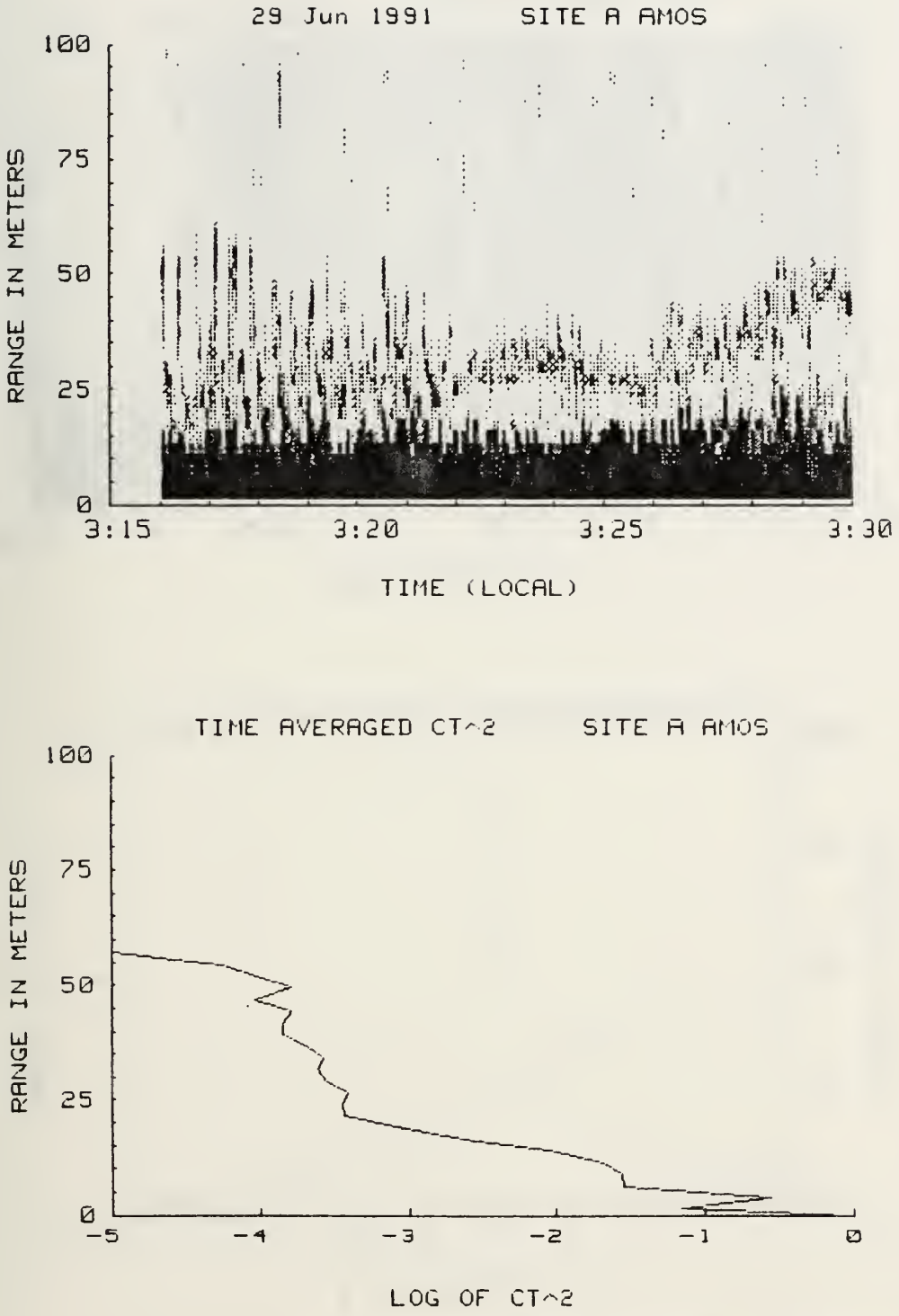

Figure 45. Echo-sounder Turbulence Profile, 29 June, 1991.

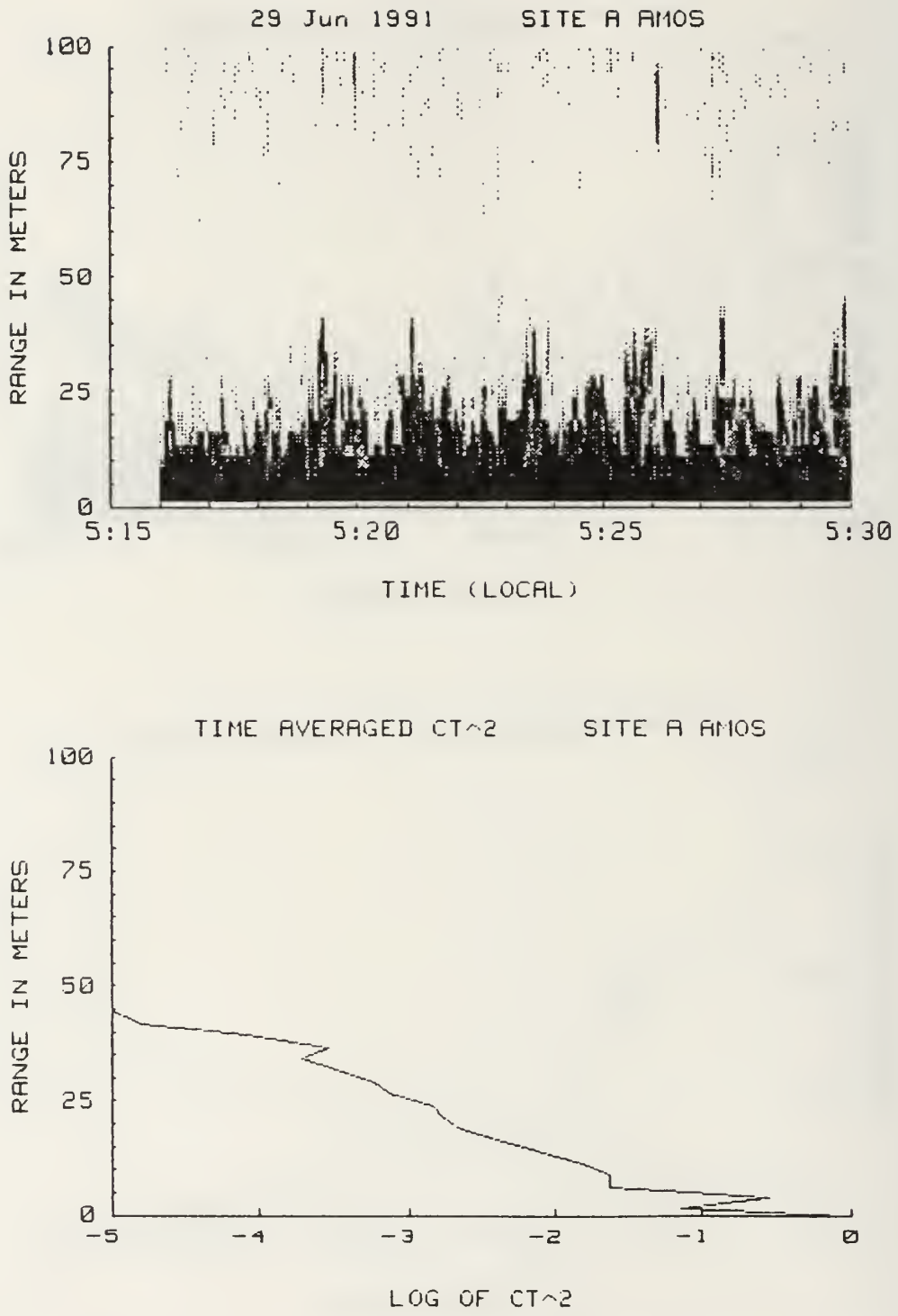

Figure 46. Echo-sounder Turbulence Profile, 29 June, 1991.

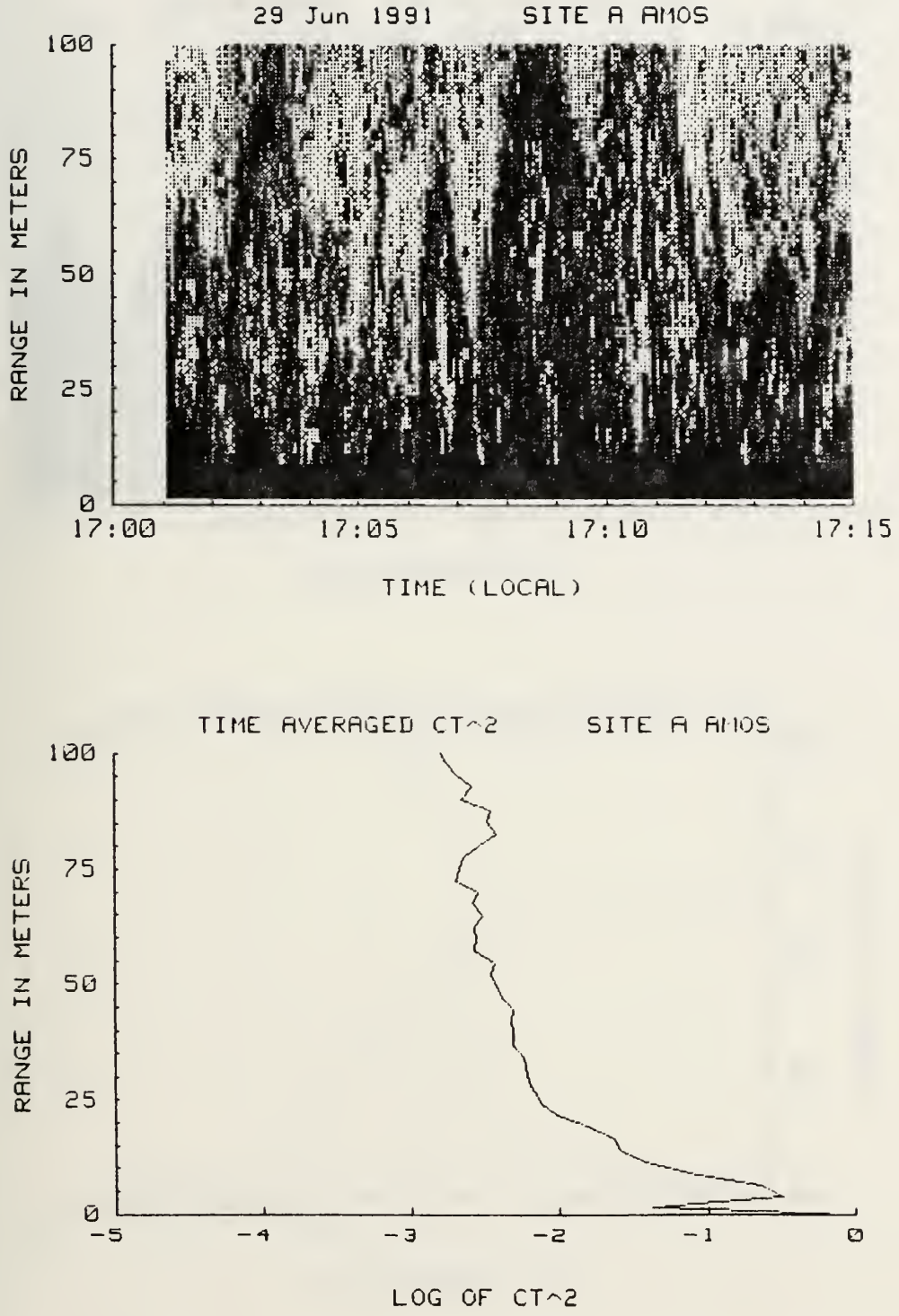

Figure 47. Echo-sounder Turbulence Profile, 29 June, 1991.

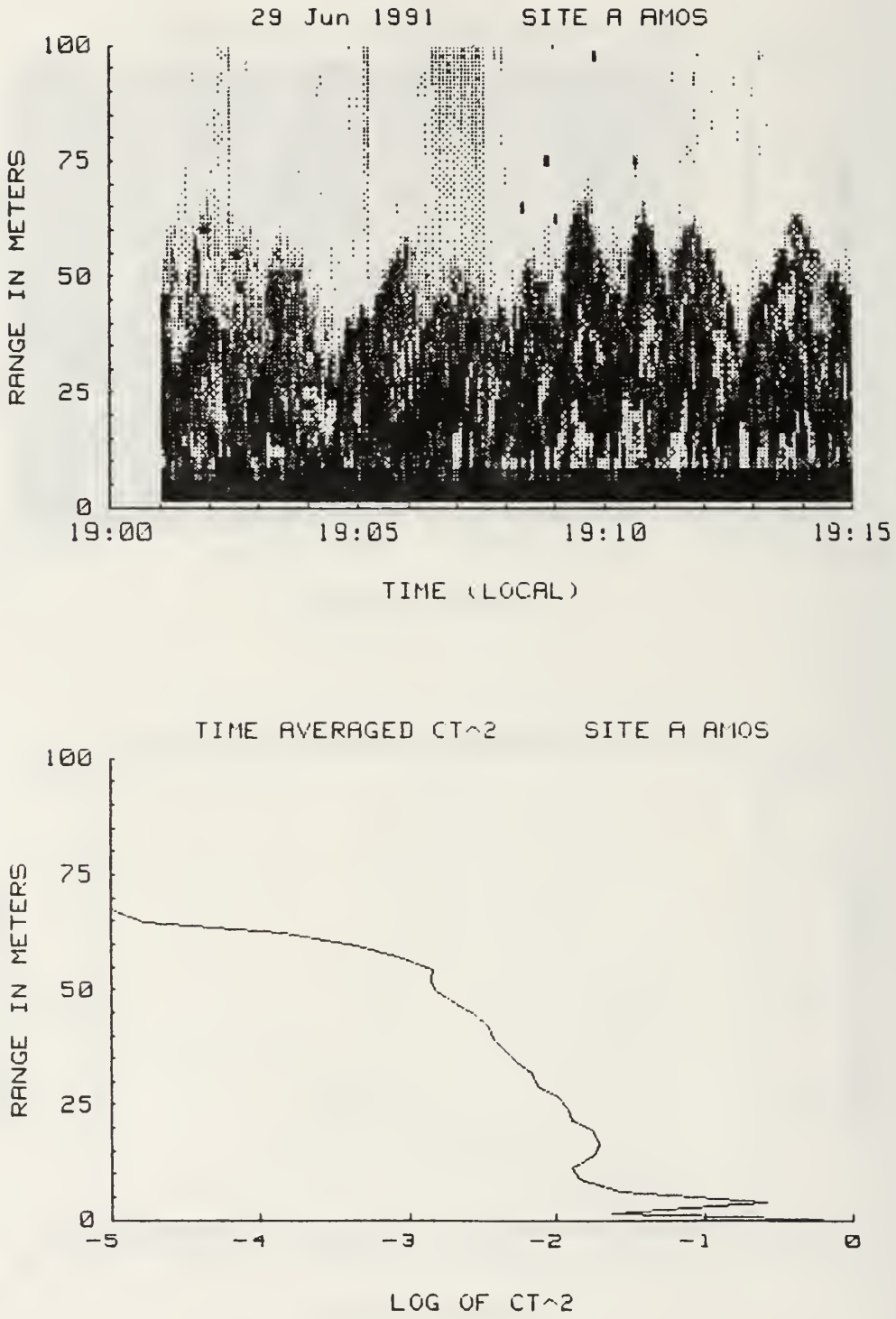

Figure 48. Echo-sounder Turbulence Profile, 29 June, 1991.

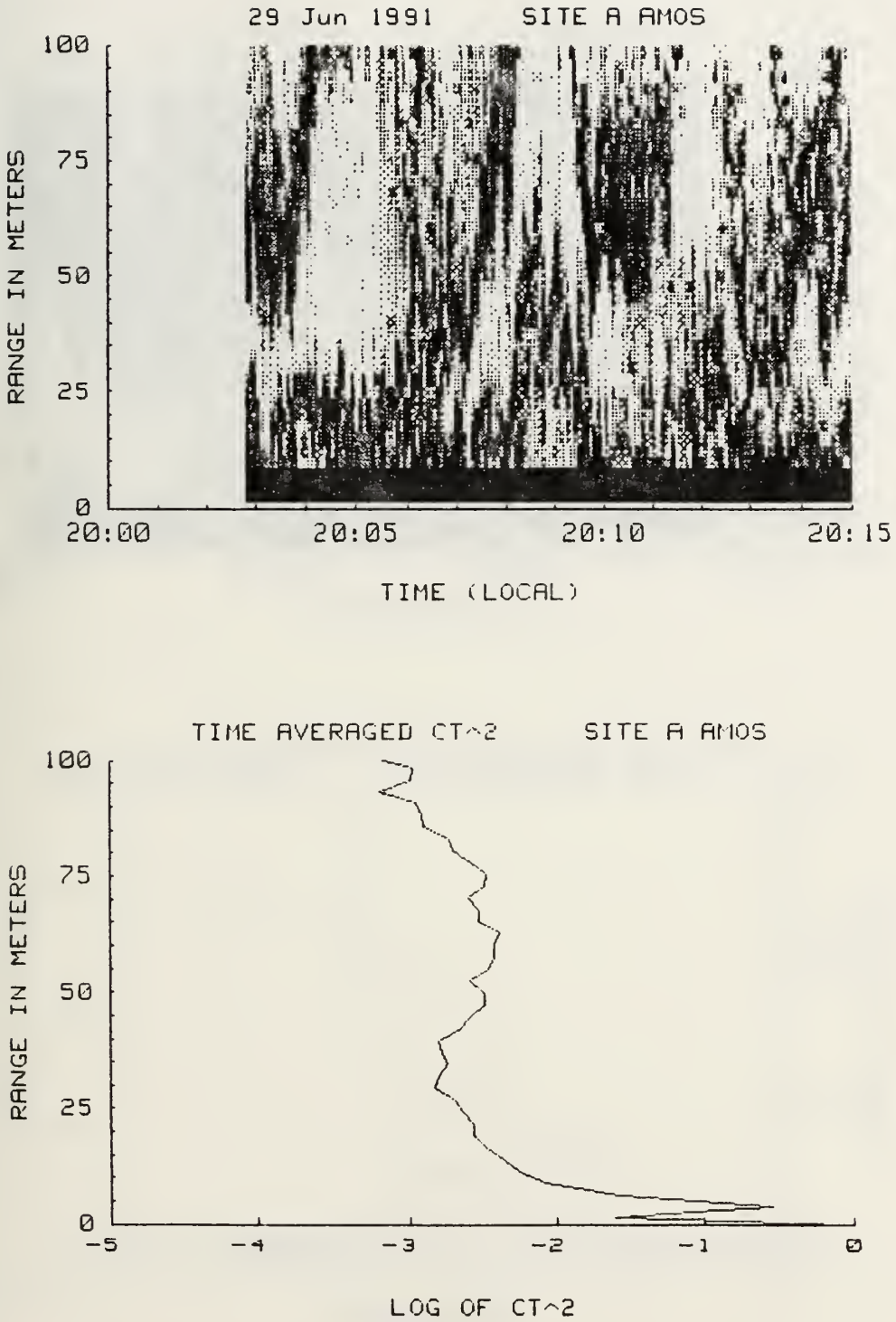

Figure 49. Echo-sounder Turbulence Profile, 29 June, 1991.

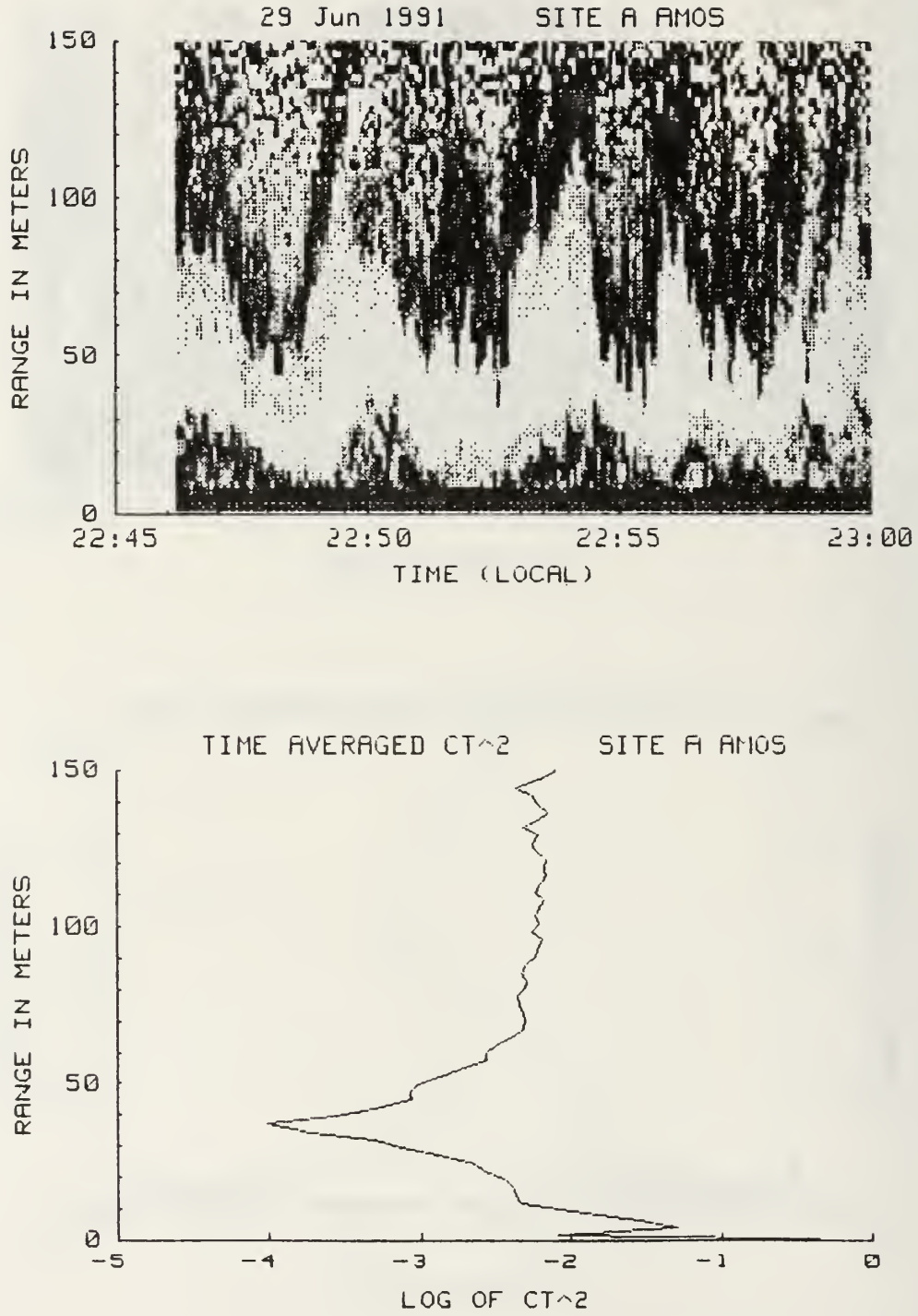

Figure 50. Echo-sounder Turbulence Profile, 29 June, 1991.

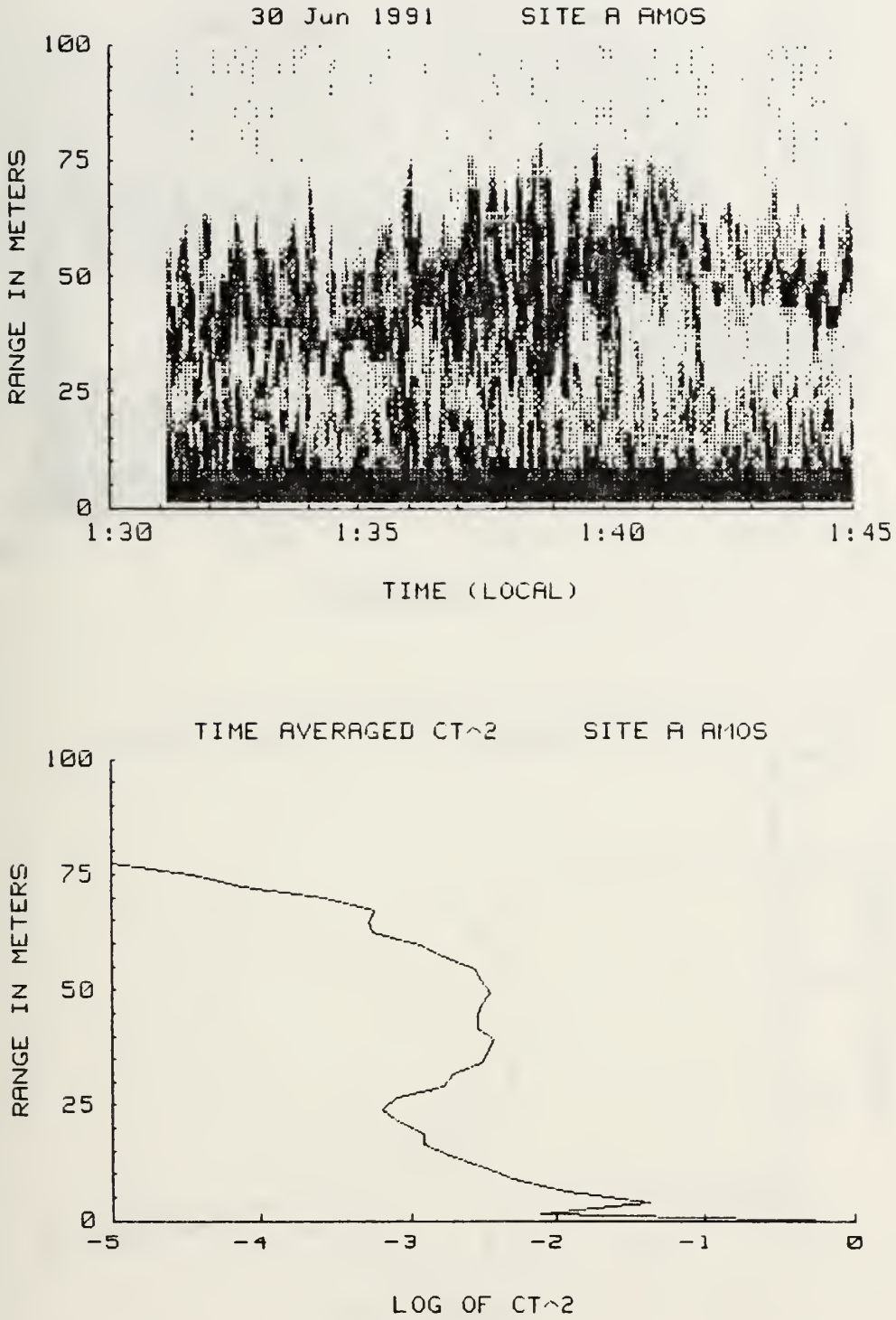

Figure 51. Echo-sounder Turbulence Profile, 30 June, 1991.

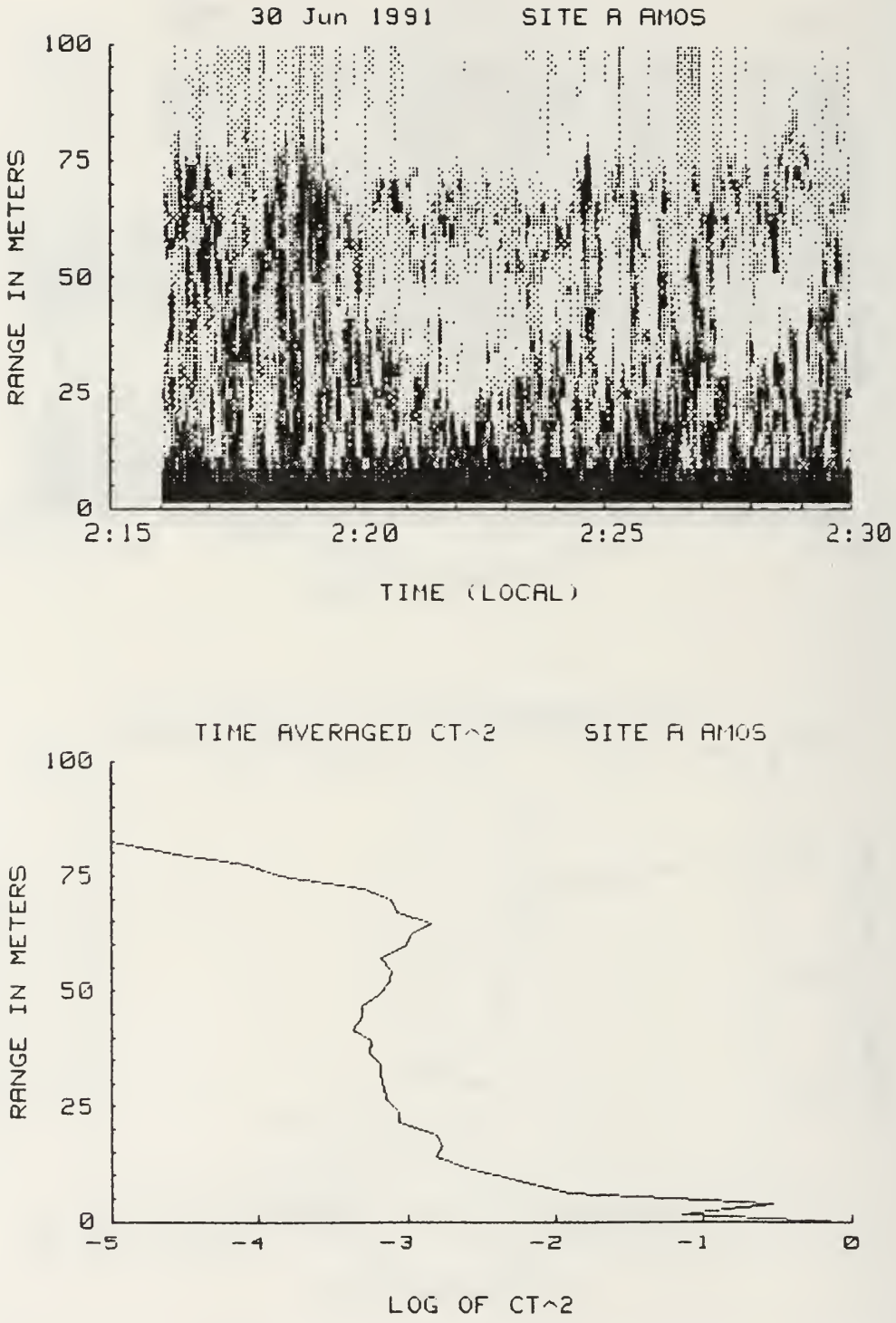

Figure 52. Echo-sounder Turbulence Profile, 30 June, 1991.

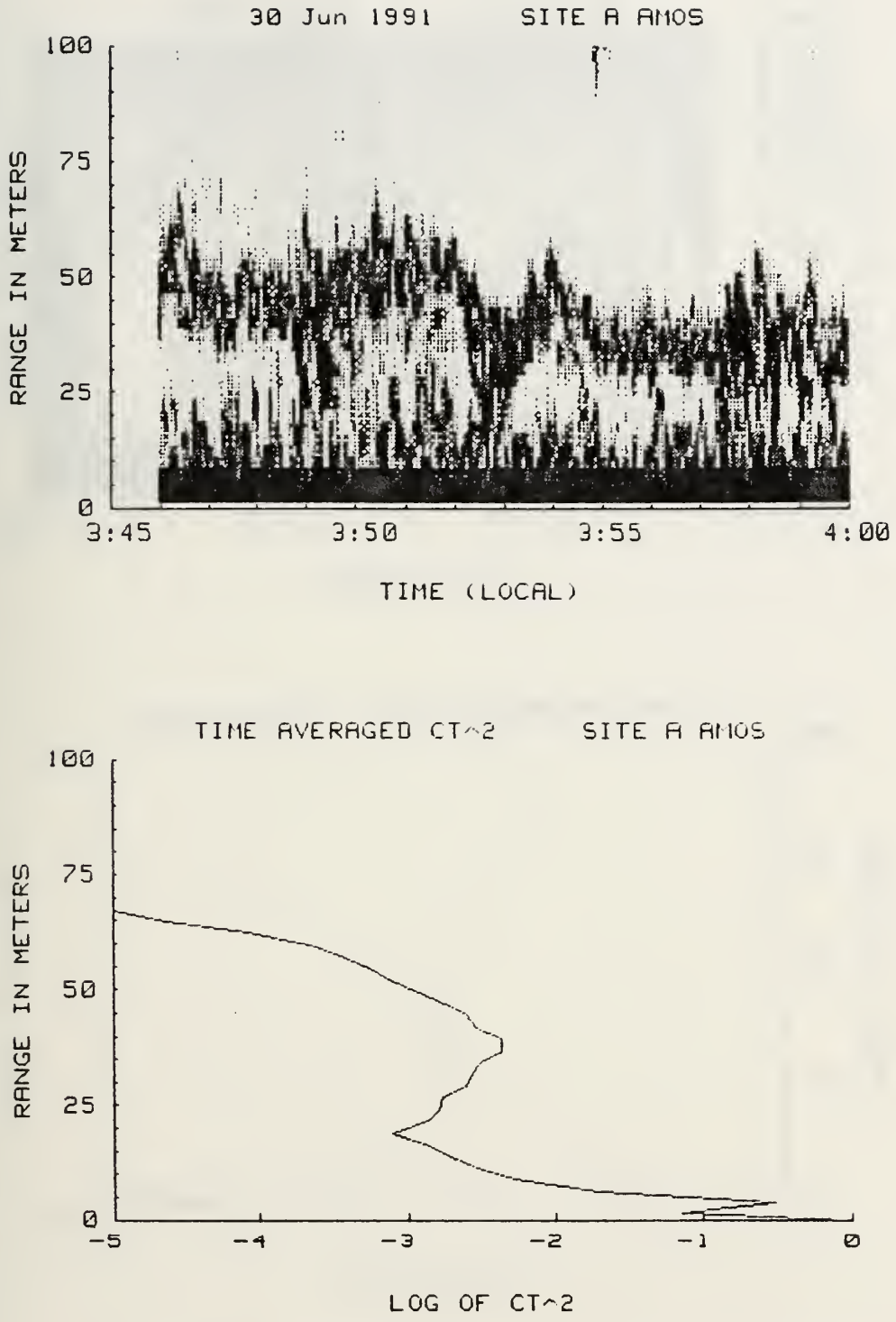

Figure 53. Echo-sounder Turbulence Profile, 30 June, 1991.

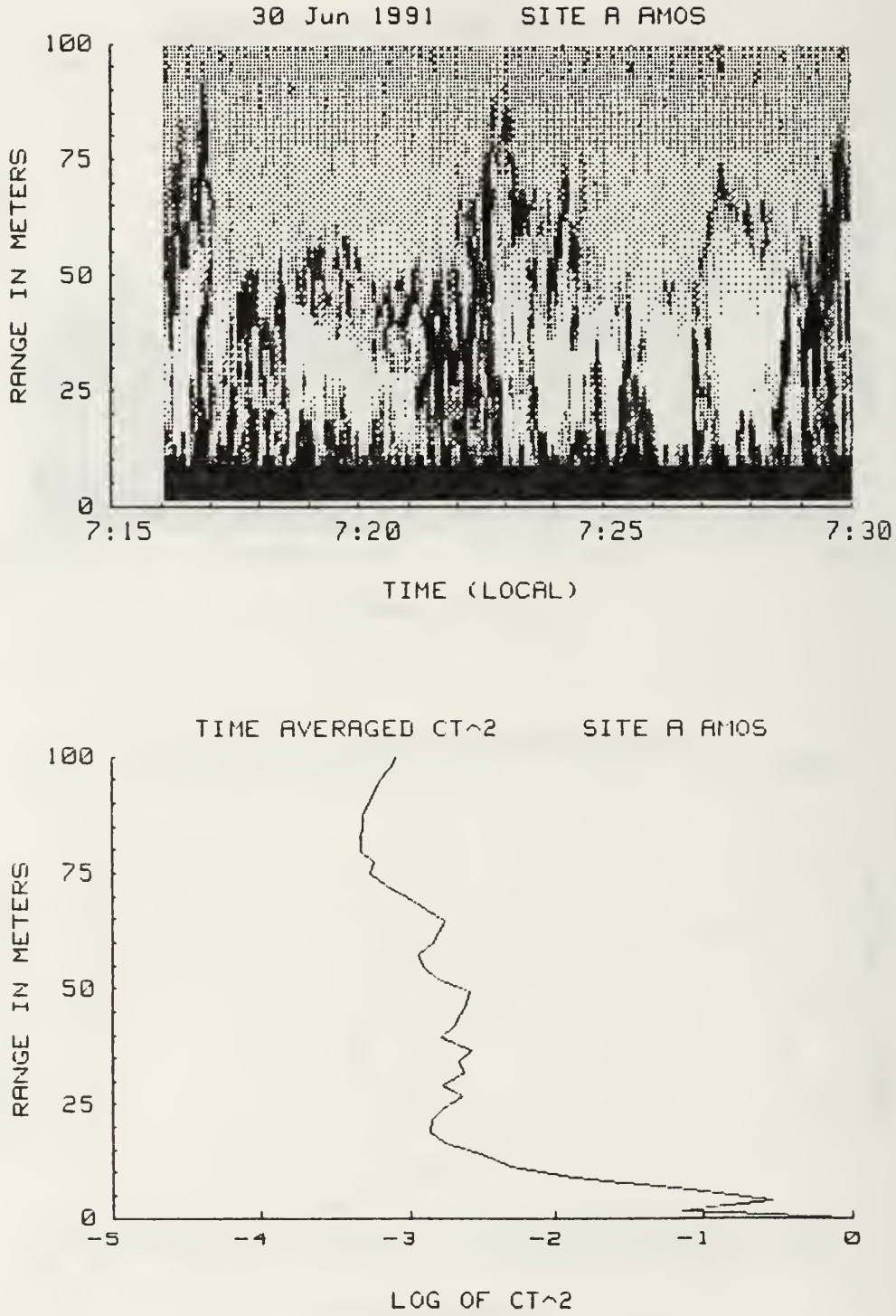

Figure 54. Echo-sounder Turbulence Profile, 30 June, 1991.

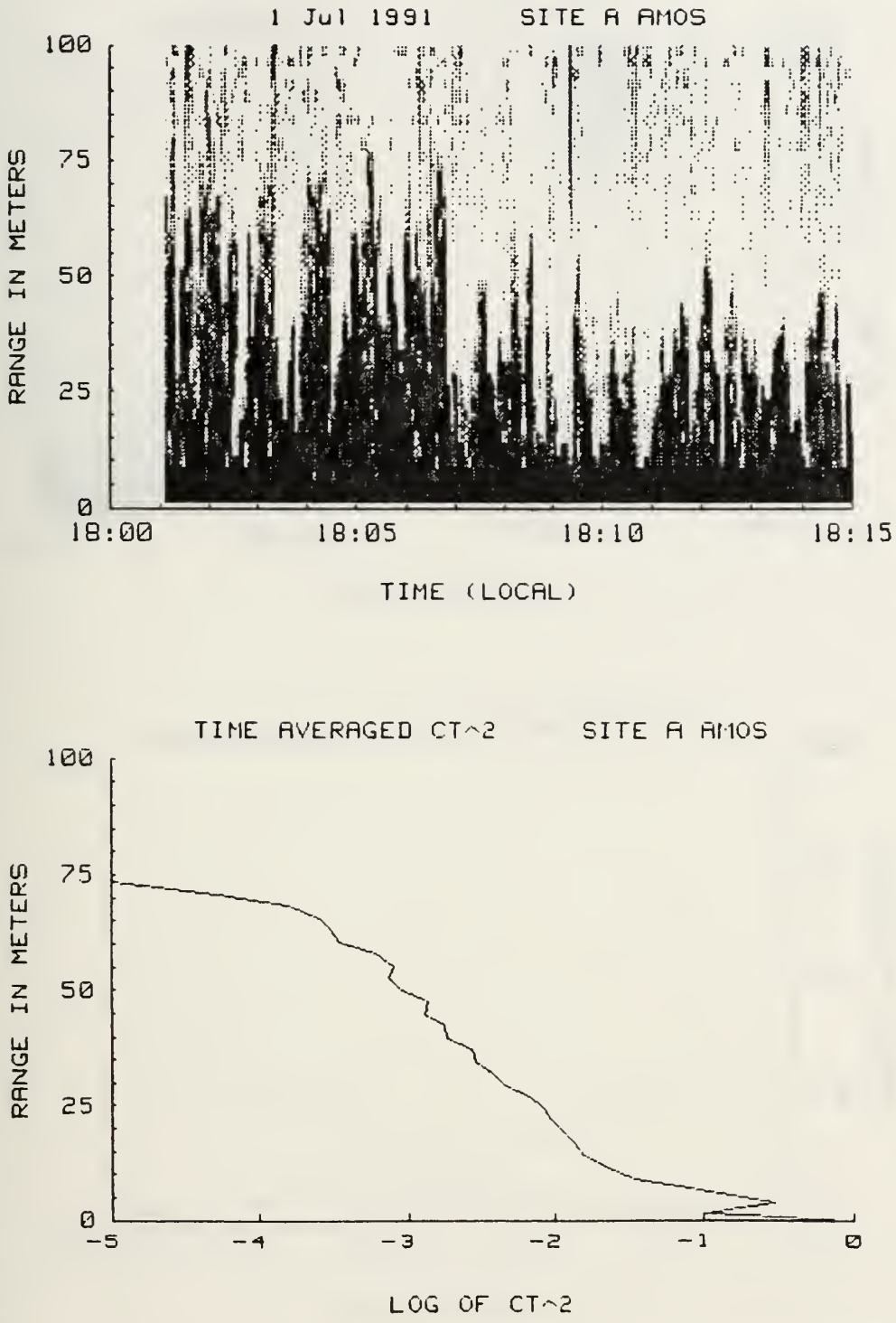

Figure 55. Echo-sounder Turbulence Profile, 01 July, 1991.

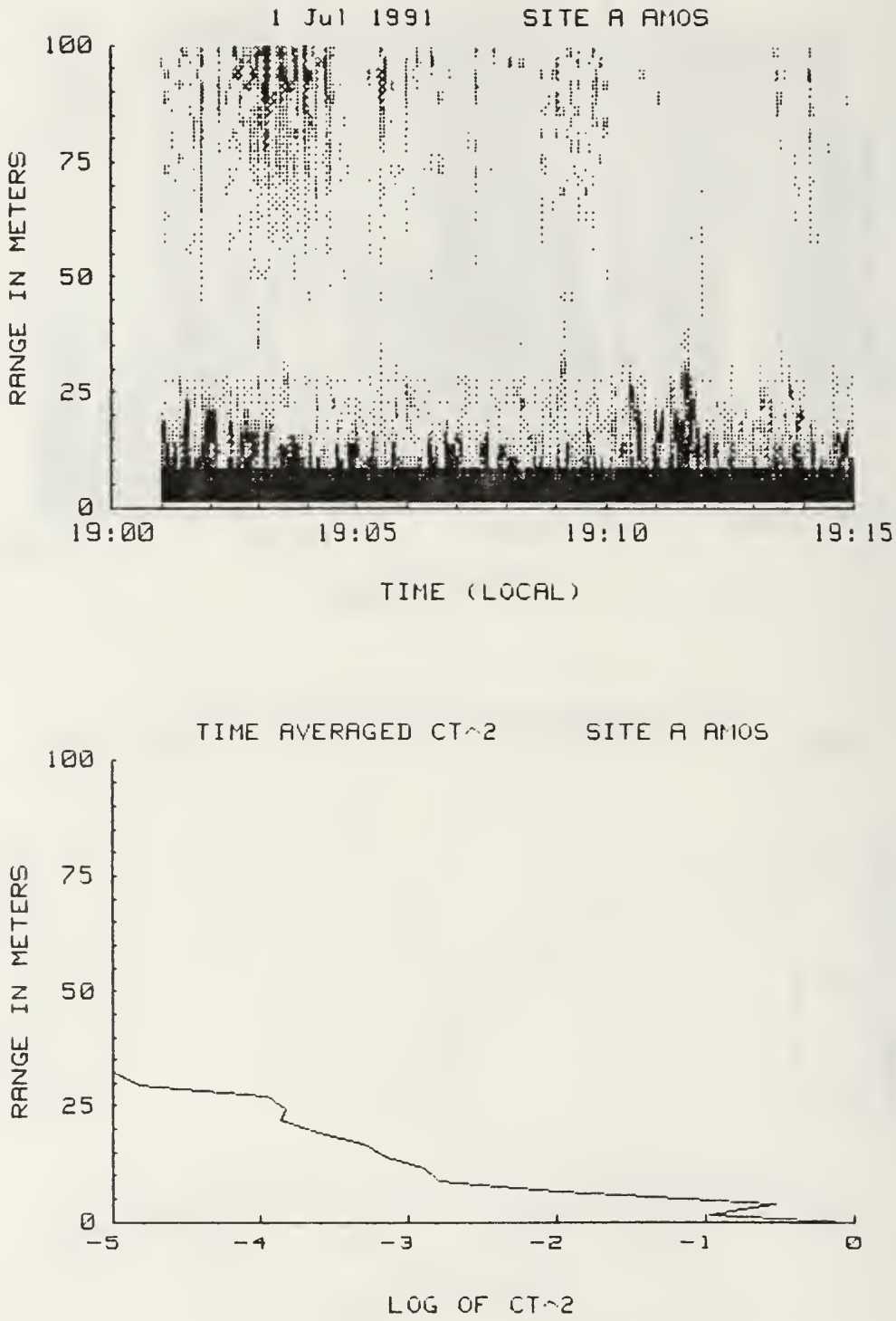

Figure 56. Echo-sounder Turbulence Profile, 01 July, 1991.

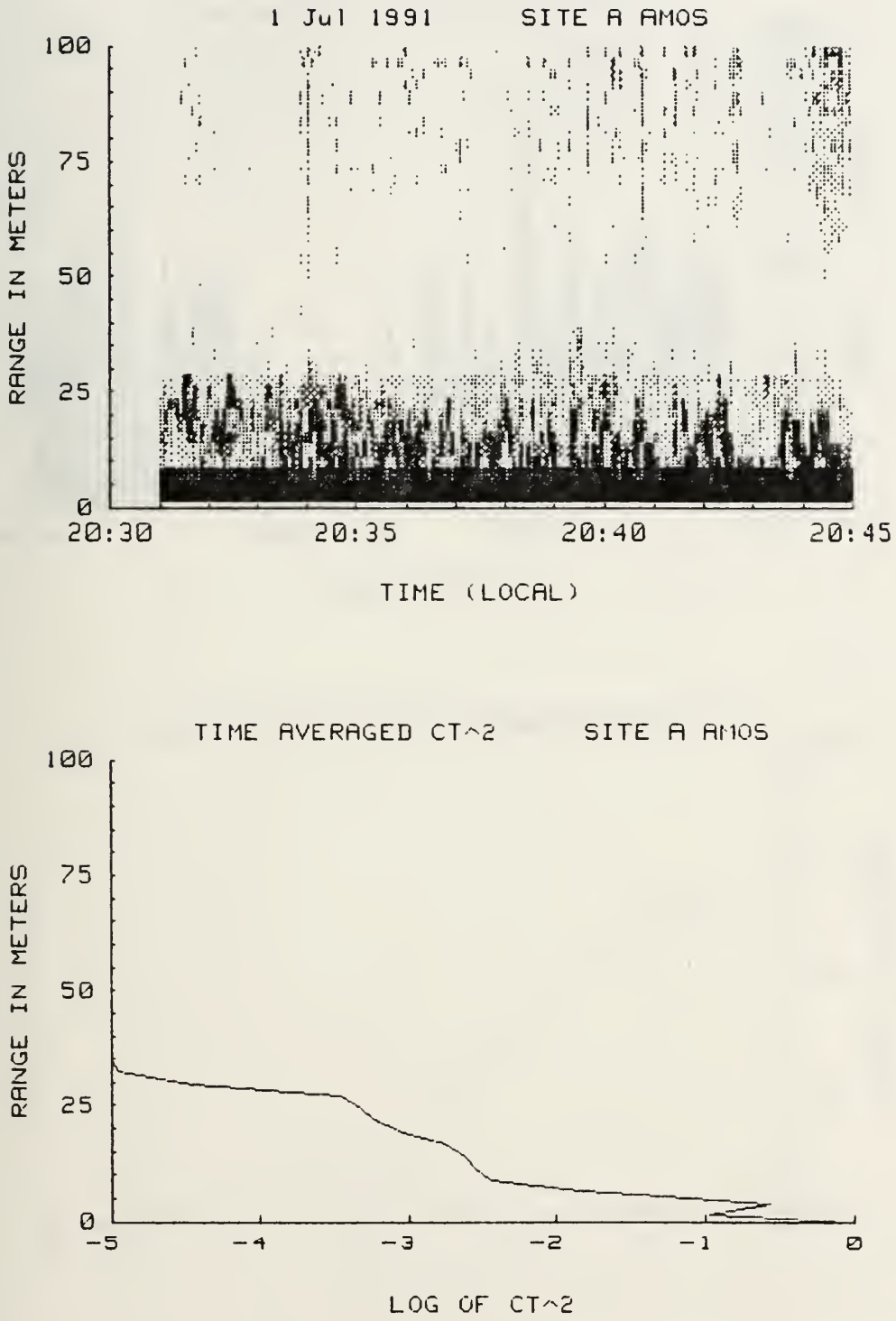

Figure 57. Echo-sounder Turbulence Profile, 01 July, 1991.

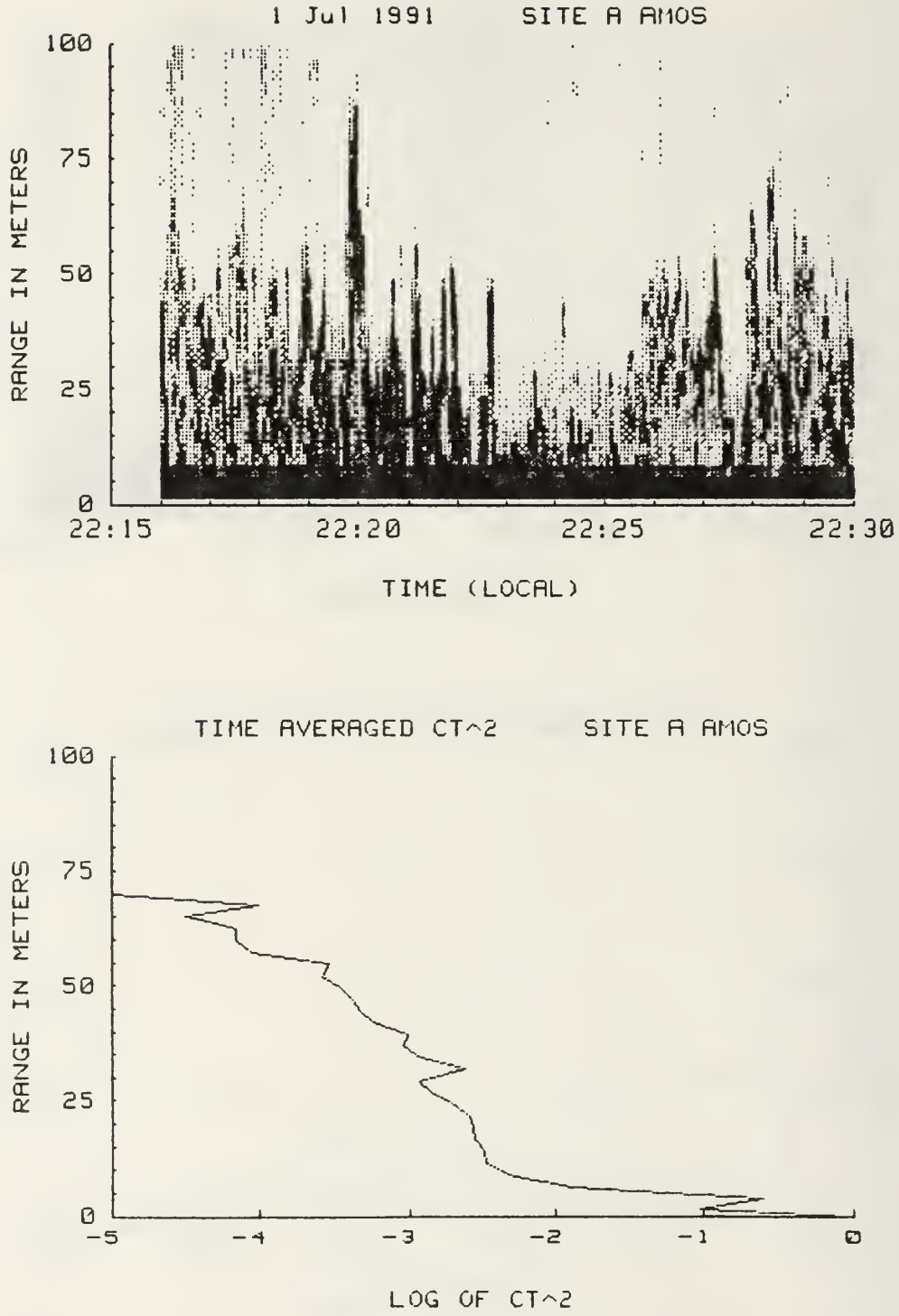

Figure 58. Echo-sounder Turbulence Profile, 01 July, 1991.

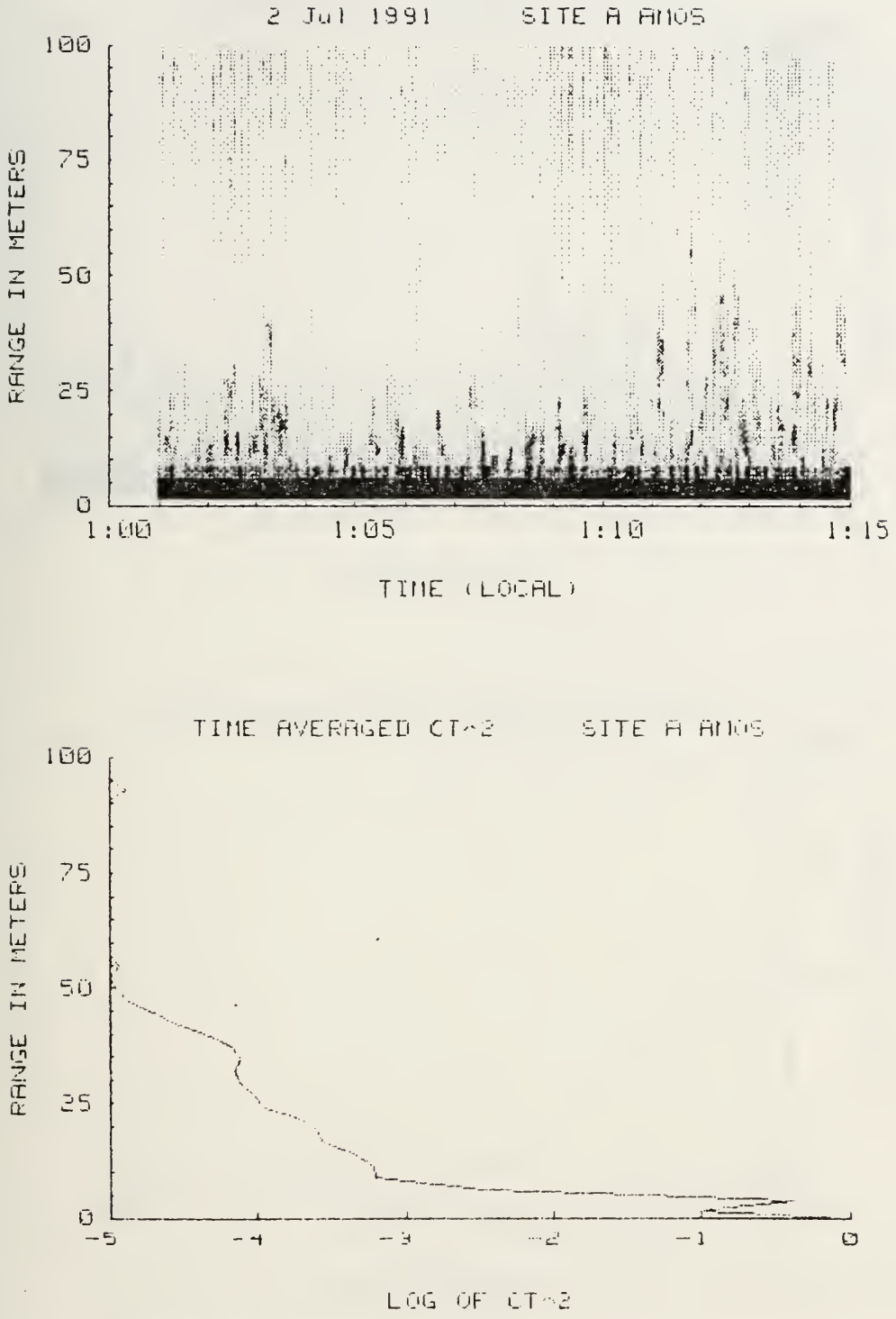

Figure 59. Echo-sounder Turbulence Profile, 02 July, 1991.

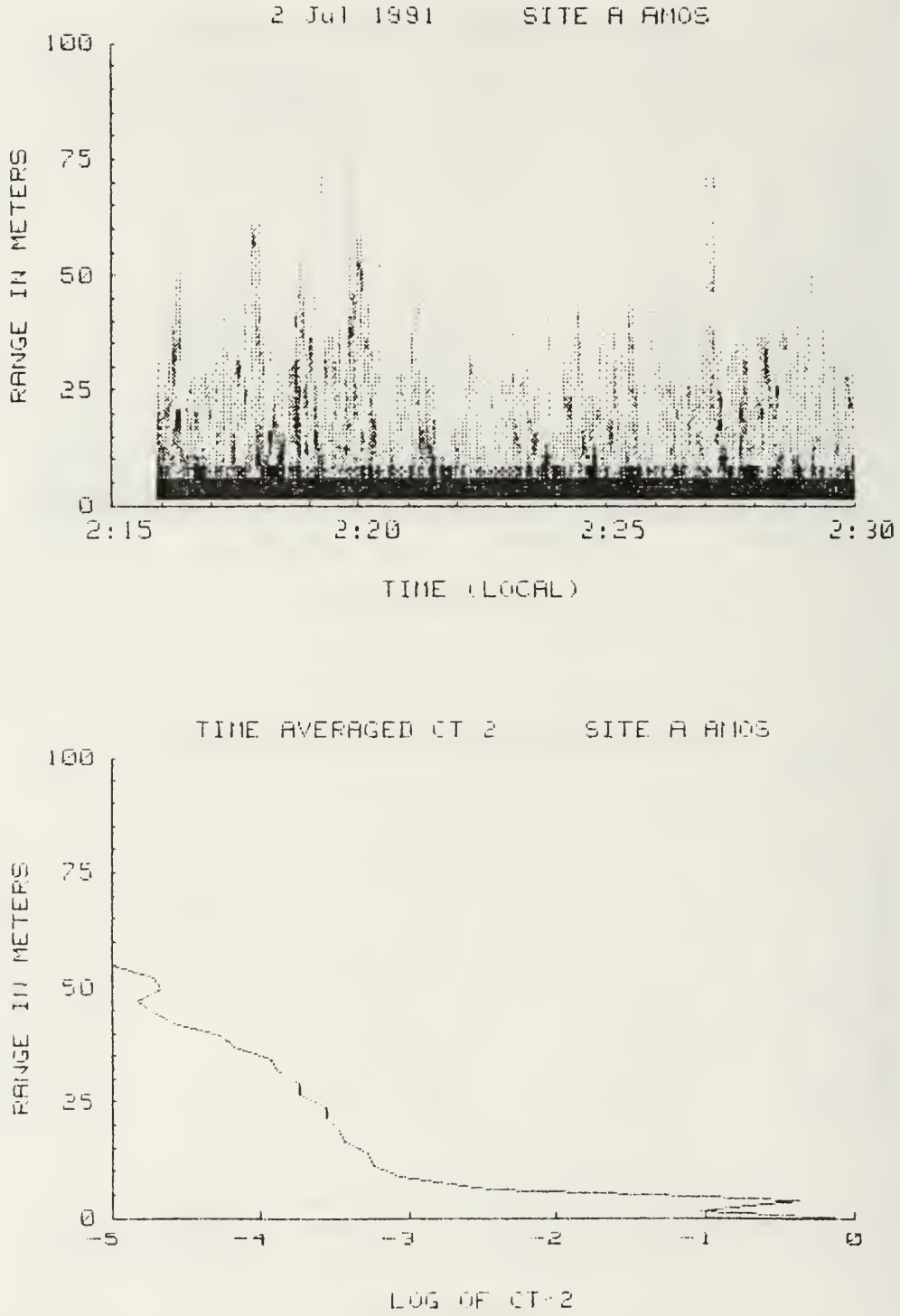

Figure 60. Echo-sounder Turbulence Profile, 02 July, 1991.

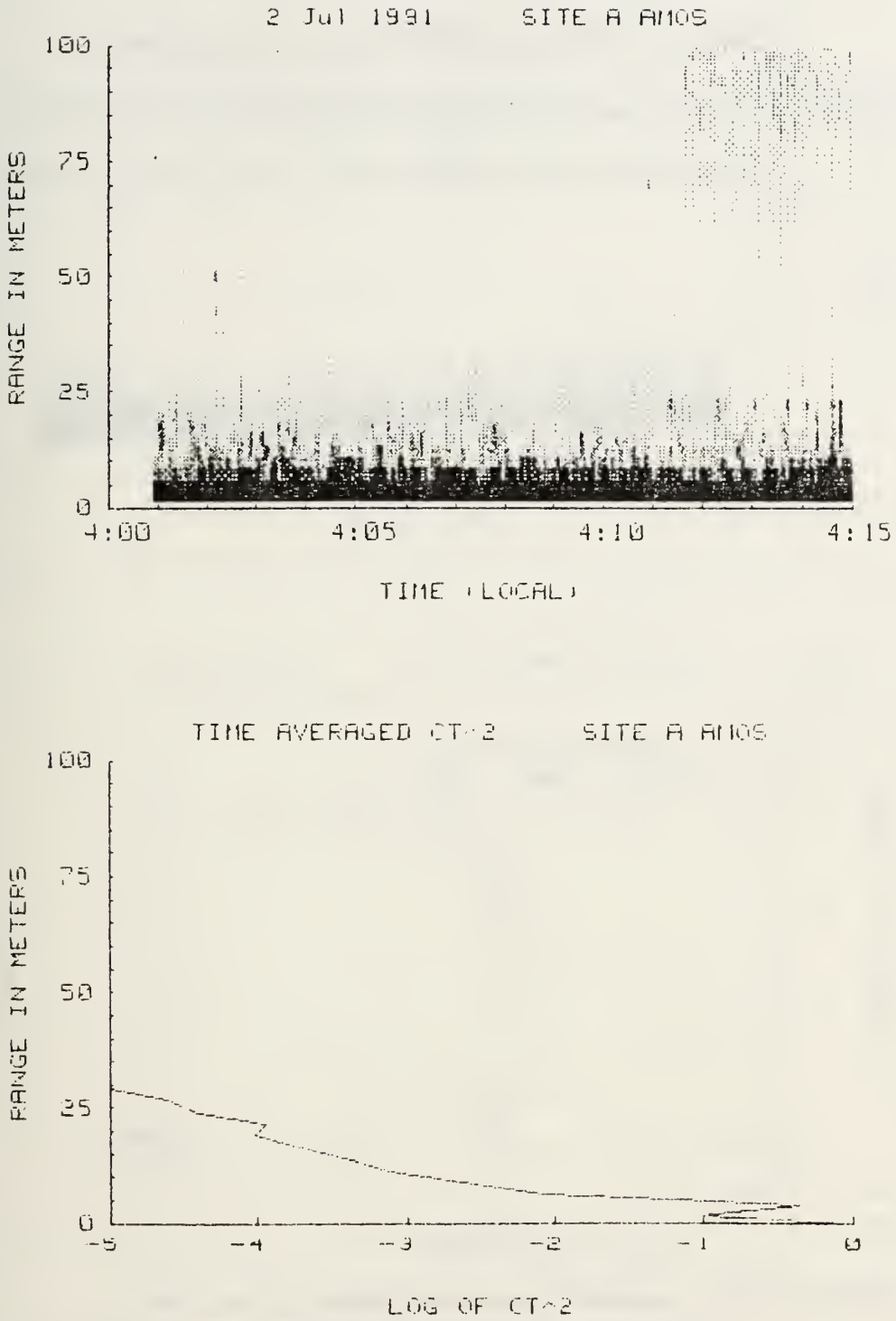

Figure 61. Echo-sounder Turbulence Profile, 02 July, 1991.

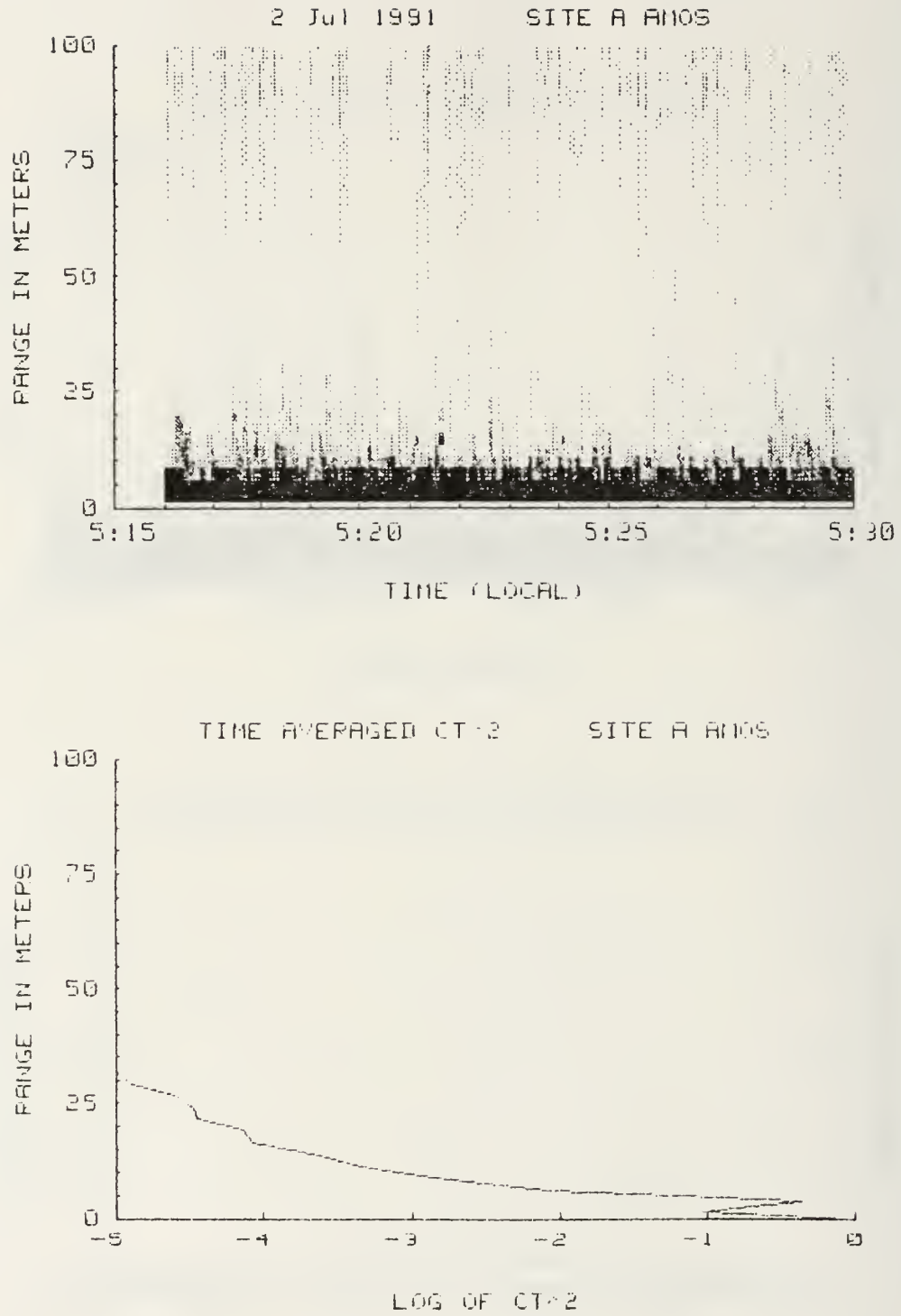

Figure 62. Echo-sounder Turbulence Profile, 02 July, 1991.

APPENDIX C. WIND PROFILE DATA FOR AMOS

In addition to C_T^2 data, wind profile data were also collected using a Doppler algorithm. The following is a representative sampling of this data.

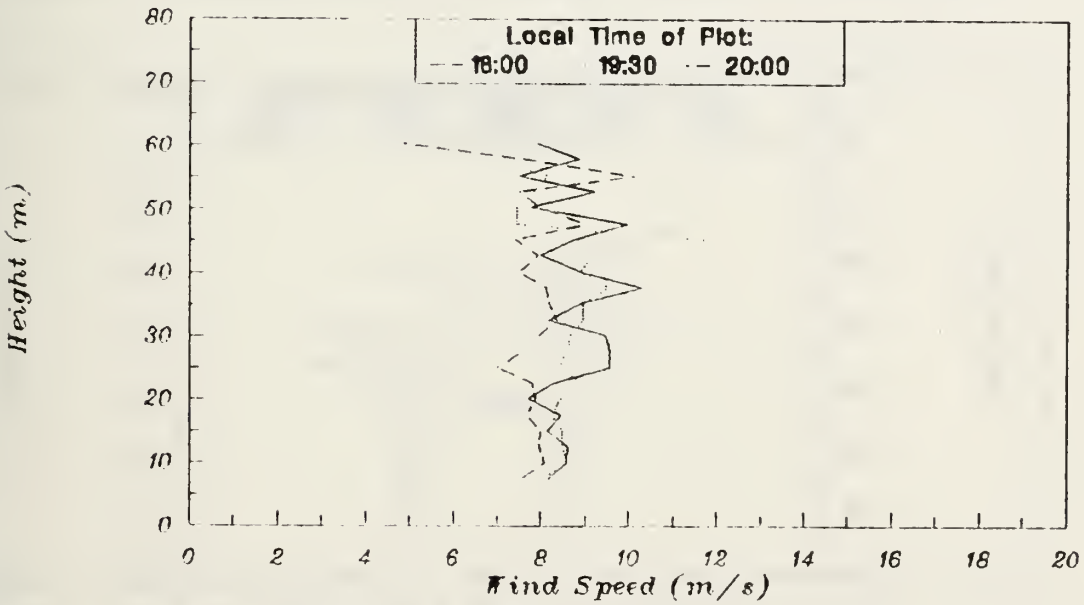

Figure 63. Echo-sounder Wind Profile, 28 June, 1991.

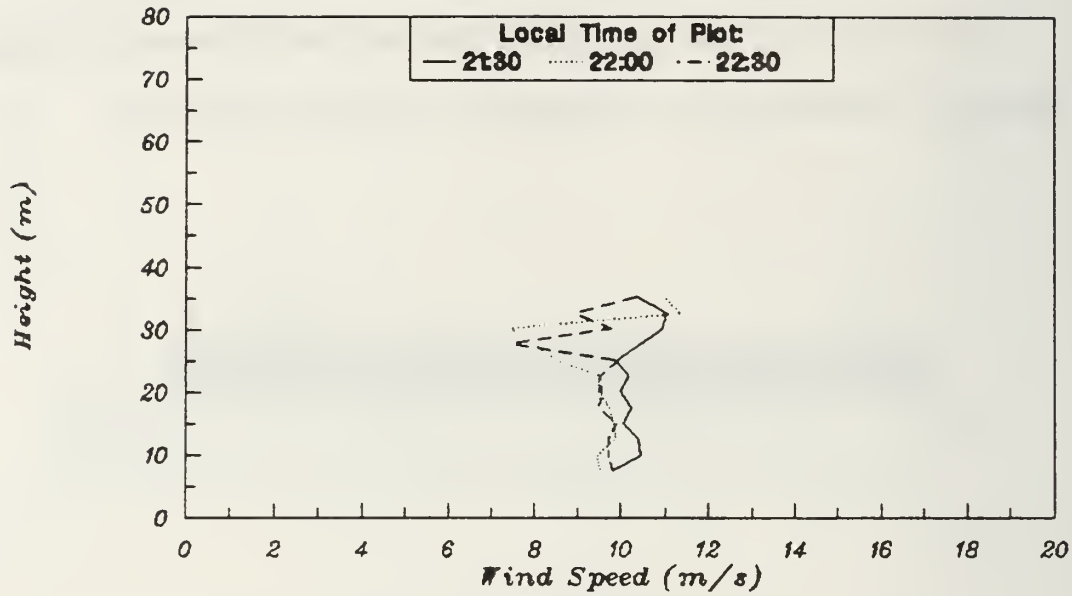

Figure 64. Echo-sounder Wind Profile, 28 June, 1991.

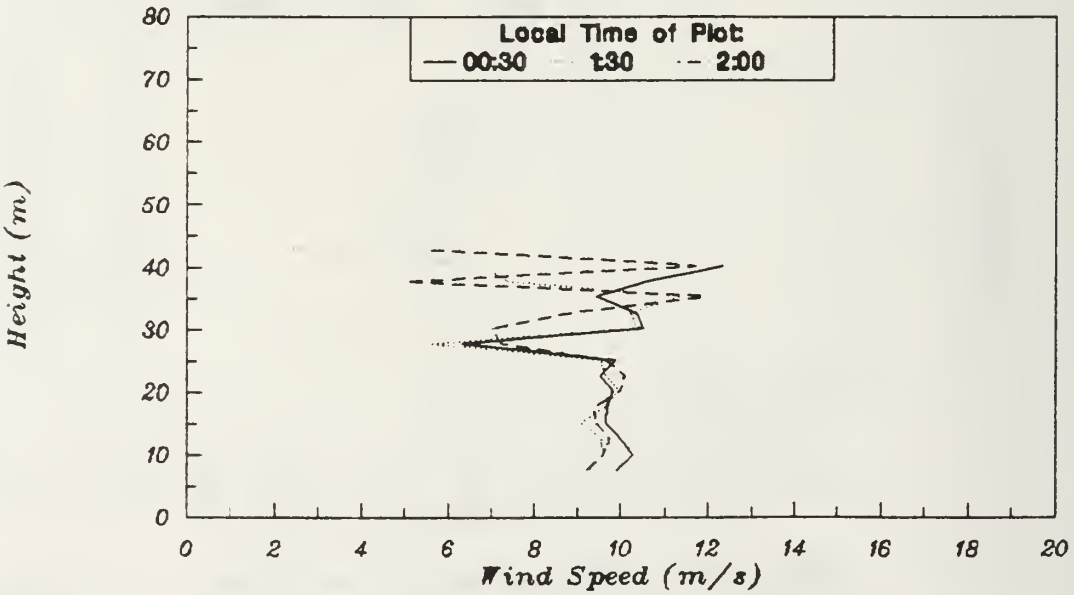

Figure 65. Echo-sounder Wind Profile 29 June 1991.

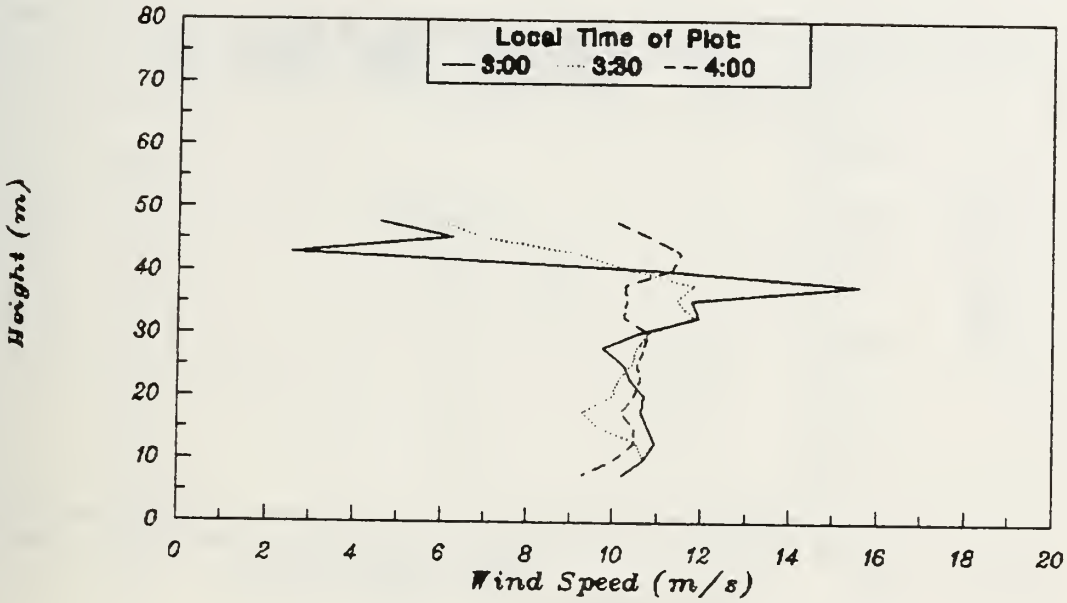

Figure 66. Echo-sounder Wind Profile, 29 June, 1991.

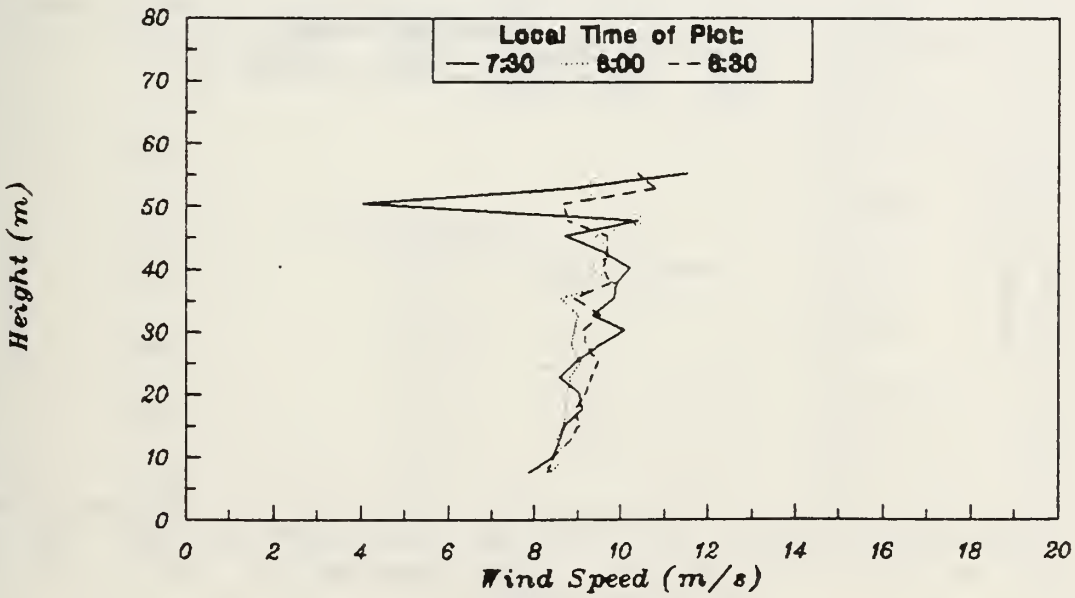

Figure 67. Echo-sounder Wind Profile, 29 June, 1991.

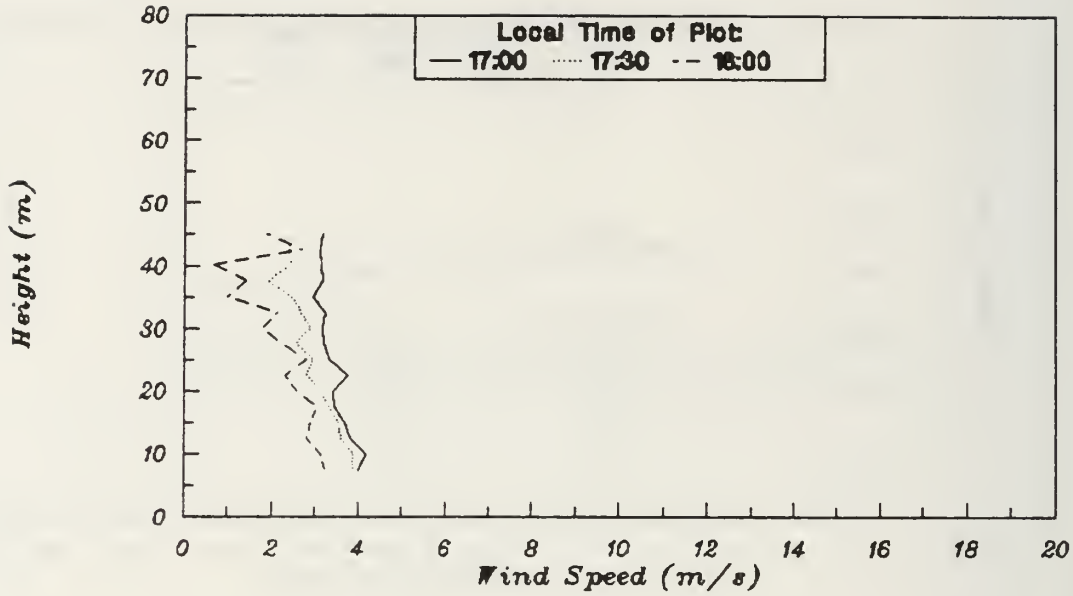

Figure 68. Echo-sounder Wind Profile, 29 June, 1991.

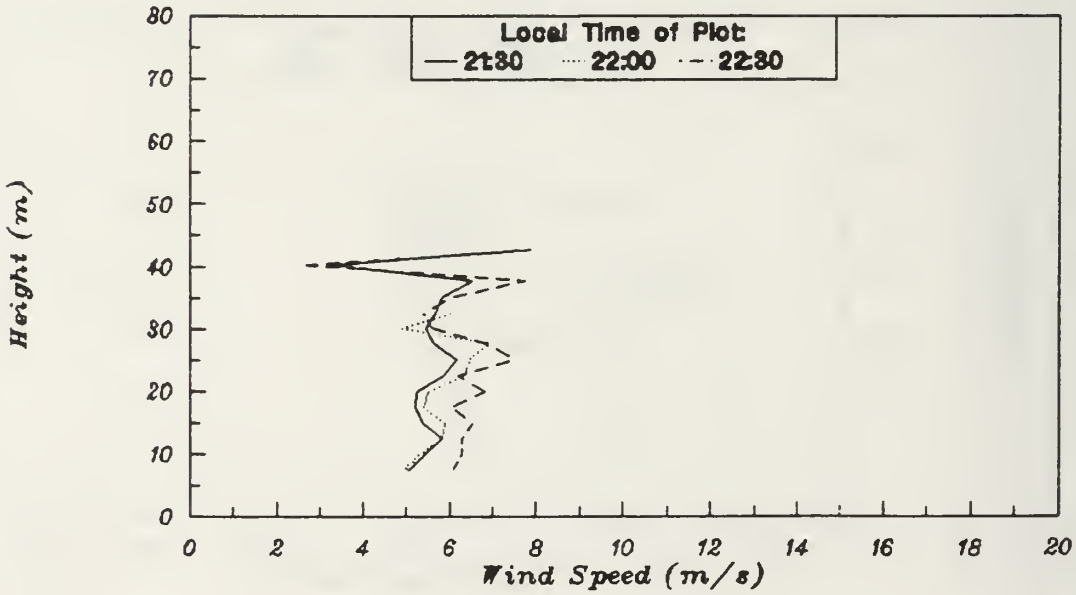

Figure 69. Echo-sounder Wind Profile, 29 June, 1991.

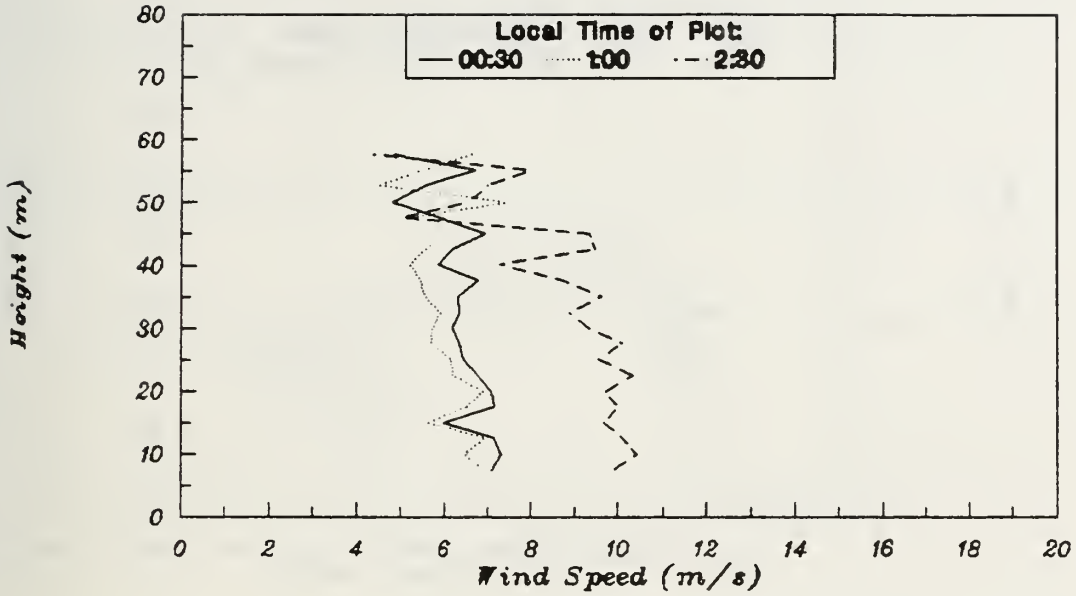

Figure 70. Echo-sounder Wind Profile, 30 June, 1991.

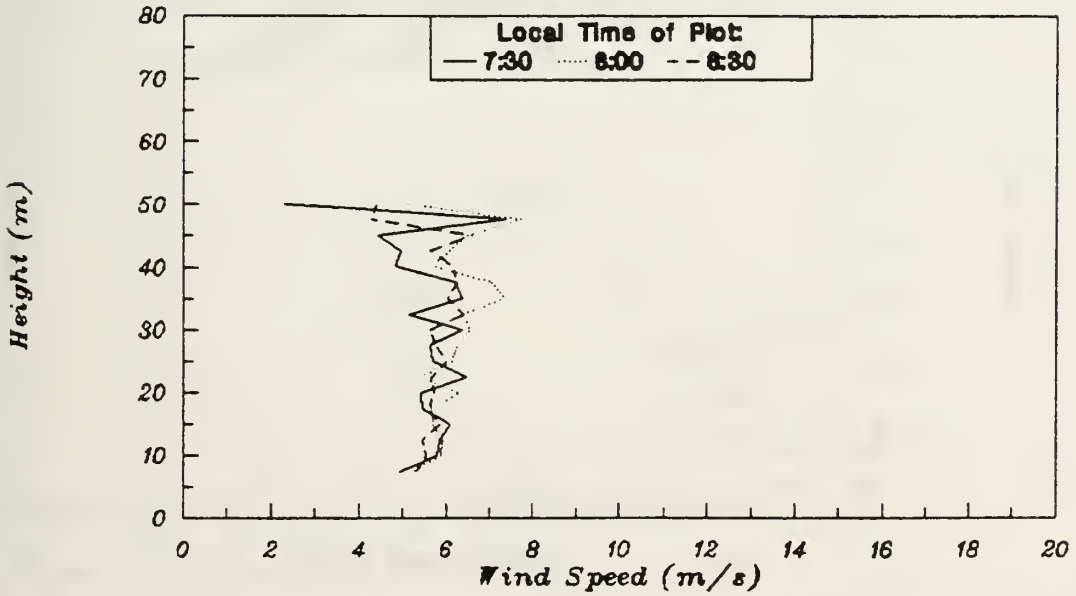

Figure 71. Echo-sounder Wind Profile, 30 June, 1991.

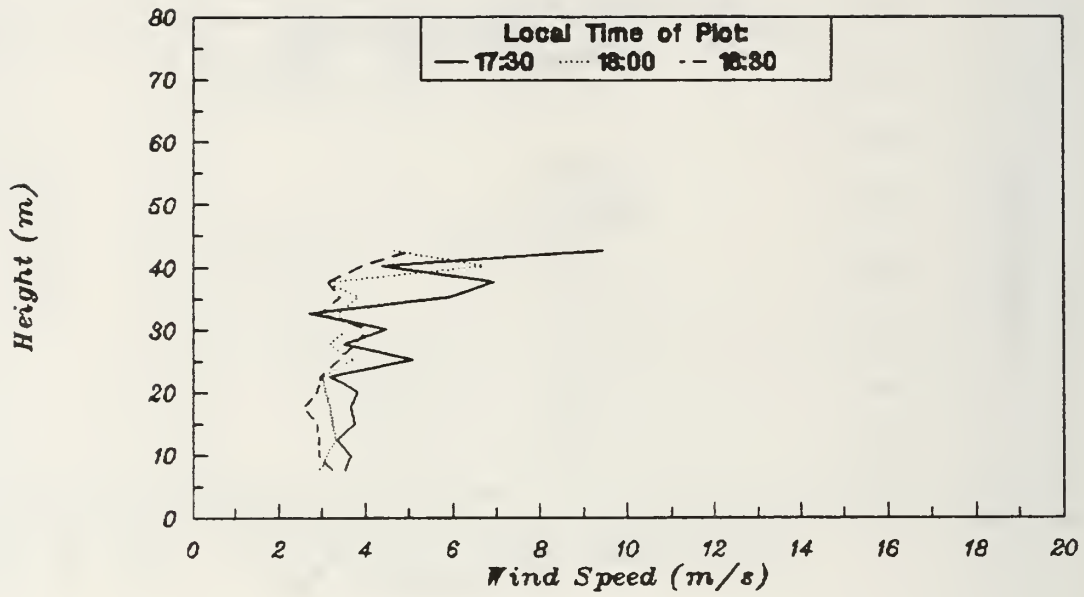

Figure 72. Echo-sounder Wind Profile, 01 July, 1991.

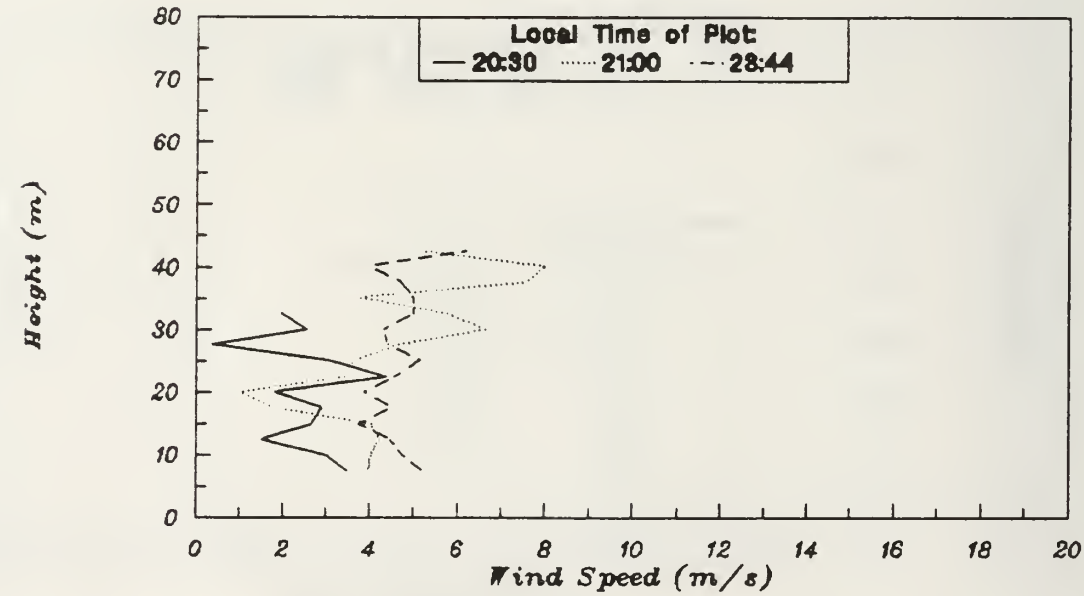

Figure 73. Echo-sounder Wind Profile, 01 July, 1991.

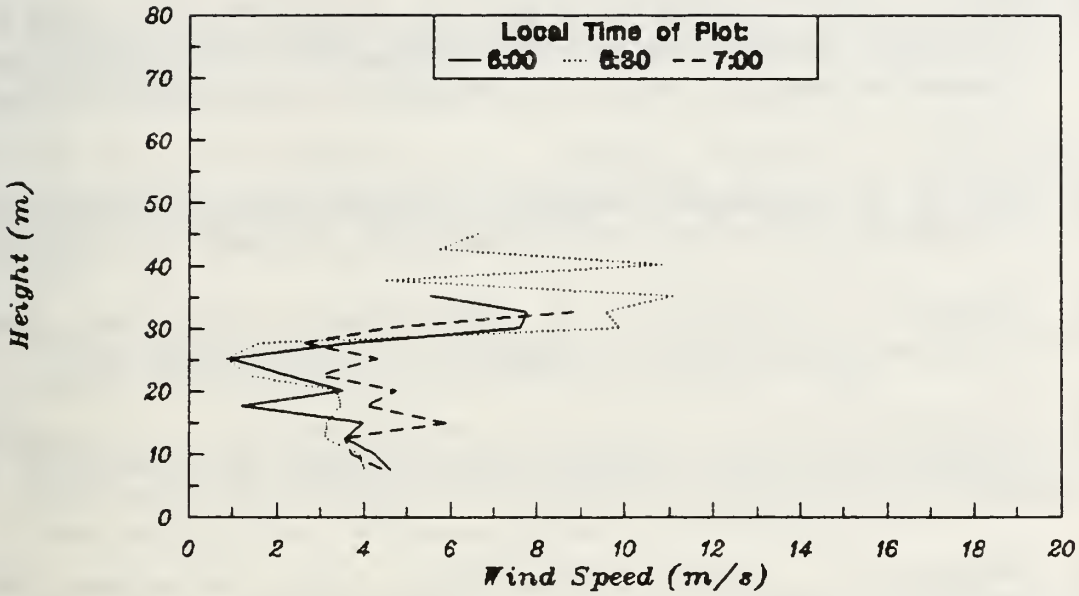

Figure 74. Echo-sounder Wind Profile, 02 July, 1991.

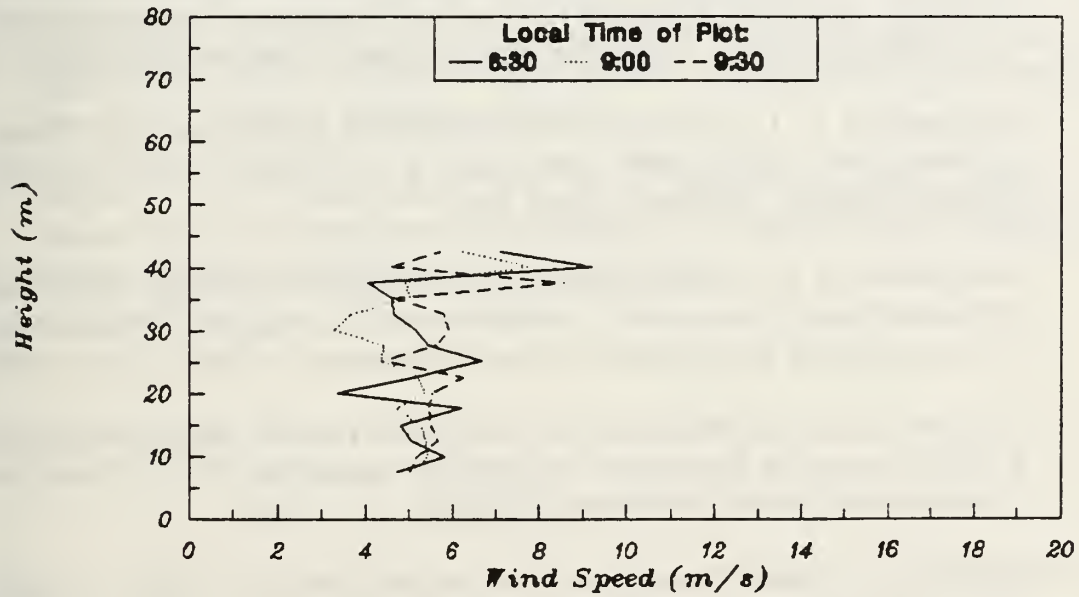

Figure 75. Echo-sounder Wind Profile, 02 July, 1991.

LIST OF REFERENCES

1. Hall, F. F. Jr., "Temperature and Wind Structure Studies by Acoustic Echo-Sounding," *Remote Sensing of the Troposphere*, U. S. Department of Commerce National Oceanic and Atmospheric Administration, 15 August, 1970.

2. Neff, W. D., "Quantitative Evaluation of Acoustic Echoes from the Planetary Boundary Layer," *NOAA Technical Report ERL 322-WPL 38,* June 1975.

3. Mousley, T. J. and Cole, R. S., "High Frequency Atmospheric Acoustic Sounders," *Atmospheric Environment,* Vol. 13, pp. 347-350, 1979.

4. Asimakopoulos, D. N., Helmis, C. G. and Stephanou, G. J., "Atmospheric Acoustic Minisounder," *American Meteorological Society,* pp. 345-350, June 1987.

5. Walters, D. L., Private Communication, Naval Postgraduate School, Monterey, California.

6. Moxcey, L. R., *Utilization of Dense Packed Planar Acoustic Echosounders to Identify Turbulence Structures in the Lowest Levels of the Atmosphere,* M. S. Thesis, Naval Postgraduate School, Monterey, California, December 1987.

7. Weingartner, F. J., *Development of an Acoustic Echosounder for Detection of Lower Level Atmospheric Turbulence,* M. S. Thesis, Naval Postgraduate School,Monterey, California, June 1987.

8. Wroblewski, M. R., *Development of a Data Analysis System for the Detection of a Lower Level Atmospheric Turbulence with an Acoustic Echosounder,* M. S. Thesis, Naval Postgraduate School, Monterey, California, June 1987.

9. McCrary, J. K., *High Resolution C_{T2} and Radial Velocity Measurements Using a High Frequency Monostatic Acoustic Echosounder,* M. S. Thesis, Naval Postgraduate School, Monterey, California, June 1990.

10. Tatarski, V. I., *Wave Propagation in a Turbulent Medium,* Dover Publications, New York, 1961.

12. Racine, R., and others, "Mirror Dome and Natural Seeing at CFHT," *Publications of the Astronomical Society of the Pacific,* Vol. 103, pp. 1020-1032, September 1991.

13. Ochs, G. R. and Hill, R. J., "Optical Scintillation Method of Measuring Turbulence Inner Scale," *Applied Optics,* Vol. 24, No. 15, pp. 2430-2432, 1 August 1985.

14. Hill, R. J. and Clifford, S. F., "Modified Spectrum of Atmospheric Temperature Fluctuations and its Application to Optical Propagation," *Journal of the Optical Society of America,* Vol. 68, No. 7, pp. 892-899, July 1978.

15. Bass, H. E., "Atmospheric Absorption of Sound: Update," *Journal of the Acoustic Society of America,* Vol. 88, No.4, October 1990.

16. Olmstead, M. R., *Development of a Differential Temperature Probe for the Measurement of Atmospheric Turbulence at All Levels,* M. S. Thesis, Naval Postgraduate School, Monterey, California, December 1988.

17. Fried, D. L., "Optical Resolution Through a Randomly Inhomogeneous Medium for Very Long and Very Short Exposures," *Journal of tthe Optical Society of America,* Vol. 56, No. 10, pp. 1372-1379, October 1966.

18. Oldenettal, J. R., "Note on the Conversion of Seeing Angle to r_o for CIS Stellar Image Data," Private Communication, Air Force Maui Observation Site, Maui, Hawaii, 4 September 1991.

19. Hoover, C. R., *Investigation of a Single Point Temperature Probe for Measurements of Atmospheric Turbulence,* M. S. Thesis, Naval Postgraduate School, Monterey, California, December 1991.

DUDLEY KNOX LIBRARY
NAVAL POSTGRADUATE SCHOOL
MONTEREY CA 93943-5101

3 2768 00307923 7